HEINRICH HEINE
UNIVERSITÄT DÜSSELDORF

Characterization of a subset of splenic plasmacytoid dendritic cells specialized for production of IFNβ and the role of type I interferon during *Toxoplasma gondii* infection

Inaugural-Dissertation

zur Erlangung des Doktorgrades
der Mathematisch-Naturwissenschaftlichen Fakultät
der Heinrich-Heine-Universität Düsseldorf

vorgelegt von

Regine Josefine Gabriele Dress
aus Staaken

Düsseldorf, Juli 2015

Aus dem Institut für Medizinische Mikrobiologie und Krankenhaushygiene
der Heinrich-Heine-Universität Düsseldorf

Gedruckt mit der Genehmigung der
Mathematisch-Naturwissenschaftlichen Fakultät der
Heinrich-Heine-Universität Düsseldorf

Referent: Frau Prof. Dr. Stefanie Scheu

Koreferent: Herr Prof. Dr. Thomas Klein

Tag der mündlichen Prüfung: 25.08.2015

Table of Contents

List of Abbreviations

Ab	Antibody
APC	Antigen presenting cell
BATF	Basic leucine zipper transcription factor
BM	Bone marrow
BST2	Bone marrow stromal cell antigen 2
CCL	Chemokine (C-C motif) ligand
CCR	Chemokine (C-C motif) receptor
CD	Cluster of differentiation
cDC	Conventional dendritic cell
CDP	Common dendritic cell progenitor
CpG	CpG containing oligonucleotide
Cy	Cyanin
d	Day
DC	Dendritic cell
DEPC	Diethylpyrocarbonat
DMSO	Dimethylsulfoxide
DLG	Discs large homolog
DNA	Desoxyribonucleic acid
dNTP	Desoxyribonucleotide
DOTAP	N-[1-(2,3-Dioleoyloxy)propyl]-N,N,N trimethylammoniummethylsulfate

E2-2	E-protein 2-2
EDTA	Ethylenediaminetetraacetic acid
ELISA	Enzyme-linked-immunosorbent assay
EpCAM	Epithelial cell adhesion molecule
EtOH	Ethanol
FACS	Fluorescent activated cell sorting
FCS	Fetal calf serum
FITC	Fluorescein isothiocyanate
Flt3	FMS-like tyrosine kinase 3
Flt3-L	FMS-like tyrosine kinase 3 ligand
Foxp	Forkhead box protein
GM-CSF	Granulocyte macrophage colony stimulating factor
GR-1	Ly6G; lymphocyte antigen 6 complex, locus G
h	hours
H_20	water
ID2	Inhibitor of DNA-binding 2
IFN	Interferon
IFNAR	Type I interferon receptor
Ig	Immunoglobulin
IL	Interleukin

i.p.	Intraperitoneal
IRF	Interferon regulatory factor
i.v.	Intravenous
LCMV	Lymphocytic choriomeningitis virus
Lin	Lineage
LN	Lymph node
LPS	Lipopolysaccharide
M-CSF	Macrophage colony stimulating factor
MDP	Macrophage dendritic cell progenitor
MHC	Major histocompatibility complex
mTOR	Mammalian target of rapamycin
MyD88	Myeloid differentiation primary response gene 88
NFκB	Nuclear factor kappa-light-chain enhancer of activated B cells
PBS	Phosphate buffered saline
PCR	Polymerase chain reaction
pDC	Plasmacytoid dendritic cell
PFA	Paraformaldehyde
p.i.	Post infection
PLP	Proteolipid protein
PMA	Phorbol 12-myristate 13-acetate

Poly(I:C)	Polyinosinic:polycitydilyc acid
PRR	Pattern recognition receptor
PSD	Postsynaptic density protein
PU.1	Spleen focus forming virus proviral integration oncogene sp1
qRT-PCR	Quantitative realtime polymerase chain reaction
RelB	avian reticuloendotheliosis viral (v-rel) oncogene related B
RIG-1	Retinoic acid-inducible gene 1
RNA	Ribonucleic acid
rpm	Revolutions per minute
RT	Room temperature
Sca-1	Stem cell antigen 1
SiglecH	Sialic acid binding Ig-like lectin H
STAT	Signal transducer and activator of transcription protein
TGF	Transforming growth factor
TH	T helper cell type
TLA	*Toxoplasma gondii* lysate antigen
TLR	Toll like receptor
TNFα	Tumor necrosis factor α
T. gondii	*Toxoplasma gondii*

List of Figures

Summary

Type I interferons are essential initiators of subsequent innate and adaptive immune responses to viruses, bacteria and other pathogens. Furthermore these cytokines can play an ambivalent role in auto-immune diseases including acting as a pathogenic factor in psoriasis or systemic lupus erythematosus or serving as a therapeutic for the case of IFNβ in multiple sclerosis. Given the central role these factors in immune responses, increasing our understanding of type I IFN and IFNβ-producing cells in infection is important to better understand how to design better therapeutics for infection and immune disorders.

We found that after TLR9 stimulation only ~5% of splenic plasmacytoid dendritic cells (pDCs) are able to produce IFNβ. This was not due to a lack of activation of the non-producing pDCs, but rather to a differential gene expression profile found in IFNβ-producing vs. non-producing pDCs. This distinct gene expression profile was accompanied by a specific localisation pattern, enhanced migration and active recruitment of NK and T cells by IFNβ-producing pDCs. Furthermore, we found the identity and function of this subset of splenic IFNβ-producing pDCs to be independent of signalling through the IFNAR. We also found the transcription factor BATF and the membrane protein PSD-93 to be differentially expressed in IFNβ-producing pDCs. Initial *in vitro* and *in vivo* analyses of $BATF^{-/-}$ and $PSD\text{-}93^{-/-}$ mice revealed that in spite being non-essential for IFNβ induction in pDCs both proteins might play a role in terminal differentiation and be involved in the IFNβ signalling pathway in pDCs.

Moreover, during *Toxoplasma gondii* infection we found that type I IFN are crucial for survival after infection. Mice lacking IFNβ or the IFNAR rapidly succumbed to *T. gondii* infection. These animals possessed higher cyst loads, and were insufficient in production of the key cytokine IFNγ, despite normal IL-12 levels and induction of mGBPs, key effector proteins in *T. gondii* clearance. We found that the main IFNβ-producing cells in infection with *T. gondii* are DCs while IFNγ was predominantly produced by NK cells. Viable or heat-killed parasites functionally activated wildtype but not type I IFN deficient DCs *in vitro*, and interaction of activated DCs with NK cells was important for NK cell activation.

Here, we describe a distinct subset of IFNβ-producing splenic pDCs, an important role for BATF and PSD-93 in IFNβ production by these pDCs and the impact of type I IFN during infection with the intracellular parasite *T. gondii*. The results of this thesis will help us to better understand type I IFN responses and type I IFN-producing cells providing a basis for new therapy strategies for infections and auto-immune disorders.

Zusammenfassung

Typ I Interferone sind essentielle Induktoren von Immunantworten des angeborenen und adaptiven Immunsystems gegenüber Viren, Bakterien und anderen Pathogenen. Des weiteren spielen sie eine ambivalente Rolle in Autoimmunerkranken. Hier können sie zum Einen detrimentelle Wirkungen haben z. B. in Erkrankungen wie Psoriasis oder Lupus oder aber dienen als Therapeutika z.B. für Multiple Sklerose. Aufgrund dieser zentralen Rolle von Typ I IFN in Immunantworten, ist es von hoher Bedeutung die Wirkung von Typ I IFN und IFNβ-produzierende Zellen besser zu verstehen. Dies ist wichtig für die Verbesserung von Therapiestrategien für diverse Infektions- und Autoimmunerkrankungen.

Wir konnten beobachten, dass nach TLR9 Stimulation lediglich ~5% aller pDCs in der Milz in der Lage sind IFNβ zu produzieren. Dies ist nicht die Folge einer fehlenden Aktivierung der nicht-IFNβ-produzierenden pDCs, als viel mehr eines unterschiedlichen Genexpressionsprofiles dieser Zellen. Zudem haben IFNβ-produzierende Zellen ein vermehrtes Migrationsvermögen und können aktiv und effizient NK- und T-Zellen rekrutieren. Des weiteren sind Identität und Funktion von IFNβ-produzierenden pDCs in der Milz unabhängig von der Typ I IFN vermittelten positiven Amplifizierung über den IFNAR. In IFNβ-produzierenden pDCs sind zudem der Transkriptionsfaktor BATF und das Membranprotein PSD-93 differentiell hoch exprimiert. In initialen *in vitro* und in *vivo* Studien an $BATF^{-/-}$ und $PSD\text{-}93^{-/-}$ -Mäusen konnten wir zeigen, dass beide Faktoren vermutlich eine Rolle in der terminalen Differenzierung von pDCs und im Signalweg der IFNβ-Produktion spielen, auch wenn sie nicht essentiell für die IFNβ-Produktion an sich sind.

Ein Infektionsmodell mit *Toxoplasma gondii* zeigte, dass Typ I IFN wichtig für das Überleben dieser Infektion sind. Mäuse, die kein IFNβ produzieren können oder denen der IFNAR fehlt, erliegen schnell der Infektion mit *T. gondii*. Trotz normaler Produktion von IL-12 bilden diese Tiere nur eine schwache IFNγ-Antwort aus und haben zudem eine erhöhte Zystenlast im Gehirn, trotz einer effizienten Aktivierung von mGBPs, Schlüsselfaktoren in der Immunabwehr gegen *T. gondii.*

Wir konnten definieren, dass während der Infektion mit *T. gondii* DCs die Hauptproduzenten von IFNβ sind, während IFNγ größtenteils von NK-Zellen sekretiert wird. Außerderm konnten wir festellen, dass sowohl lebendige, als auch Hitze-inaktivierte Parasiten in der Lage sind Wildtyp-DCs *in vitro* funktionell zu aktivieren, während dies nicht der Fall war für DCs von Typ I IFN-defizienten Mäusen. Zudem konnten wir zeigen, dass vollständig aktivierte DCs wichtig für die Aktivierung von NK-Zellen sind.

In dieser Arbeit beschreiben wir eine einzigartige Subpopulation IFNβ-produzierender pDCs in der Milz und eine wichtige Rolle für die Proteine BATF und PSD-93 in der IFNβ-Produktion durch diese pDCs. Zudem zeigen wir, dass Typ I IFN von essentieller Bedeutung während der Infektion mit dem intrazellulären Parasiten *T. gondii* sind. Die Ergebnisse dieser Arbeit werden uns helfen Typ I IFN-Antworten und –produzierende Zellen besser zu verstehen und stellen damit eine Grundlage für die Entwicklung neuer Therapiemethoden für diverse Infektions- und Autoimmunerkrankungen dar.

1. Introduction

The immune system has evolved to protect us from a plethora of parasites, bacteria and viruses, while limiting autoimmunity. The immune system relies on an efficient interplay of innate and adaptive branches of immunity. This thesis will focus mostly on innate immunity, the following chapters will introduce the importance of type I interferon and dendritic cells (DCs), key components of the innate immune system, which also provide an important link to the adaptive immune system.

1.1 Type I IFN in host defence

Type I IFN, including different IFNα subtypes and IFNβ, are crucial for host protection against viruses but have also important functions in non-viral infections. These factors can be rapidly secreted in large quantities following infection primarily by DCs and macrophages. Plasmacytoid dendritic cells (pDCs) are especially well equipped for IFN production due to their endosomal expression of the toll like receptors (TLR) 7 and 9, as well as constitutive expression of the transcription factor IRF7 (interferon regulatory factor 7). TLR7 and 9 recognize viral single-stranded RNA and unmethylated DNA respectively, and trigger activation of IRF7. IRF7 subsequently translocates into the nucleus where it promotes expression of type I IFNs (Honda et al., 2005). This configuration allows pDCs to produce massive amounts of IFNα and IFNβ very early after infection (Gilliet et al., 2008; Reizis et al., 2011; Swiecki and Colonna, 2011). Furthermore, type I IFN production can be enhanced by a positive feedback loop via the type I IFN receptor. Here, secreted IFNα or IFNβ binds to the IFNAR on either the cytokine producing cell itself or neighbouring cells inducing a cascade of signalling leading to the expression of interferon stimulated genes (ISGs) along with production of more type I IFN (Ivashkiv and Donlin, 2014; Platanias, 2005). The IFNAR consists of two subunits, IFNAR1 and IFNAR2. Recently a unique complex of IFNAR1 and IFNβ was identified that signals independently of IFNAR2 and induces a distinct set of ISGs. This

suggests that IFNAR1 may play a more prominent role than IFNAR2 during IFNβ signalling responses (de Weerd et al., 2013).

In addition to their crucial role in host defence against viruses, type I IFN also play a role in other aspects of the immune system. These factors can modulate responses of the innate and the adaptive immune system by promoting maturation of DCs and B cells, and activation of T and NK cells. Type I IFNs have complex and sometimes seemingly contradictory roles during bacterial and parasitic infections, tumour surveillance and autoimmune processes. For instance type I IFN have been shown to have a detrimental impact during infection with the gram-positive bacterium *Listeria monocytogenes*. Here, induction of type I IFNs leads to apoptosis of T cells and macrophages and thereby loss of important effector cells (Carrero et al., 2004; Stockinger et al., 2002). On the other hand, type I IFN were shown to positively influence suppression of tumour cell growth (Bogdan et al., 2004; Decker et al., 2005). Administration of IFNβ is a common treatment for the autoimmune disease multiple sclerosis where it drastically reduces severity of disease in many cases (Inoue et al., 2012; Takaoka and Yanai, 2006). Precisely how IFNβ supresses this auto-immune disease remains to be elucidated.

Type I IFN and especially IFNβ, essential for host protection, are mostly produced by DCs and macrophages. In previous studies we have shown that during viral infection IFNβ is produced predominantly by pDCs (Scheu et al., 2008).

1.2 Dendritic cells

Dendritic cells provide the first line of innate immune defence against viruses and other pathogens which have breached epithelial barriers. These cells are often the first to recognize pathogens and induce immune responses necessary to ultimately clear an infection. Dendritic cells were first recognized for their potent ability to activate naïve T cells (Nussenzweig and Steinman, 1980; Steinman and Witmer, 1978) but since then, our knowledge of the diverse functions of these cells has continued to grow. Among the cells classified as DCs there are different subtypes which appear to have distinct functions during immune responses,

despite sharing common features. In general, four cell types have been typically classified as members of the DC family – conventional DCs (cDCs), plasmacytoid DCs (pDCs), Langerhans cells and monocyte-derived DCs. In this thesis we focused on cDCs and pDCs. Both of these cell types are derived from hematopoietic stem cells which have the potential to differentiate into common myeloid progenitors (CMP) or common lymphoid progenitors (CLP) that subsequently can give rise to pDCs, $CD8\alpha^+$ cDCs and $CD11b^+$ cDCs in a Flt3-L-dependent manner (see Fig. A) (Karsunky et al., 2003; Manz et al., 2001). CMP give rise to macrophage/DC progenitors (MDP) which are able to give rise to $Ly6C^{+/-}$ monocytes, macrophages, and under the influence of Flt3-L and M-CSFR to common DC progenitors (CDP) (Geissmann et al., 2010; Onai et al., 2007). Flt3-L and M-CSFR themselves were found to be under the control of the transcription factor PU.1 (Carotta et al., 2010). CDP are thought to be the immediate pre-cursor of pDCs and pre-cDCs, the immature pre-cursors of cDC lineages (Liu et al., 2009; Naik et al., 2006). However, development of cDCs also depends on various transcription factors e.g. PU.1 as mentioned above, STAT3 and Ikaros (Dakic et al., 2005; Laouar et al., 2003). On the other hand, the transcription factors IRF8, BATF3 and ID2 (DNA-binding protein inhibitor 2), were shown to be crucial for development of $CD8\alpha^+$ cDCs (Aliberti et al., 2003; Hacker et al., 2003; Hildner et al., 2008; Poltorak and Schraml, 2015), whereas IRF2, IRF4 and RelB are crucial for $CD11b^+$ cDCs (Ichikawa et al., 2004; Poltorak and Schraml, 2015; Suzuki et al., 2004). In the case of pDCs, E2-2 was shown to be crucial in inducing pDC commitment (Cisse et al., 2008; Ghosh et al., 2010; Reizis et al., 2011). However, the detailed mechanisms of pDC commitment are still poorly understood. Lack of any of the transcription factors mentioned above leads to severe developmental defects and/or loss of these DC populations. Recently, in attempts to analyse commitment of different pre-cursor states to one or the other DC lineages more intermediate pre-cursor stages have been described (Naik et al., 2007; Schlitzer et al., 2015b). Of note, it was reported that $CCR9^-$ immature pDCs can differentiate into cDC subsets *in vitro* and *in vivo*, suggesting early pDC development can be diverted towards the cDC lineage (Schlitzer et al., 2012; Schlitzer et al., 2011). However, pDCs and cDCs in general appear to be clearly distinguishable by their morphology, unique surface

molecule expression patterns, gene expression and cytokine profiles (Blasius et al., 2006a; Blasius et al., 2006b; Colonna, 2004; Reizis et al., 2011).

DCs are important in transmitting information from the innate to the adaptive immune system. As antigen presenting cells they are able to capture and process antigens from different pathogens and present those antigens to naïve T cells and/or co-stimulate T cells thereby activating them. Therefore, DCs are important in transmitting information from the innate to the adaptive immune system, but also in shaping the adaptive response e.g. driving T cell differentiation towards the specialized Th1, Th2 or Th17 states depending on the pathogen encountered and cytokines produced by DCs.

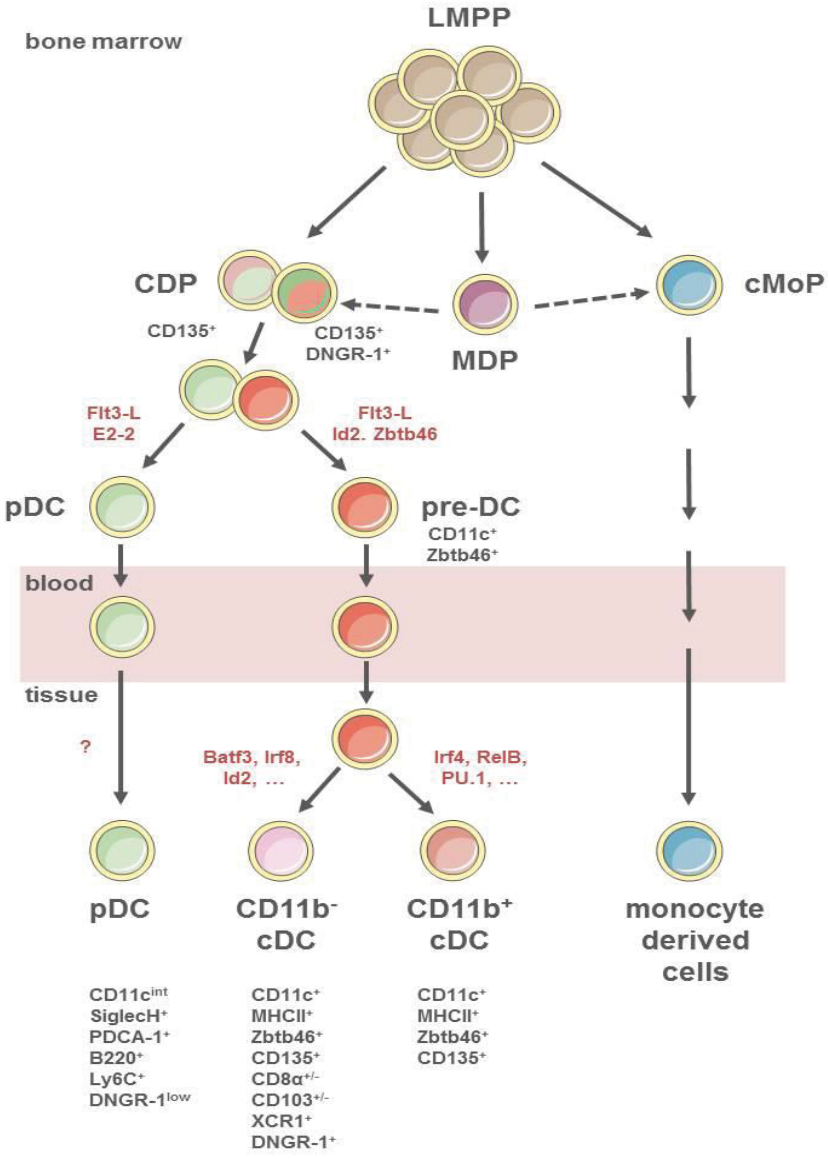

Fig.A Scheme of DC development (for illustration the servier medical art database was used; after Poltorak and Schraml, 2015).

1.2.1 Subsets of dendritic cells

1.2.1.1 Conventional dendritic cells

Conventional DCs are the largest population of DCs. They are relatively short-lived and therefore continuously replaced in the periphery by BM-derived pre-cursors assisted by expression of Flt3-L, c-kit (receptor for stem cell factor), and Zbtb46 (zink finger transcription factor) during development and CCR7 (Karsunky et al., 2003; Ogawa et al., 1991; Satpathy et al., 2012) expression enabling their migration into the periphery (Liu et al., 2007; McKenna et al., 2000; Waskow et al., 2008). cDCs can be found in all tissues analysed so far and are able to capture antigens from pathogens or the environment, process these antigens and present them to T cells (Villadangos and Schnorrer, 2007). As such, cDCs are able to induce immunity to foreign antigens but also tolerance to self-antigens. cDCs express high levels of CD45, CD11c, MHC class I and II and chemokine receptors facilitating their migration into lymphoid tissues (Inaba et al., 2000; Mellman and Steinman, 2001; Pierre et al., 1997). Furthermore, they are able to mature in response to viral or bacterial stimuli, this involves engagement of different pathogen recognition receptors and their downstream pathways e.g. TLRs and RIG-I like receptors (intracellular RNA receptors). Maturation upon TLR stimulation is dependent on intracellular signalling adaptors e.g. MyD88 (via TLR 1, 2, 4, 5, 6, 7, 8, 9, 11, 12 and 13) and Trif (via TLR 3 and 4) and leads to induction of pro-inflammatory cytokines such as IL-6 or IL-12 and to upregulation of cell surface molecules like CD80, CD86 or CD40, which are important for efficient T cell activation (Barchet et al., 2005). Up to now several cDC subsets have been described based on surface marker expression and functional characteristics, often specific for their tissue of residence e.g. spleen, lung, liver, gut or skin. In lymphoid organs including the spleen, three types of $CD11c^{+}MHCII^{+}$ cDCs can be distinguished, $CD4^{+}CD11b^{+}$ cDCs, $CD8\alpha^{-}CD11b^{+}$ cDCs and $CD8\alpha^{+}CD11b^{-}$ cDCs (Shortman and Liu, 2002). Interestingly, $CD8\alpha^{+}CD11b^{-}$ cDCs produce large amounts of IL-12 in response to viral stimuli or LPS thereby inducing Th1 T cell responses (Hildner et al., 2008; Hochrein et al., 2001) whereas $CD8\alpha^{-}CD11b^{+}$ cDCs which are able to produce large amounts of IL-6 instead induce Th2 responses (Moser and Murphy, 2000) Furthermore, $CD8\alpha^{+}CD11b^{-}$ cDCs are able to efficiently cross-present antigens via MHC class

I to $CD8^+$ T cells while $CD8\alpha^-CD11b^+$ cDCs fail to perform cross-presentation (Hildner et al., 2008). Of note, in addition to several other subsets in different tissues, like Langerhans cells in the skin or CX3CR1-dependent DCs in the intestine, a subset of lung $CD11b^-CD103^+$ DCs exists which is able to actively migrate into the draining lymph nodes after encountering antigens preferentially inducing Th2 responses (Lambrecht and Hammad, 2009; Merad et al., 2008; Niess et al., 2005).

1.2.1.2 Plasmacytoid dendritic cells

Compared to cDCs, pDCs have been much less well described. They accumulate mainly in blood and lymphoid tissues like the spleen, and are able to enter the lymph nodes through the blood circulation where they migrate to the T cell areas in a CCR7 dependent manner (Seth et al., 2011). pDCs are characterized by their plasma cell like morphology with an excentered nucleus. They display intermediate expression of CD11c, but a high expression of surface molecules like Ly6C, B220, mPDCA-1 and SiglecH but no expression of CD11b, and rather variable expression of CD4 and CD8 (Asselin-Paturel et al., 2005; Blasius et al., 2006a; Blasius et al., 2006b; Zhang et al., 2006). pDCs also can be further distinguished by their expression of CCR9 and CD9. Bone marrow-pDCs highly express CD9 but can be either positive or negative for CCR9 (Hadeiba et al., 2008; Schlitzer et al., 2011; Segura et al., 2009) while pDCs in the periphery downregulate expression of CD9 (Bjorck et al., 2011). Co-stimulatory molecules such as CD80, CD86 and MHC class II are highly upregulated on pDCs upon appropriate stimulation. However, the most striking properties of pDCs are their endosomal expression of TLR7 and 9, and a constitutive high expression of the transcription factor IRF7 under naïve conditions. Therefore, pDCs are able to immediately produce massive amounts of type I IFN in response to viral stimuli (Asselin-Paturel et al., 2005; Izaguirre et al., 2003). Furthermore, this type I IFN production can be enhanced via involvement of the IFNAR (Blasius and Beutler, 2010). Besides type I IFN production, pDCs can also secrete other cytokines like TNFα or IL-12, and are able to prime T cells or recruit T and NK cells to the site of infection by secretion of different chemokines including CCL3 (Krug et al., 2002; Liu et al., 2008; Sapoznikov et al., 2007). Furthermore, there have been

studies indicating an important role for pDCs in cancer immunology (Le Mercier et al., 2013) and in tolerance. For example, auto-immune diseases like psoriasis or systemic lupus erythematosus (SLE) are associated with pDCs and type I IFN produced by these cells, yet the exact mechanisms of action here remain elusive (Nestle et al., 2005; Sisirak et al., 2014).

1.3 IFNβ-producing pDCs

One of the main focuses of this thesis is IFNβ-producing pDCs. Unlike cDCs, where relevant transcription factors and pre-cursors required for subset development, e.g. for cDC1 and cDC2 (Schlitzer et al., 2015b), have been described, barely anything is known about differentiation of pDC subsets. Rather, pDCs are frequently thought to constitute a homogenous population. In this thesis, it will be shown that pDCs are a heterogeneous population and those pDCs that produce IFNβ harbour specific properties. To this end, we have characterized global gene expression profiles of pDCs associated with IFNβ-production. Furthermore, in the work described here I have examined the function of two genes found highly differentially expressed in IFNβ-producing pDCs, namely BATF and PSD-93.

1.4 BATF

BATF is a transcription factor of the basic leucine zipper protein family or AP-1 (activator protein) family. Currently three BATF family members are described: BATF, BATF2 and BATF3, of which BATF3 is probably the best understood. Interestingly, it was shown that BATF and BATF3 have some functional redundancy and that lack of BATF3 can be partially compensated by functions of BATF. Recent publications demonstrated, that BATF forms heterodimers with Jun to interact with transcription factors of the IRF (interferon regulatory factor) family, like IRF4 or IRF8 (Li et al., 2012; Murphy et al., 2013; Tussiwand et al., 2012). These BATF-IRF complexes translocate into the nucleus where they bind to AIC elements (AP-1–IRF composite elements) of respective target genes.

BATF-IRF interactions are thereby able to regulate gene expression in different immune cell types, e.g. DCs, B and T cells (Murphy et al., 2013).

Therefore, transcription factors of the BATF family have pivotal functions in immune cell development and regulation of innate and adaptive immune responses. BATF- or BATF3-deficient mice display defects in development of T follicular helper cells (Tfh) and Th17 cells, while Th1 and Th2 cells develop normally. Furthermore loss of these molecules causes defects in class switch recombination in B cells and in development of $CD8\alpha^+$ cDCs, leading to an almost complete loss of this DC population (Edelson et al., 2010; Ise et al., 2011; Schraml et al., 2009).

Mice deficient for BATF3 that lack $CD8\alpha^+$ cDCs, also lack normal IL-12 production and are therefore highly susceptible to infection by the protozoan parasite *Toxoplasma gondii* (Mashayekhi et al., 2011). Interestingly, mice deficient for BATF are protected in a murine model for the auto-immune disease multiple sclerosis. Furthermore, through collaborative work with other groups, we were able to show that BATF cooperating transcription factor IRF4 appear to function in a similar manner in promote $CD8^+$ T cell responses following LCMV infection. Despite normal initial proliferation of BATF- and IRF4-deficient virus specific $CD8^+$ T cells, loss of IRF4 or BATF resulted in an inability to sustain cytotoxic T cell responses and consequently caused persistence of LCMV in various tissues as indicated by higher viral titres in $BATF^{-/-}$ mice (Grusdat et al., 2014). However, until now there are no descriptions in the literature about the impact of BATF in pDC development or type I IFN production by DCs. Therefore, these questions were investigated as part of this thesis.

1.5 PSD-93

PSD-93 (postsynaptic density 93), also known as DLG2 (discs, large homolog 2) or chapsyn110 (channel-associated protein of synapse-110) is a member of the family of membrane associated guanylate kinases (MAGUK). Proteins in this family have been described to have three tandem PDZ domains (PSD-95/DLG/Zo-1; N-terminal), a central SH (Src homology) domain and a guanylate kinase domain (C-terminal) (Fitzjohn et al., 2006; Zheng et al., 2011) Ten

different splice variants of PSD-93 are known of which only four are predicted to be protein coding. Whether these splice variants have different functions remains to be determined. PSD-93 is described to be enriched in postsynaptic sites where it functions in processes maintaining synaptic networks and transmission (Xu, 2011). At postsynaptic sites it also interacts with its family member PSD-95 forming heterodimers that act as scaffold proteins specifically binding to the NR2A/2B subunits of the NMDA receptor to enable and facilitate assembling and signalling of this receptor (Brenman et al., 1996; Carlisle et al., 2008; Kim et al., 1996). PSD-93 is also thought to act as a scaffold protein in the formation of lipid rafts (Delint-Ramirez et al., 2010). Furthermore, PSD-93 has been shown, to interact with the nitric oxide synthase, potassium-channels (Ogawa et al., 2008), microtubule-associated protein 1 A (Brenman et al., 1998), and is a direct target of the extracellular signal-regulated kinase (ERK) (Guo et al., 2012). Although this protein and its family members have been intensively studied in the field of neuroscience there are no descriptions of PSD-93 in the context of innate or adaptive immunity up to now. PSD-93 appears to be involved in multiple signalling processes, and is also highly differentially expressed in IFNβ-producing pDCs which classifies it as a protein of high interest for our studies. Therefore the role of PSD-93 in IFNβ-producing pDCs was investigated in this thesis.

1.6 *Toxoplasma gondii*

Toxoplasma gondii is an intracellular protozoan parasite belonging to the phylum Apicomplexa. It is of great interest for medical research since at least 30 % of the human population are persistently infected with *T. gondii*. This number is even higher among elderly people and varies between different countries worldwide. Symptoms of infection with *T. gondii* are generally mild and the infection is relatively harmless and largely asymptomatic in healthy individuals. However, in individuals suffering from immune deficiencies Toxoplasmosis can be life threatening. Another high risk group are pregnant women newly infected with the parasite, as *T. gondii* is able cross the blood-placenta barrier frequently leading to deformations or even abortion of the embryo (Joynson and Wreghitt, 2001; McLeod et al., 2012). The outcome of infection with *T. gondii* is highly dependent

on a range of factors including the genotype (strain) of the parasite. In North America and Europe three clonal variants of *T. gondii* are described: type I, II or III strains which are characterised by their different virulence in animal models (Hunter and Sibley, 2012; Sibley, 2009) Type I strains are the most virulent, with a lethal dose as low as one parasite per mouse, whereas type II and type III strains are considered intermediate or even avirulent (with a lethal dose of >1000 parasites per mouse) (Sibley and Boothroyd, 1992). Nevertheless, virulence and the susceptibility to *T. gondii* can differ between different mouse strains and genotypes. Interestingly, humans are mostly infected by type II strains such as *T. gondii* ME49 with intermediate virulence (Kim and Weiss, 2004). Therefore it is important to carefully study the immune response to *T. gondii* infection in order to gain a better understanding of host pathogen interactions, but also to find new potential targets for therapeutic or even vaccination strategies.

1.6.1 Life cycle of *T. gondii*

The life cycle of *T. gondii* is highly complex involving multiple differentiation steps and stages within different hosts (Fig. B). Sexual reproduction via merogony and gametes occurs only within intestinal epithelial cells of cats, the primary hosts of *T. gondii*. Sexual reproduction results in development and shedding of oocysts in the faeces and ultimately release into the environment. Unsporulated oocysts are able to sporulate which results in the conversion of sporoblasts to sporozoites within the oocysts. Sporulated oocysts can contaminate food and water and consequently can be up taken orally by intermediate hosts, e.g. mice. Within the intermediate host, the asexual replication of *T. gondii* takes place. During this process sporozoites are released from the oocysts and develop into tachyzoites which rapidly replicate within host cells and spread throughout various tissues of the body during the acute phase of infection. Tachyzoites then further differentiate into bradyzoites, a metabolically less active and slower replicating stage. Bradyzoites are able to form cysts within muscular and neuronal tissue preferentially in the brain. Tissue cysts predominantly occur in the chronic phase of infection and help the parasite to persist in the host's body since they are relatively protected from host immune responses. Ingestion of cysts, mostly by

cats that are the natural predators of mice, closes the cycle and allows another round of sexual reproduction in the primary host leading again to shedding of oocysts and continuation of the life cycle of *T. gondii*. Of note, even if mice are the preferred intermediate host, all vertebrates can be infected by *T. gondii*. Asexual replication can take place and tissue cysts can persist throughout the whole life of these accidental hosts (e.g. humans), but in general hosts which are not prey for cats are a dead end for the *T. gondii* life cycle (Hunter and Sibley, 2012; Yarovinsky, 2014).

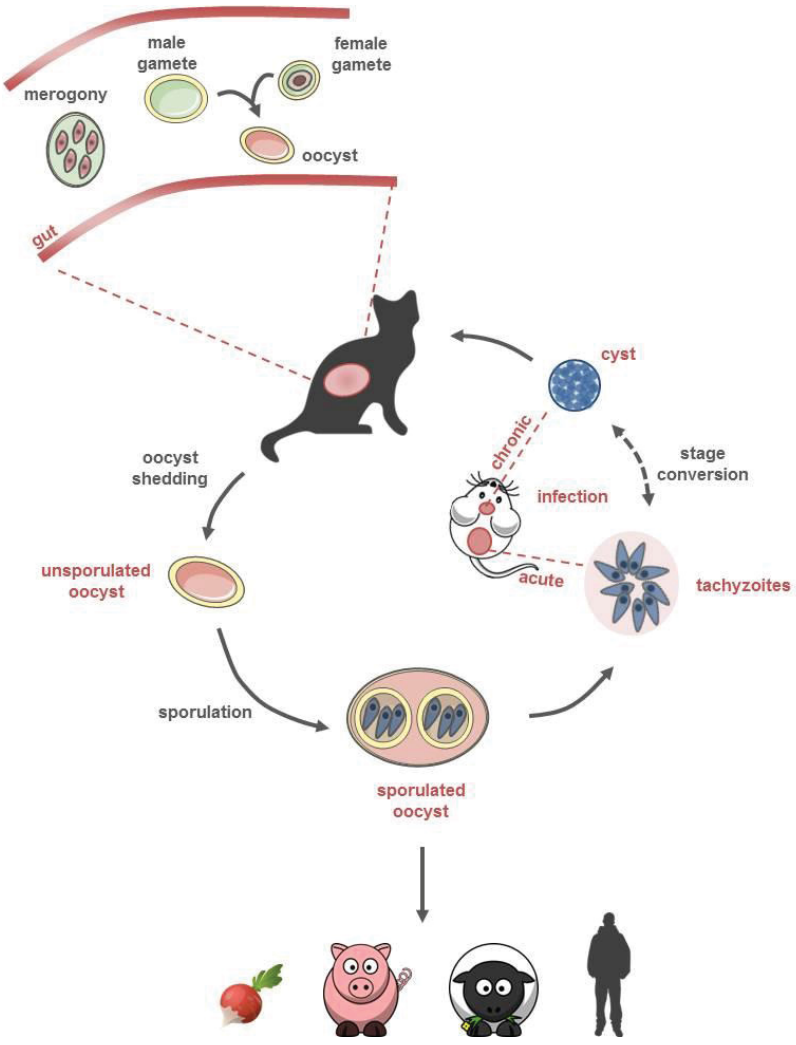

Fig. B Life cycle of *Toxoplasma gondii* (for illustration the servier medical art and pixabay databases were used; after Hunter and Sibley, 2012).

1.6.2 Immune defence against *T. gondii*

The immune response to *T. gondii* infection is highly complex and involves an interplay of various components of the innate and the adaptive immune system. Following infection, early secretion of the pro-inflammatory cytokine IL-12 mostly by DCs and monocytes (Bierly et al., 2008; Mashayekhi et al., 2011; Pepper et al., 2008; Robben et al., 2004) is essential for stimulation and activation of NK and $CD4^+$ and $CD8^+$ T cells which respond with production of IFNγ (Gazzinelli et al., 1993; Hunter and Sibley, 2012; Hunter et al., 1994; Johnson, 1992; Khan et al., 1994) inducing a strong Th1 response (Denkers and Gazzinelli, 1998). Of note, mice deficient for IFNγ or the IFNγ receptor rapidly succumb to *T. gondii* infection (Deckert-Schluter et al., 1996) due to a failure in inducing Th1 responses and downstream anti-parasitic effects. Another important cytokine during the immune response to *T. gondii* is TNFα, which is secreted by activated monocytes upon infection (Daubener et al., 1996). In line with this, MyD88 was found to play an important role in host resistance to *T. gondii* infection (Scanga et al., 2002). MyD88 is an adaptor protein essentially required for function of several TLRs and cytokine production. Interestingly, deletion of individual TLRs barely has an effect on outcome of infection, whereas mice deficient in multiple TLRs, e.g. triple knock-outs for TLR3, 7 and 9 or those carrying a point mutation in UNC93B1 are highly susceptible to *T. gondii* infection (Gazzinelli and Denkers, 2006; Melo et al., 2010; Pifer et al., 2011). Furthermore it was shown that TLR11 and 12 are very important for parasite recognition by DCs. TLR11 and 12 are able to recognize a profilin-like molecule on the parasite forming a heterodimer complex. This leads to subsequent activation of IRF8 and production of IL-12 by DCs, also suggesting an important role for IRF8 dependent $CD8\alpha^+$ cDCs in host resistance to *T. gondii* (Raetz et al., 2013; Yarovinsky, 2014; Yarovinsky et al., 2005). $CD8\alpha^+$ cDCs are dependent on the transcription factor BATF3, and it was shown that mice deficient for BATF3 fail to induce adequate IL-12 responses to control the infection with *T.* gondii (Mashayekhi et al., 2011). This data further strengthens the assumption of a role for $CD8\alpha^+$ cDCs in host resistance to *T. gondii* infection. However, possibly the most important cytokine in host protection during *T. gondii* infection is IFNγ, which initiates mechanisms that lead to clearance of the parasite. One of these mechanisms is the production of reactive

oxygen species (ROS) and nitrogen intermediates (e.g. nitrogen monoxide) upon STAT1 signalling by IFNγ-activated phagocytes (monocytes and macrophages) (Adams et al., 1990). This mechanism was nicely described in mice deficient for the inducible nitric oxide synthase (iNOS) showing that there is an iNOS independent but IFNγ dependent mechanism in host resistance during the acute phase of *T. gondii* infection (Scharton-Kersten, 1997). Hereby, IRGs (immunity related Guanosine Triphosphatases (GTPases)) can be directly induced by IFNγ-signalling. It was shown that these GTPases e.g. GBPs (guanosine nucleotide-binding proteins) are immediately recruited to the parasitophorous vacuole surrounding *T. gondii*. This, on the one hand, leads to inhibition of parasite growth e.g. via activation of autophagy protein 5 (ATG5) (Howard et al., 2011; Yamamoto et al., 2012) and on the other hand to rupture of the vacuole leading to release of the parasite into the cytosol and its digestion (Degrandi et al., 2007; Degrandi et al., 2013). The exact mechanisms of GBP-parasite interactions and GBP-signalling as well as specific interactions between innate and adaptive immune system, e.g. *T. gondii*-antigen-presentation by DCs in order to prime T cells, unfortunately still are poorly understood and are the focus of current research.

While the importance of IL-12 production by DCs and monocytes in *T. gondii* infection is clear, the role of type I IFN produced by these cells during *T. gondii* infection remains largely unknown. In 1989 Schmitz et al. demonstrated that treatment of human macrophages with rIFNβ *in vitro* results in inhibition of *T. gondii* growth (Schmitz et al., 1989). This later was confirmed by *in vivo* experiments in mouse models (Orellana et al., 1991). Recently it was shown that inflammatory monocytes are the main source of IFNβ, at least in mesenteric lymph nodes, after infection with *T. gondii* (Han et al., 2014). IFNβ production was dependent on phagocytosis of the parasite and subsequent TLR and MyD88 signalling. Furthermore, mice lacking the type I IFN receptor were shown to have higher parasite levels than wildtype mice (Han et al., 2014). Although this publication by Han et al. did investigate the importance of IFN-producing cells but not directly the impact of the produced type I IFN itself during infection with *T. gondii* this work strengthens our hypothesis that in addition to IL-12 and IFNγ,

IFNα as well as IFNβ might play an important role in host protection against this intracellular parasite.

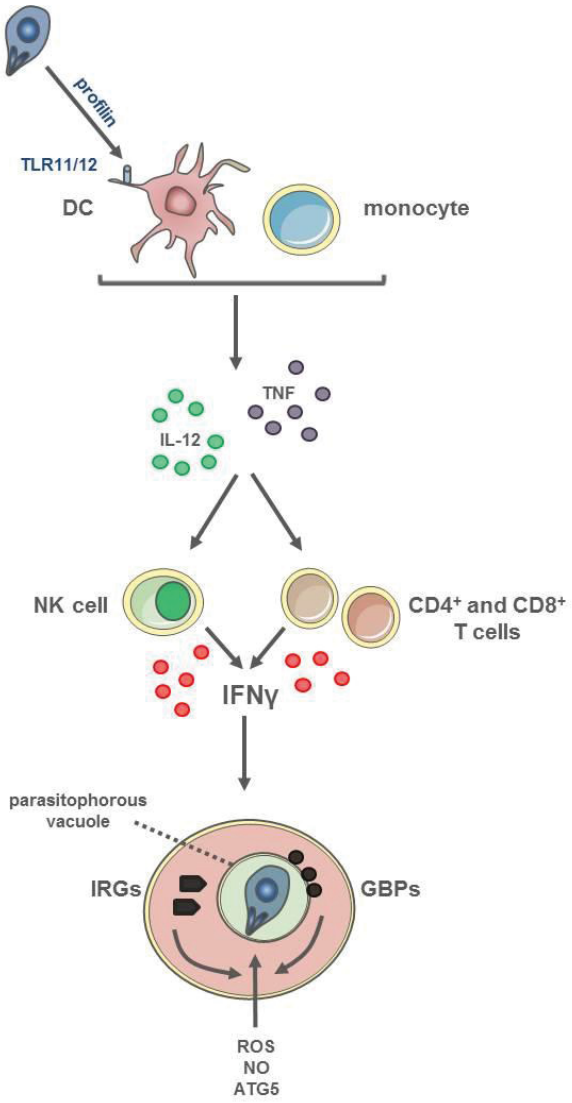

Fig. C Immune response to *Toxoplasma gondii* (for illustration the servier medical art database was used; after Hunter and Sibley, 2012).

1.7 Aims of the study

Type I IFN are crucial in initiating host immune responses during viral, bacterial or parasitic infection and even play an important role in auto-immune diseases. Analysis of IFNβ expression and its producing cells has traditionally been quite difficult due to low levels of this cytokine and lack of robust staining methods e.g.

for FACS analysis of the endogenous protein. Now, using an IFNβ-reporter mouse model (IFNβ$^{mob/mob}$ mouse) we are able to track IFNβ producing cells. Therefore the primary aim of this study was to characterize IFNβ-producing cells, especially pDCs, in the spleen using this mouse. Another aim was to characterize genes that might be involved in IFNβ production in these cells and describe their function in pDCs. This knowledge could be of impact in designing future therapeutic strategies e.g. to fight infection of block auto-immune diseases.

Furthermore, type I IFN are important initiators of immune responses and their impact in viral and bacterial infections has been extensively studied. However, the importance of these factors in parasitic infections is poorly understood. Therefore, another aim of this work was to investigate the impact of type I interferon during infection with the protozoan parasite *Toxoplasma gondii*.

2. Materials and Methods

2.1 Materials

2.1.1 Chemicals

Chemicals	Manufacturer
Acetone	Merck, Darmstadt
Aqua ad injectabilia	Braun, Melsungen
Avidin/Biotin blocking solution	Vector Laboratories, Burlingame, USA
β-Mercaptoethanol (β-ME)	Invitrogen, Karlsruhe
Bovine Serum Albumin (BSA)	Sigma-Aldrich, Taufkirchen
Chloroform	Roth, Karlsruhe
DEPC	Sigma-Aldrich, Taufkirchen
desoxynucleotides	Roche, Mannheim
distilled water	Invitrogen, Karlsruhe
DMEM medium VLE	Biochrom, Berlin
Dimethylsulfoxide (DMSO)	Sigma-Aldrich, Taufkirchen
donkey normal serum	Jackson Laboratories, Suffolk, UK
DOTAP	Roche, Mannheim
EDTA	Sigma-Aldrich, Taufkirchen
EGTA	Sigma-Aldrich, Taufkirchen
Erythrocyte lysis buffer	Morphisto, Frankfurt am Main

ethanol	Merck, Darmstadt
FACS Clean solution	BD Biosciences, Heidelberg
FACS Flow solution	BD Biosciences, Heidelberg
FACS Rinse solution	BD Biosciences, Heidelberg
Fetal Calf Serum (FCS)	PAN, Aidenbach
Ficoll Paque™ Plus	GE Healthcare, Freiburg
goat normal serum	DakoCytomation, Hamburg
HBSS	Gibco, Paisly
hydrochloric acid	Roth, Karlsruhe
hydrogen peroxide, 30 %	Merck, Darmstadt
IMDM	Lonza, Verviers
L-glutamine	Biochrom, Berlin
methanol	Merck, Darmstadt
mouse normal serum	Jackson Immuno Research, Suffolk, UK
Oligo-(dT)-Primer	Fermentas, St.Leon-Roth
paraformaldehyde	Merck, Darmstadt
PBS chemical powder	Biochrom, Berlin
PBS, 0,5 l, sterile	Invitrogen, Karlsruhe
PBS, 10x	Gibco, Paisly
PCR Nukleotid-Mix (dNTPs)	Fermentas, St.Leon-Roth
penicillin/streptomycin	Biochrom, Berlin
Percoll	GE Healthcare, Freiburg

potassium chloride	Sigma-Aldrich, Taufkirchen
rat normal serum	Jackson Immuno Research, Suffolk, UK
RNase Zap	Applied Biosystems/Ambion, Darmstad
RPMI 1640 VLE	Biochrom, Berlin
saline solution, physiologica	DeltaSelect, Dreireich
sodium azide	Merck, Darmstadt
sodium hydroxide	Merck, Darmstadt
sucrose	Serva, Heidelberg
TissueTek™ O.C.T. Compound™	Sakura, Staufen
Triton X-100	Biochrom, Berlin
Trypan blue	Sigma-Aldrich, Taufkirchen
Trypsin/EDTA	Biochrom, Berlin
Vectashield mounting medium with DAPI	Vector Laboratories, Burlingame, USA

2.1.2 Enzymes

Enzyme	Manufacturer
collagenase type VIII	Sigma-Aldrich, Taufkirchen
DNAse I	Roche, Mannheim
SuperScript III	Roche, Mannheim
Trypsin/EDTA, 0.25 %	Gibco, Paisly

2.1.3 Anaesthetics

Anaesthetic	Manufacturer
Isofluran	Baxter, Munich
Narketan, 100 mg/ml	Vectoquinol GmbH, Ravensburg
Xylapan, 20 mg/ml	Chassot, GmBH, Ravensburg

2.1.4 Kits and other reagents

Kits/Reagents	Manufacturer
BD AccuDrop Beads	BD Biosciences, Heidelberg
BD Compensation Beads	BD Biosciences, Heidelberg
DakoCytomation Pen	DakoCytomation, Hamburg
Fluka RNA isolation kit	Sigma Aldrich, Taufkirchen
Hemacolor staining kit	Merck, Darmstadt
IFNα ELISA	eBioscience
IFNβ ELISA	Biolegend
LS MACS columns and magnets	Miltenyi, Bergisch-Gladbach
Miltenyi anti-biotin microbeads	Miltenyi, Bergisch-Gladbach
mirVana miRNA isolation kit	Applied Biosystems/Ambion, Darmstadt
NK cell isolation kit II	Miltenyi, Bergisch-Gladbach
Reverse Transcription Kit	Invitrogen, Karlsruhe
TissueTek	Sakura Finetek, Staufen
TSA FITC/Biotin System	Perkin Elmer, Rodgau

2.1.5 TLR agonists

TLR agonist	Manufacturer
CpG ODN 1668	TIB MolBiol, Berlin
CpG ODN 2216	TIB MolBiol, Berlin
LPS	List Biologial Laboratories, Campbell, CA
Poly(I:C)	GE Healthcare, Freiburg

2.1.6 Antibodies

Antigen	Clone	Fluorochrome	Manufacturer
donkey anti rabbit	polyclonal	biotinylated	Jackson Immuno Research
B220	Ra3-6B2	APC, FITC, PerCP	BD Biosciences
CD3ε	145-2C11	PercP	BD Biosciences
CD8α	53-6.7	APC, APC-Cy7	BD Biosciences
CD9	MZ3	biotinylated, APC	BioLegend
CD11b	M1/70	APC, APC-Cy7	BD Biosciences
CD11c	HL3	APC, APC-Cy7	BD Biosciences
CD16/CD32	2.4G2	unconjugated	BioLegend
CD19	1D3	PerCP	BD Biosciences
CD69	H1.2F3	PE	eBioscience
CD86	GL1	biotinylated, PE-Cy7	eBioschience
CD103	2E7	APC	Biolegend

CCR9	eBioCW-1.2	PE-Cy7	eBioscience
GFP	polyclonal	Biotinylated	Abcam
GR-1	RB6-8C5	biotinylated	BD Biosciences
IgG2A	C1.18.4	unconjugated	BioXCell
IL-12p40	C17.8	PE	BD Biosciences
IFNγ	4S.B4	PE	BD Biosciences
Ly6C	AL-21	APC, biotinylated	BD Biosciences
MHCII (I-a/I-b)	M5/114	APC, biotinylated, FITC, PE	BD Biosciences
mPDCA-1	JF05-1C2.4.1	biotinylated, PE	Miltenyi Biotec
NK1.1	PK136	APC, biotinylated, FITC	BD Biosciences
NK1.1	PK136	unconjugated	BioXCell
NKp46	29A1.4	FITC	eBioscience
SA-APC	-	APC	Invitrogen
SA-APC-Cy7	-	APC-Cy7	BD Biosciences
SA-Cy3	-	Cy3	Invitrogen
SA-FITC	-	FTC	Biolegend
SA-PE-Cy7	-	PE-Cy7	BD Biosciences
SiglecH	55.3D3	APC, biotinylated	Miltenyi Biotec
TNFα	MP6-XT22	PE	eBioscience

2.1.7 Oligonucleotides

Gene	Primer sequence (5'-3')	Probe
β-Actin	TGA CAG GAT GCA GAA GGA GA CGC TCA GGA GGA GCA ATG	106
BATF	AGA AAG CCG ACA CCC TTC A CGG AGA GCT GCG TTC TGT	85
CCL3	TGC CCT TGC TGT TCT TCT CT GTG GAA TCT TCC GGC TGT AG	40
CCL5	TGC AGA GGA CTC TGA GAC AGC GAG TGG TGT CCG AGC CAT A	110
CD86	GAA GCC GAA TCA GCC TAG C CAG CGT TAC TAT CCC GCT CT	107
CCR7	CTC CTT GTC ATT TTC CAG GTG TGG TAT TCT CGC CGA TGT AGT	29
CCR9	TTC CCC TCC TGA AGC TGA T CAT GCC AGG AAT AAG GCT TG	105
mGBP1	CAG ACT CCT GGA AAG GGA CTC CTT GGA CCT GGA ACA TTC ACT GAC	41
mGPB2	TGA GTA CCT GGA ACA TTC ACT GAC AGT CGC GGC TCA TTA AAG C	17
mGPB5	TCA CTG AAG CTG AAG CAA GG GCG TCA AAA ACA AAG CAT TTC	48
IFNα	TCA AGC CAT CCT TGT GCT AA GTC TTT TGA TGT GAA GAG GTT CAA	3
IFNβ	CAG GCA ACC TTT AAG CAT CAG CCT TTG ACC TTT CAA ATG CAG	95
IFNγ	ATC TGG AGG AAC TGG CAA A TTC AAG ACT TCA AAG AGT CTG AGG	21
IL-12p40	TCT TCA AAG GCT TCA TCT GCA A ACA GCA CCA GCT TCT TCA TCA	-
IL-28b	TCA GCC CTG ACC ACC ATC CTG TGG CCT GAA GCT GTG TA	33
IRF7	AGC GTG AGG GTG TGT CCT TCT TCG TAG AGA CTG TTG GTG CT	56
ISG56	TCT AAA CAG GGC CTT GCA G GCA GAG CCC TTT TTG ATA ATG GT	6
MHCII (H2-Ab1)	GTG GTG CTG ATG GTG CTG CCA TGA ACT GGT ACA CGA AAT G	26
PSD-93	ATT TGA AGA AAT TAC ATT GGA GAG G TCC AAT GTG GGG ATT ATC TGT	63
STAT1	AAA TGT GAA GGA TCA AGT CAT GTG CAT CTT GTA ATT CTT CTA GGG TCT TGA	15
TLR3	GAT ACA GGG ATT GCA CCC ATA TCC CCC AAA GGA GTA CAT TAG A	26
TLR9	GAG AAT CCT CCA TCT CCC AAC CCA GAG TCT CAG CCA GCA C	79

TNFα	TCT TCT CAT TCC TGC TTG TGG GGT CTG GGC CAT AGA ACT GA	49

2.1.8 Cell lines, media and buffers

2.1.8.1 Media

Cells	Concentration	Components
BMDMs		RPMI 1640 VLE
	10 %	FCS
	0.1 %	β-mercaptoethanol
	10 %	M-CSF
Flt3-L DCs		RPMI 1640 VLE
	10 %	FCS
	0.1 %	β-mercaptoethanol
	5 %	Flt3-L
HFF		IMDM
	10 %	FCS
HEK-293T cells		DMEM
Naïve NK cells (cultured after MACS depletion of primary splenocytes)		RPMI 1640 VLE
	10 %	FCS
	0.1 %	β-mercaptoethanol
	1 %	Penicillin/Streptomycin

2.1.8.2 Buffers

Buffer	Components	
Collagenase VIII	100 mg/ml	in PBS
DNase I	3000 U/ml	in PBS
FACS buffer	1x	PBS
	2 %	FCS

	2 mM	EDTA
MACS buffer	1x	PBS
	0,5 %	BSA
	2 mM	EDTA
PFA fixation buffer, pH 7.4	1x	PBS
	4 %	Paraformaldehyde
	2 mM	$MgCl_2$
	1.25 mM	EGTA
Stop buffer	1x	PBS
	10 mM	EDTA
Tissue digest buffer	93 %	PBS
	6 %	Collagenase type VIII solution
	1 %	DNase I solution
TNB	0.1 mM	Tris-HCl, pH 7.5
	0.15 mM	NaCl
	0.5 %	blocking reagent from TSA kit

2.1.9 Equipment

Device	Manufacturer
Axiovert 11 Mikroskop	Zeiss
Biofuge A (centrifuge)	Heraeus
Biological safety cabinet	Kendro
Confocal microscope (LSM510Meta)	Zeiss
Cryotom (HM 650)	Thermo Fisher Scientific
Dewar	Nalgene Laboratories
Digital camera: Powershot G2	Canon

FACS Aria II	BD Biosciences
FACS Canto II	BD Biosciences
Heat block Techne DB3	Biostep
Heidolph Polymax 1040 (shaker)	Heidolph Polymax 1040
iCycler iQ5 (qRT-PCR)	Bio-Rad
Millipore Elix advantage 3	Millipore
Multistep-Dispenser Handystep	Brand
NanoDrop 1000 (photometer)	Peqlab
Neubauer chamber	LO-Laboroptik
pH Meter MP 225	Mettler-Toledo
Photometer: TECAN Sunrise	Tecan
Rotana 46 RC (centrifuge)	Hettich
Scale Precisa 600c	Oehmen Labortechnik
Single- and multichannel pipette	Thermo Fisher Scientific
Surgery tools	Fine Science Tools
TE2000 (microskope)	Nikon
Thermocycler T1	Biometra
Tissue culture incubator (Heraeus Heracell 20)	Heraeus
Ultra Turrax T25	IKA
Vortex shaker VVR	VWR
Water bath	Köttermann Labortechnik

2.1.10 Animal experiments

Mice were kept under pathogen-free conditions in the animal facility of the University of Düsseldorf. All experiments in this thesis were done in accordance with the guidelines of the protection of animals act § 8 and approved by the government of North-Rhine Westphalia.

2.1.10.1 Mice

Mouse strain	Description
C57BL/6	Wildtype mouse
IFNAR1$^{-/-}$	*Ifnar1* knockout mouse (Hwang et al., 1995)
IFNβ$^{-/-}$	*Ifnb* knockout mouse (Erlandsson et al., 1998)
IFNβ$^{mob/mob}$	IFNβ reporter mouse (Scheu et al., 2008)
IFNAR1-/-xIFNβ$^{mob/mob}$	*Ifnar1* deficient IFNβ reporter mouse
BATF$^{-/-}$	*Batf* knockout mouse (Schraml et al., 2009)
BATF$^{-/-}$xIFNβ$^{mob/mob}$	*Batf* deficient IFNβ reporter mouse (generated in our lab)
PSD-93$^{-/-}$	*Psd-93* knockout mouse (McGee et al., 2001)
PSD-93$^{-/-}$xIFNβ$^{mob/mob}$	*Psd-93* IFNβ reporter mouse (generated in our lab)

2.2 Methods

2.2.1 Cell culture

Cell lines were cultured in tissue-culture-treated flasks. Primary cells were cultured in untreated petri dishes. All cell lines and primary cells were cultured at 37 °C and 10 % CO_2 in a humidified incubator.

Cell lines were passaged once a week or when necessary. Therefore adherent cells were rinsed with PBS and incubated with Trypsin/EDTA for 1-5 min at 37 °C. Single cell solutions were diluted in a 1:2 or 1:4 ratio and cells were seeded into new tissue culture flasks.

2.2.1.1 Isolation of murine bone marrow

Mice of an age of 8-14 weeks were sacrificed, hind legs removed and femurs and tibias were dissected. Bones were disinfected in 70 % EtOH followed by a washing step in cold PBS. Subsequently bones were opened on both sides and bone marrow was flushed out with RPMI using a 20 ml syringe with a 23 G needle. After carefully pipetting it up and down the bone marrow single cell solution was transferred into a 50 ml tube and centrifuged for 5 min at 1200 rpm at RT. Supernatant was aspirated and the cell pellet was resuspended in 3 ml erythrocyte lysis buffer and incubated for 3 min at RT. The reaction was stopped by adding 10 ml RPMI media, followed by a second centrifugation for 5 min at 1200 rpm at RT. Afterwards cells were seeded in petri dishes containing media and responding growth factors and differentiated into myeloid cells.

2.2.1.2 Differentiation of BMDMs

To differentiate BM cells into BMDMs 1.5-2x10^6 cells/10 ml were seeded into a petri dish containing RPMI media with M-CSF. Medium was supplemented with additional 5 ml after 3 days and after 6 days cell were fully differentiated. Fully differentiated cells were either left untreated or stimulated with TLR agonists or pathogens (see 2.2.6).

2.2.1.3 Differentiation of Flt3-L-derived DCs

To differentiate BM cells into pDCs or cDCs 20x10^6 cells/10 ml were seeded into a petri dish containing RPMI media with Flt3-L. After 5 days 5 ml of the media were removed and replaced by fresh Flt3-L-containing media and after 7 days cell were fully differentiated. Fully differentiated cells were either left untreated or stimulated with TLR agonists or pathogens (see 2.2.6).

2.2.1.4 *In vitro* passage of *T. gondii*

Tachyzoites from the *T. gondii* strain ME49 were maintained by serial passage in confluent monolayers of HFF cells as host cells. After infection of cells, parasites were harvested from culture supernatant and purified from host cell debris by differential centrifugation (5 min, 50 × g; 15 min, 500 × g) 3–4 d after infection. Parasites were resuspended in medium, counted, and immediately used for inoculation of the host cells or infection of BMDMs or Flt3-L-DCs (see 2.2.6).

2.2.1.5 Stimulation and infection of *in vitro* differentiated cells

Stimulation of *in vitro* differentiated BMDMs and DCs with TLR agonists, parasites or viruses was done as shown in the tables below. Stimuli were pipetted directly into the cell supernatant, gently mixed and left on for 6 h, 12 h or 24 h, as indicated in the single experiments.

Agonist	Responding PRR	Concentration
CpG 1668/B	TLR9	6 µg/ml
CpG 2216/A	TLR9	6 µg/ml
Poly(I:C)	TLR3, MDA5	50 µg/ml

For endosomal application CpG 1668/B was complexed to DOTAP as follows:

- 6 µg CpG 1668/B *ad* 100 µl with HBSS or PBS
- 20 µl DOTAP *ad* 100 µl with HBSS or PBS
- both solutions were mixed and incubated for 15 min at RT
- 200 µl were added into the cell culture supernatant.

Virus	Dosage
MCMV C3X	MOI 1

Parasite	Parasites per cell
Toxoplasma gondii ME49 (viable)	15
Toxoplasma gondii ME49 (heat killed)	15

2.2.1.6 Immunofluorescence staining of Flt3-L-derived DCs

For immunofluorescence staining BM-derived FLt3-L differentiated DCs were harvested, counted and seeded into 24-well plates ($1x10^6$ cells/well) containing gelatin coated cover slips. Cells were either left untreated or stimulated with CpG 1668/B complexed to DOTAP (see 2.2.6). After stimulation media was aspirated, cells were washed twice with PBS and fixed with 4 % PFA for 15 min at RT. PFA was aspirated, cells washed twice with PBS and permeabilized using 0.2 % Triton-X for 10-15 min at RT. Following this cells were washed again and covered with a blocking solution containing sera (n-goat, n-donkey, n-rat, n-mouse) and FC block (αCD16/CD32) to block unspecific binding sites for at least 30 min at RT. After another washing round cells were stained with primary and secondary antibodies against mPDCA-1, YFP, BATF or PSD-93 as indicated in the specific experiments. Stained cells then were covered in Vectashield containing DAPI, cover slips were placed onto slides and frozen at -20 °C till being analysed on a confocal microscope.

2.2.2 *In vivo* experimental procedures

2.2.2.1. *In vivo* stimulation with TLR agonists

6-12 week old mice were i.v. injected with either CpG 1668/B or CpG 2216/A complexed to DOTAP. CpG-DOTAP mixture was prepared as follows:

- 10 µg CpG *ad* 100 µl HBSS
- 30 µl DOTAP *ad* 100 µl HBSS
- combined, well mixed reagents were incubated for 15 min at RT
- 200 µl CpG/DOTAP were injected per mouse.

Prior to injection mice were illuminated with a heat lamp to dilate the tail vein. The tail was disinfected and CpG/COTAP was injected using a sterile 30 G needle.

2.2.2.2 Infection with MCMV

6-8 weeks old mice were i.p. injected with $1x10^5$, $2x10^5$ or $1x10^6$ PFU of MCMV C3X. Virus was kindly provided by Dr. Albert Zimmermann, Institute for Virology, Heinrich Heine University Düsseldorf.

2.2.2.3 Infection with *Toxoplasma* gondii

6-10 weeks old mice were co-housed prior infection starting at 4 weeks of age. Mice then were i.p. infected with either 20 cysts or 40 cysts of *T. gondii* ME49 as indicated in the specific experiments.

For i.p. infection of *T. gondii* ME49 CD1 mice were sacrificed and their cyst-containing brains were mashed up using different needles starting with 18 G to 25 G. Brain suspensions then were resuspended in 5 ml of sterile PBS, underplayed with 10 ml Ficoll and centrifuged at 2500 rpm for 25 min at RT. Following this, the supernatant was discarded, the cyst-containing pellet was washed with PBS and resuspended in 500 µl of PBS. Cysts were counted and the required amount of cysts was lysed using Trypsin/EDTA. Lysis was stopped by adding FCS and cysts were washed with PBS. For maintaining *T. gondii* ME49 CD1 mice were i.p. injected with 20 cysts and for experiments mice were i.p. injected with 20 or 40 cysts.

2.2.2.4 Harvesting of murine tissue

For analysis of blood or serum mice were bled from the retro-orbital plexus or the submandibular (facial) vein. After cervical dislocation different organs like spleen, liver, lung, mesenteric LNs, peripheral LNs or cervical LNs were harvested.

For serum preparation blood samples were centrifuged at maximum speed for 20 min at 4 °C. Clear supernatant was transferred into a new tube and centrifuged a second time at maximum speed for 20 min at 4 °C. The clear serum then was frozen at -20 °C till further analysis

For preparation of RNA or DNA samples were snap frozen in liquid nitrogen and stored at -80 °C till further processing.

For histology samples were carefully embedded in TissueTek-containing cryomolds, frozen on dry ice and stored at -80 °C till further processing or in case of YFP-staining tissue samples were processed as described in 2.2.3.6.

For FACS analysis organs were transferred into 6-well plates containing tissue digest buffer (containing DNase and collagenase VIII), carefully disrupted using tweezers and digested at 37 °C for 30 min. Afterwards the digest was stopped by adding 3-5 ml of Stop buffer. Cell suspensions were pipetted up and down several times, then transferred into a 50 ml tube over a 40 or 100 µm cell strainer and centrifuged at 1200 rpm for 5 min at 4 °C. Cell pellets then were prepared as described in 2.2.2.5-8 and 2.2.3.1-4.

2.2.2.5 Preparation of spleen and LNs for FACS analysis

For FACS analysis of spleen and LNs, cell suspensions were prepared as described in 2.2.2.4. Following this erythrocytes were lysed by adding 3 ml of erythrocyte lysis buffer to each sample for 3 min at RT. Lysis was stopped by adding 10 ml of FACS buffer and samples were centrifuged at 1200 rpm for 5 min at 4 °C. Supernatant was discarded and cell pellet was resuspended in 1 ml (for LNs) or 10 ml (for spleen) of FACS buffer and cells were counted. Samples were aliquoted into FACS tubes and stained as described in 2.2.3.1 and 2.2.3.2.

2.2.2.6 Preparation of liver und lung for FACS analysis

For FACS analysis of liver and lung, cell suspensions were prepared as described in 2.2.2.4. Following this cell pellets were resuspended in 30 % Percoll, underlayed with 70 % Percoll and centrifuged at 2130 rpm for 25 min at RT with no break. Cell debris in the very top layer was aspirated and immune cells from the middle layer were carefully collected using a 1 ml pipette and transferred into a new 50 ml tube. Collected immune cells were washed with 50 ml PBS, centrifuged at 1800 rpm for 15 min at 4 °C, supernatant was discarded and the washing step repeated. Afterwards cell pellets were resuspended in FACS buffer, cells counted, aliquoted into FACS tubes and stained as described in 2.2.3.1 and 2.2.3.2.

2.2.2.7 Preparation of primary cell cultures from different tissues for analysis of IFNγ, IL-12p40 and TNFα production after infection with *T. gondii*

For preparation of primary cell cultures from liver, lung, spleen, LNs and peritoneal lavage mice were dissected under sterile conditions within the biological safety cabinet. Liver, lung, spleen and LNs were prepared as described in 2.2.2.4. For the peritoneal lavage mice were narcotized, i.p. injected with 20 ml of sterile PBS and gently agitated. PBS, now containing peritoneal cells, was removed from the peritoneum and transferred into a 50 ml tube over a 100 µm cell strainer. Peritoneum was rinsed a second time with 5 ml PBS which was then added on into the 50 ml tube. Cell suspension was centrifuged at 1200 rpm for 5 min at 4 °C. Cells from all samples (liver, lung, spleen, LNs, peritoneal lavage) were counted, seeded into 96-well plates and rested overnight. After this, cells were either left untreated, stimulated with PMA/Ionomycin for 4 h, with TLA plus rIL-12 for 24 h and with LPS or TLA for 24 h. At the end of stimulation cells were collected and stained for FACS analysis as described in 2.2.3.1 and 2.2.3.2.

2.2.2.8 MACS separation of splenic NK cells

For separation of NK cells naïve spleens from C57BL/6 or IFNAR1$^{-/-}$ mice were harvested under sterile conditions and prepared as described in 2.2.2.4 and 2.2.2.5. Cells were resuspended in MACS buffer, counted, stained for MACS depletion following the manufacturer's description (NK cell isolation kit II, Miltenyi Biotec) and purified using LS columns. Purified NK cells were seeded into 6-well plates and rested for at least 6 h before being treated with either stimulated or unstimulated Flt3-L-derived BMDCs or rIFNβ overnight or left untreated.

2.2.3 Immunological methods

2.2.3.1 Extracellular FACS staining

Cell suspensions were centrifuged at 1200 rpm for 5 min at 4 °C and supernatant was aspirated. 25 µl of FC block solution (FACS buffer containing 1:100 Ab dilution of αCD16/CD32) was added to each sample to block unspecific binding sites, mixed well and incubated for 10 min at 4 °C. Subsequently 25 µl of primary antibody cocktail (Ab dilution 1:100) was added to the samples, mixed well and incubated for another 10 min at 4 °C. After this samples were washed by adding 2-3 ml of FACS buffer and centrifuged at 1200 rpm for 5 min at 4 °C. Supernatant was discarded and, if necessary, 50 µl of secondary antibody cocktail (Ab dilution 1:300) was added to the samples, mixed well and incubated for 10 min at 4 °C. After incubation cells were washed with 2-3 ml of FACS buffer, centrifuged at 1200 rpm for 5 min at 4 °C and supernatant was discarded. Samples then were resuspended in 100 µ of FACS buffer containing DAPI (dilution 1:200) to discriminate for living and dead cells and analysed on a FACS Aria II or FACS Canto II or further processed for an intracellular staining as described in 2.2.3.2.

2.2.3.2 Intracellular FACS staining

In case of primary cell cultures a protein transport inhibitor (Golgi Stop) was added to the cell culture supernatant 4-6 h prior harvesting, for staining of secreted cytokines like IFNγ or IL-12. For intracellular staining of cells, samples

were prepared as described in 2.2.2.4 - 2.2.3.1 prior fixation with 4 % PFA for 10 min at 37 °C. Tubes then where chilled on ice for a minute, centrifuged at 1200 rpm for 5 min at 4 °C and supernatant was discarded. For permeabilization cells were resuspended in 90 % ice cold methanol and incubated on ice for 30 min. Methanol was washed off by adding FACS buffer, samples were centrifuged at 1200 rpm for 5 min at 4 °C, supernatant was discarded and cells were stained with 100 µl of diluted antibody for 1 h at RT. Primary antibody was washed off by centrifugation, cell pellet was resuspended in fluorochrome-conjugated secondary antibody and incubated for 30 min at RT. Subsequently, secondary antibody was washed off and cell pellet was resuspended in 100 µl of FACS buffer and analysed on a FACS Canto II.

2.2.3.3 FACS cell sorting

For cell sorting organs of stimulated or unstimulated mice were harvested and prepared as described in 2.2.2.4 and 2.2.2.5. Non B- and T cells were enriched and purified using a MACS depletion system directed against B and T cells, following the manufacturer's instructions. Cells then were stained as described in 2.2.3.1, resuspended in 1 ml of FACS buffer per $2x10^6$ cells and populations were separated on a FACS Aria II. For further analysis or processing separated cells were collected in FCS coated tubes and stored on ice.

2.2.3.4 Preparation of cytospins

FACS sorted pDCs were washed with PBS by centrifugation at 1200 rpm for 5 min at 4 °C and supernatant was discarded. Cells were resuspended in 200 - 400 µl PBS and centrifuged onto slides using a cytospin centrifuge (Cellspin II, Tharmac) at 1500 rpm for 5 min at RT. After preparations were dry, cells were stained with an eosin-G/azur-B staining using a fast-stain kit (Hemacolor, Merck) following the manufacturer's instructions. Stained cells were analysed on a microscope and pictures were analysed and edited using Adobe Photoshop CS1.

2.2.3.5 ELISA

Serum and organ ELISA were done as sandwich-ELISA for IFNα, IFNβ, IFNγ and IL-12p40 following the manufacturer's instructions. All samples were measured as triplicates for IFNγ and Il-12p40 or duplicates for IFNα and IFNβ and analysed at 450 nm with an ELISA reader. Protein concentrations were calculated based on the responding standard curves.

2.2.3.6 Histology and Immunohistochemistry

For staining of IFNβ/YFP spleens were fixed in PLP solution (containing 4 % PFA) at 4°C overnight. Subsequently, spleens were immersed sequentially in 10 %, 20 % and 30 % sucrose at RT. Upon this procedure organs were placed into cryomolds containing TissueTek and carefully frozen on dry ice. Organs were stored at -80 °C till further processing.

Frozen organs were cut into 8 µm thick sections using a cryotome (ThermoFisher Scientific) and fixed to a slide. Slides were either stored at -20 °C or processed for immuno- or HE staining.

For non-IFNβ/YFP staining slides were thawed, rehydrated in PBS and fixed in acetone for 10 min.

All tissue slices were surrounded with a DAKOPen (wax/fat pen) and staining procedure was done in a humid chamber. In-between every staining step slides were carefully rinsed with PBS two or three times. Initially, slides were incubated in a H_2O_2 (1 %) -NaN_3 (0,1%) -PBS solution for 1 h at RT under constant shaking. Subsequently, unspecific binding sites were blocked by incubating the slides in a blocking solution, containing different sera (n-goat, n-donkey, n-rat, n-mouse) and FC block (αCD16/CD32) in TNB, for 25 min at RT. Endogenous biotin then was blocked by using an avidin/biotin blocking kit, each solution was left on for 20 min at RT. Following this, slides were stained with the primary antibody solution (1:100 – 1:2000 in TNB) for 1 h at RT. If the primary antibody was biotin-conjugated signal intensities were enhanced by incubating the slides with SA-HRP (in TNB, 1:200) for 25 min at RT followed by incubation with a tyramid solution (either conjugated to FITC or biotin) for 6-8 min. For multiple colour stainings slides were incubated a second time in a H_2O_2 (1 %) -NaN_3 (0,1%) -

PBS solution followed by avidin/biotin block before incubation with the second primary antibody. At the end of the staining procedure, slices were embedded in Vectashield containing DAPI and slides were stored at -20°C till further processing or immediately analysed on a fluorescence microscope (TE2000, Nikon) or confocal microscope (LSM510Meta, Zeiss).

2.2.4 Molecular-biological methods

2.2.4.1 Isolation of RNA from sorted cells

RNA from purified FACS sorted cells was isolated using the mirVana miRNA isolation kit, following the manufacturer's instructions (Ambion). Purity and RNA concentration of each sample was measured at 260 nm using a NanoDrop 1000 photometer and RNA samples were stored at -80 °C till further analysis.

2.2.4.2 Isolation of RNA from organs

For isolation of RNA from different tissues, organs were harvested as described in 2.2.2.4. Subsequently organs were taken up in 1 ml SolD and homogenized using an UltraTurrax. RNA was isolated using the Fluka RNA isolation kit, following the manufacturer's instructions (Sigma Aldrich). Purity and RNA concentration of each sample was measured at 260 nm using a NanoDrop 1000 photometer and RNA samples were stored at -80 °C till further analysis.

2.2.4.3 Preparation of cDNA from RNA samples

For the preparation of cDNA 0.1 – 5 µg RNA from sorted cells or tissue samples were used. RNA was digested by adding DNase I to the samples for 30 min at 37 °C. DNase I then was heat-inactivated at 70 °C for 10 min. Subsequently RNA was added into a tube containing a mix of:

- 1 µl Oligo (dT)20 (50µM)
- 1 µl 10 mM dNTP Mix

- 6 µl RNase free H_2O.

This mixture was incubated at 65 °C for 5 min, rested on ice for a minute and centrifuged for a couple seconds. Following this, mixture was transferred into a PCR-reaction tube containing:

- 1 µl 0.1M DTT
- 4 µl 1 x First Strand Buffer
- 1 µl SuperscriptTM RTase (200U/µl)
- 1 µl RNase free H_2O.

Reverse transcription PCR was run at 50 °C for 1 h, followed by an inactivation step at 70 °C for 15 min and a cooling down step to 4 °C. cDNA was stored at -20 °C till further processing.

2.2.4.3 Quantitative real time PCR

For analysing gene expression cDNA (prepared as in 2.2.4.3) was diluted either 1:5 or 1:10 and 5 µl were pipetted into each well of a 96-well plate containing 20 µl of the responding the mastermix. Mastermix was prepared as follows:

- 12.5 µl Fast Start Mastermix (Invitrogen)
- 6.5 µl H_2O
- 0.3 µl primer forward
- 0.3 µl primer reverse
- 0.5 µl probe.

The qRT-PCR reactions were done in an iQ5 cycler (Bio-Rad) under following conditions:

1. DNA denaturation at 95 °C for 7 min
2. DNA denaturation at 95 °C for 20 s
3. hybridisation and elongation of at 60 °C for 1 min

4. hold at 4 °C
5. steps 2 - 3 were periodically repeated for 45 times

Relative gene expression was calculated using the Pfaffl method (Pfaffl, 2001). For every new primer pair there was a cDNA free control as a negative control included for the qRT-PCR reaction. As reference gene for normalization and quantification β-Actin and or GAPDH were used and every sample was run as a triplicate.

2.2.4.4 Luciferase Assay

For analysing a potential interaction of BATF with the Ifnβ promoter a luciferase assay was performed as follows:

Plasmids (hBATF, Ifnβ-luciferase, Tbk1, renilla-luciferase, empty vector) were set to a concentration of 2000 ng/ml. Out of this, 50 ng of Ifnβ-luciferase, 50 ng of renilla-luciferase, 10 ng (or 100 ng) Tbk1 and 50 ng (or 250 ng or 500 ng) hBATF were mixed with media and lipofectamine LTX and incubated for 45 min.

HEK293T were harvested from tissue culture flasks, centrifuged and the pellet was resuspended in media and $5x10^5$ cells per well were seeded into a 24-well plate in a total volume of 400 µl. The lipofectamine-plasmid cocktail was added into the supernatant of the HEK293T cells and media was changed carefully 6 h after incubation.

After 24 h cells were harvested und luciferase activity was measured using the Dual Luciferase kit (Promega) following the manufacturer's instructions and the illuminometer (Berthold) in a 96-well black bottom plate for 12 s (exposure time) for Ifnβ-luciferase and 1 s exposure time for renilla-luciferase. Fold induction of Ifnβ- luciferase was calculated as follows:

$$\frac{\text{Ifnβ-luciferase reading}}{\text{Renilla-luciferase reading}} \times 100$$

2.3 Data analysis and statistics

2.3.1 Analysis of FACS data

FACS data were analysed using the FlowJo Software (Tree Star, Ashland, USA). For *in vitro* experiments cells were pre-gated on living ($DAPI^-$) cells and as indicated in the specific experiments. For *in vivo* experiments cells were pre-gated on living ($DAPI^-$), non-B- and T-cells ($CD19^-$ and $CD3\varepsilon^-$) and as indicated in the specific experiments.

2.3.2 Processing and analysis of fluorescent and confocal images

Confocal images (LSM510Meta, Zeiss) were primarily analysed using the Zen2010 and Zen2012 software (Zeiss). Single pictures were exported as jpegs and analysed, edited in the identical manner and merged using Adobe Photoshop CS1.

Fluorescent images (TE2000, Nikon) were analysed, edited in the identical manner and merged using Adobe Photoshop CS1.

2.3.3 Statistical analysis of results

For statistical analysis of results shown in this thesis One-Way or Two-Way Anova with Bonferroni Post Test or Student's t-test (unpaired, two-tailed) was used to test for statistical significance * indicates $p< 0.05$; ** indicates $p< 0.01$; *** indicates $p< 0.001$.

3. Results

3.1 IFNβ expression in the spleen is restricted to a subpopulation of pDCs exhibiting a specific immune modulatory transcriptome (Bauer, Dress et al., *in revision*)

During the initial response to viral infections type I interferons (IFN) are crucial initiators of subsequent protective immune responses. Type I IFNs are produced by a large variety of immune cells, like DCs and macrophages or non-immune cells, such as fibroblasts. In previous studies from our lab using an IFNβ/YFP reporter-knockin mouse model (IFNβ$^{mob/mob}$ mouse) we have shown that after *in vivo* stimulation with the TLR9 ligand CpG, IFNβ is almost exclusively produced by pDCs (Scheu et al., 2008). In the work described here, we performed a comprehensive analysis of phenotype, gene expression profile and functionality of these IFNβ-producing pDCs. The data presented in this part of the thesis are part of the manuscript submitted to The Journal of Immunology (Bauer, Dress et. al., 2015) which is attached to the appendix section of this thesis.

3.1.1 IFNβ expression is restricted a low frequency subset of splenic CCR9^{+}CD9^{-} pDCs after TLR9 stimulation

We found pDCs to be the almost exclusive source of IFNβ in the spleen (Scheu et al., 2008). To further analyse these splenic IFNβ-producing pDCs we examined IFNβ$^{mob/mob}$ mice following injection with either CpG or infection with MCMV. We found that the majority of IFNβ/YFP^{+} cells within the spleen were CD11c^{int}, mPDCA-1^{+} and B220^{+}, thus expressing classical pDC surface markers (Fig. 3.1.1A). IFNβ/YFP expression was restricted to only ~5% (4.62±0.70%) of all splenic pDCs after TLR9 stimulation as determined by FACS analysis (Fig. 3.1.1B).We also performed dose titration experiments, to see if we could trigger a higher IFNβ response using a higher dose of CpG or virus. However, the low frequency of IFNβ/YFP^{+} pDCs could neither be enhanced by using a lower nor a higher dose of any these stimuli (Supplemental Fig. 1B and C of the manuscript attached). Furthermore, the co-stimulatory molecules like CD86 were highly up

regulated on both IFNβ/YFP$^-$ and IFNβ/YFP$^+$ pDCs following stimulation with CpG or infection with MCMV. This indicates that both subsets were equally activated early after stimulation (Fig. 3.1.1C and Supplemental Fig. 1D and E of the manuscript attached). Also, IFNβ/YFP$^+$ pDCs as well as IFNβ/YFP$^-$ pDCs exhibited typical plasmacytoid morphology with a round, smooth cellular body and an excentered nucleus (Fig. 3.1.1D). To further characterize the IFNβ/YFP$^+$ subset we analysed the expression of various surface markers by FACS at 0, 6, 12, and 24 h post CpG injection. We found, that besides the classical pDC markers mPDCA-1, B220, and SiglecH, IFNβ/YFP$^+$ pDCs also highly expressed Ly6C and CCR9 but not CD9. This surface marker profile on IFNβ/YFP-producing pDCs was stable for at least 24 h (Fig. 3.1.1A and Fig. 3.1.1E). Taken together, while all splenic pDCs are highly activated, IFNβ production is restricted to only ~5% of pDCs which are CD11c^{int} mPDCA-1$^+$ B220$^+$ SiglecH$^+$ CCR9$^+$ but CD9$^-$.

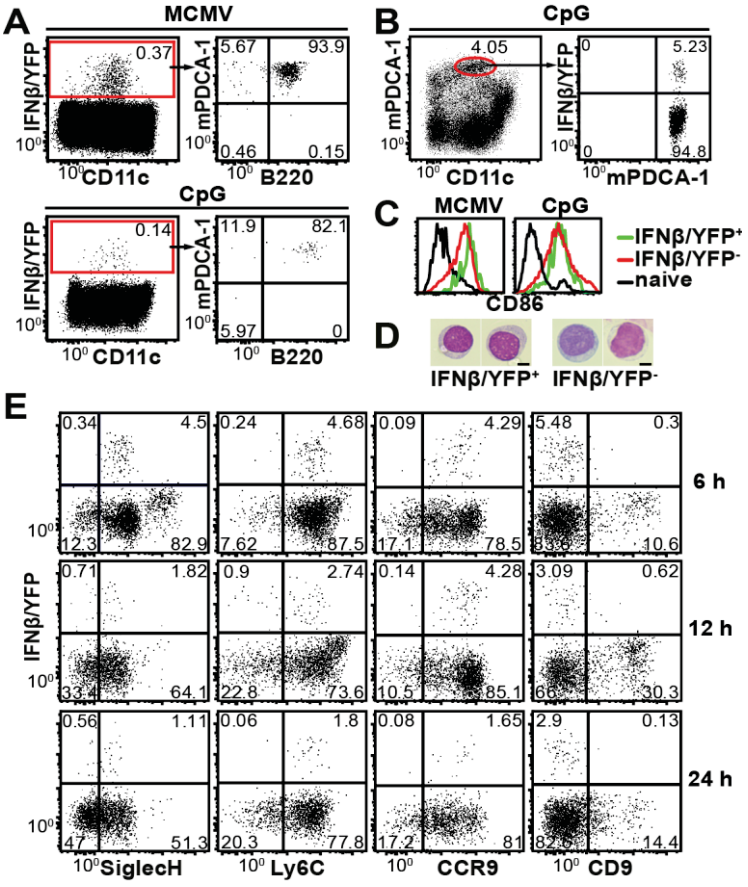

Fig. 3.1.1 IFNβ expression is restricted a low frequent subset of splenic CCR9$^+$CD9$^-$ pDCs after MCMV infection or TLR9 stimulation.

(A) IFNβ/YFP expression in splenic CD11c^{int}mPDCA-1^{+}B220^{+} pDCs in IFNβ$^{mob/mob}$ mice 6h after MCMV infection or CpG injection. (B) Percentages of IFNβ/YFP^{+} cells within CD11c^{int}mPDCA-1^{+} splenic pDCs after CpG injection. (C) CD86 expression on IFNβ/YFP^{+} (green) and IFNβ/YFP^{-} pDCs (red) in comparison to pDCs of untreated mice (black) was determined 6h after MCMV infection or CpG injection. (D) Cytospins of ex vivo sorted pDCs after CpG administration. Bar, 2µm. (E) Expression of IFNβ/YFP was analysed in comparison to pDC surface markers in splenocytes at the indicated timepoints after CpG stimulation. Cells are pre-gated on living CD3ε^{-}CD19^{-} cells (A, B) or additionally on CD11c^{int}mPDCA-1^{+}(C) or CD11c^{int}mPDCA-1^{+}CD11b^{-} cells (D, E). See Supplemental Fig. 1F of the manuscript attached for gating.

3.1.2 Differential localization of IFNβ-producing pDCs within the splenic microarchitecture

Next, we were wondering, if IFNβ/YFP^{+} pDCs have a different localization within the spleen than IFNβ/YFP^{-} pDCs. Therefore, we performed immunofluorescence analysis of spleen sections following 6 h CpG stimulation *in vivo*. We found, that in naïve mice ~60% of all pDCs were located within the marginal zone (Fig. 3.1.2A and Fig. 3.1.2C). Following CpG stimulation most pDCs formed clusters around the former marginal zone in accordance with observations published by Asselin-Paturel et al. (2005) but some pDCs also were found to be within the B and T cell area of the splenic white pulp (Fig. 3.1.2A and Fig. 3.1.2D). Remarkably, more than 97% of the IFNβ/YFP^{+} pDCs were located within B and T cell area upon stimulation with CpG (Fig. 3.1.2B and Fig. 3.1.2E). These data demonstrate that IFNβ-producing pDCs have a distinct localization within the spleen.

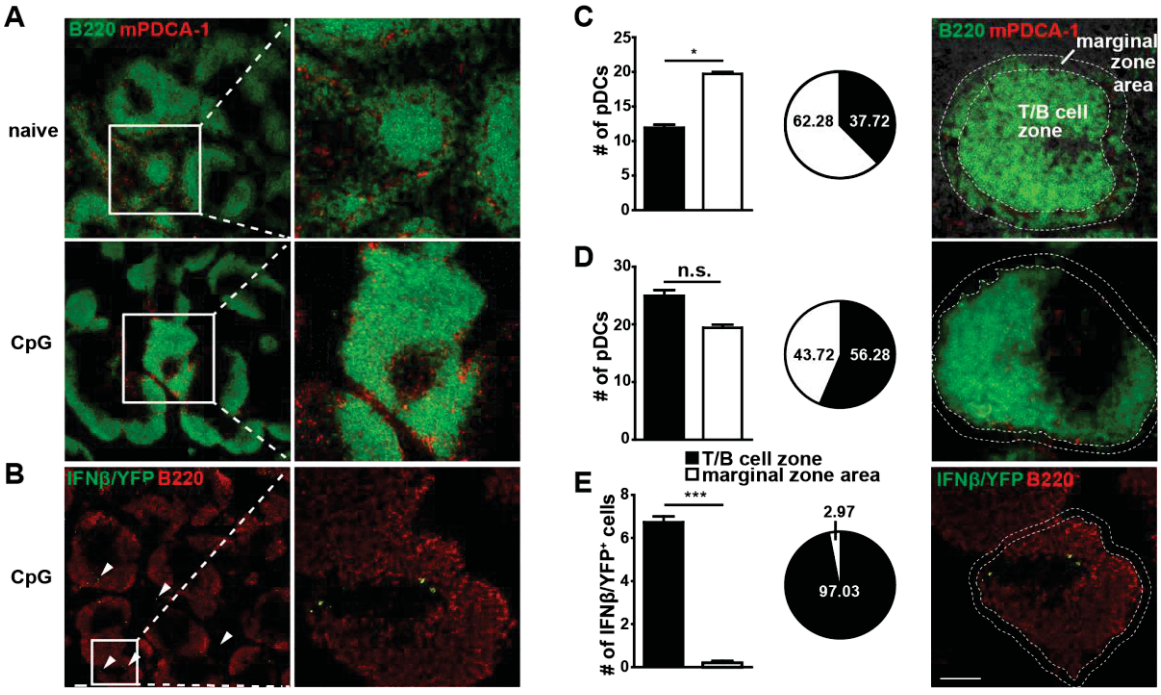

Fig. 3.1.2 Differential localization of IFNβ-producing pDCs within the splenic microarchitecture.

(A, B) Immunofluorescence of the spleen of naïve or CpG stimulated C57BL/6 or IFNβ$^{mob/mob}$ mice. Arrows: exemplary IFNβ/YFP^{+} cells. (C-E) Distribution of pDCs in naive (C) and CpG stimulated mice (D) and of IFNβ/YFP^{+} cells in CpG stimulated mice (E) within the T and B cell zone and the marginal zone (dotted lines). Cell counts are shown as absolute numbers (left) or percentage distribution (middle) per white pulp area; n=17-20. 4x original magnification (A, C, D). Bar, 100µm (B, E).

3.1.3 IFNβ-producing pDCs harbour a proinflammatory gene expression profile

To understand the key differences between IFNβ-producing and non-producing pDCs, we analysed the gene expression profile of both subsets. Therefore splenic CD11c^{int} mPDCA-1^{+} CD11b^{-} IFNβ/YFP^{-} and IFNβ/YFP^{+} pDCs were FACS sorted *ex vivo* 6 h after stimulation with CpG (Fig. 3.1.3.A). Sorted IFNβ/YFP^{-} and IFNβ/YFP^{+} pDCs were subjected to a microarray analyses (performed by Miltenyi Biotech, see description in Materials and Methods part of Bauer, Dress et al., 2015). This microarray analyses indeed revealed that there are 1446 genes >2-fold over- or underrepresented in IFNβ/YFP^{+} vs. IFNβ/YFP^{-} pDCs ($p \leq 0.01$) (Fig. 3.1.3B). There were no significantly different expression levels for classical pDC surface markers like mPDCA-1, the hallmark transcription factor E2-2 (Ghosh et al., 2010) nor activation markers like CD86 in IFNβ/YFP^{+} vs. IFNβ/YFP^{-} pDCs. However, genes associated with pDC activation in general, including TLR9, STAT1, MHCII and CD86, were found to be expressed at different levels in IFNβ/YFP^{-} pDCs (and IFNβ/YFP^{+} pDCs) as compared to naïve pDC (Supplemental Fig. 1H of the manuscript attached). In contrast, the genes for IFNβ, other type I IFNs, the type III IFN Il28b, T helper cell differentiation cytokines such as Il12b and Il12a, and genes involved in chemotaxis, e.g. CCL3, CCL5, and CCR7 were found amongst the highest overrepresented genes in IFNβ/YFP^{+} pDCs. Expression and overrepresentation of selected immune response genes was confirmed by independent qRT-PCR analyses (Supplemental Fig. 1I of the manuscript attached). Multi-level gene ontology analysis (http://www.helmholtz-muenchen.de/icb/mona) identified genes involved in immune effector processes and regulation of localization as highly represented specifically in IFNβ-producing pDCs). To see, if the differential expression of chemokines has an impact on the function of IFNβ/YFP^{+} pDCs, we performed *in vitro* transwell migration assays. These highlighted, that indeed significantly more

IFNβ/YFP$^+$ pDCs, which highly express CCR7, also actively migrate towards the CCR7 ligands CCL19 and CCL21 as compared to IFNβ/YFP$^-$ pDCs (Fig. 3.1.3C). This correlates with their specific localization within the splenic white pulp as described in 3.1.2. Furthermore, to confirm that the specific gene expression profile is the key difference between IFNβ/YFP$^-$ and IFNβ/YFP$^+$ pDCs and not simply a stochastic expression of the IFNβ gene, we performed a re-stimulation experiment. For this purpose, IFNβ/YFP$^-$ and IFNβ/YFP$^+$ pDCs were FACS sorted as described previously and *ex vivo* stimulated a second time with CpG for 6 h. Interestingly, IFNβ/YFP$^+$ pDCs retained their IFNβ/YFP expression, independent of the re-stimulation, for at least 24 h, while the sorted IFNβ/YFP$^-$ pDCs remained unable to produce IFNβ even after this second stimulation (Supplemental Fig. 1J of the manuscript attached). Taken together, this indicated that the ability to produce IFNβ is a functional phenotype of these splenic pDCs due to a distinct gene expression profile.

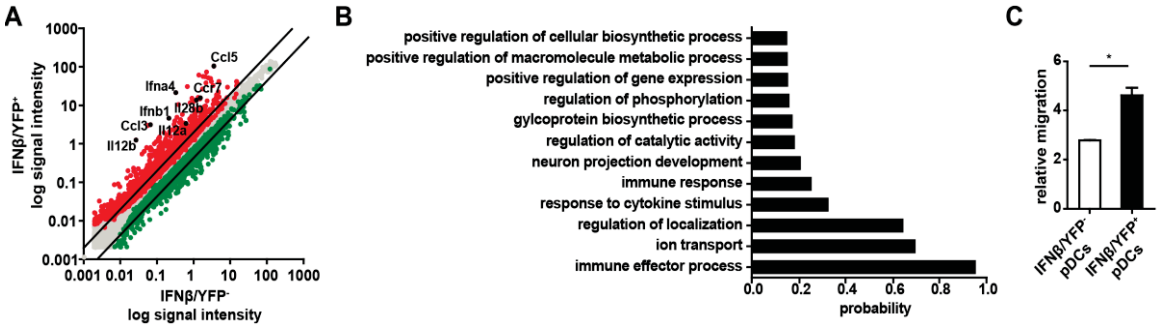

Fig. 3.1.3 IFNβ-producing pDCs harbour a proinflammatory gene expression profile.

(A) Pairwise comparison of the log signal intensities for transcripts as analysed by microarray. Red and green dots indicate genes differentially expressed in IFNβ/YFP$^+$ and IFNβ/YFP$^-$ pDCs, respectively. (B) MONA for overrepresented genes in IFNβ/YFP$^+$ vs. IFNβ/YFP$^-$ pDCs. (C) Transwell migration assay of CpG activated BM-derived IFNβ/YFP$^+$ and IFNβ/YFP$^-$ pDCs in response to CCL19 and CCL21. Shown is one representative of two independent experiments.

3.1.4 IFNAR1-deficiency does not affect the functional properties of IFNβ-producing splenic pDCs after CpG stimulation

It is well described that a positive feedback loop via the type I IFN receptor has a tremendous impact of amplifying the type I IFN response and thereby inducing a higher number of cells to produce IFNα and IFNβ (Ivashkiv and Donlin, 2014).

We were wondering if the IFNAR also has an impact on IFNβ production by this specific splenic pDC subset after TLR9 stimulation. Therefore we did the same comprehensive phenotype, localization and gene expression analyses on IFNAR1$^{-/-}$ mice as we did for IFNAR1$^{+/+}$ mice. We found, that following TLR9 activation, even in the absence of the IFNAR the majority of IFNβ-producing pDCs were located within the B and T cell are of the spleen similar to their localization in IFNAR1$^{+/+}$ mice (Fig. 3.1.2A, Fig. 3.1.2B, Fig.3.1.4A and Fig. 3.1.4B). There were no significant differences in the percentages or absolute numbers of total and IFNβ/YFP^{+} pDCs in IFNAR1$^{-/-}$ mice early after CpG stimulation as compared to IFNAR1$^{+/+}$ mice (Fig. 3.1.4C and Fig. 3.1.4D). Indeed, this is in line with previous studies demonstrating that type I IFN production by pDCs occurred independently of the IFNAR-mediated feedback loop (Barchet et al., 2002). Also, IFNβ serum levels were found to be similar in IFNAR1$^{-/-}$ and IFNAR1$^{+/+}$ mice while IFNα levels appeared to be reduced in the absence of IFNAR1 (Supplemental Fig. 1K and L of the manuscript attached). To elucidate whether type I IFN signalling is involved in the regulation of the specific gene expression profile seen in IFNβ/YFP^{+} pDCs, we FACS sorted splenic IFNβ/YFP^{+} and IFNβ/YFP^{-} pDCs from IFNAR1$^{-/-}$xIFNβ$^{mob/mob}$ mice 6 h after stimulation with CpG. qRT-PCR analysis on these subsets revealed that the gene expression profile of IFNβ/YFP^{+} and IFNβ/YFP^{-} pDCs from IFNAR1$^{-/-}$ and IFNAR1$^{+/+}$ mice is comparable since there were no significant differences in expression levels of e.g. *Ifnb*, *Il-28*, *Ccr7* or *Il-12* (Fig. 3.1.4E). Taken together, these data demonstrate that IFNβ/YFP^{+} pDCs are a distinct, functional subset independent of the IFNAR.

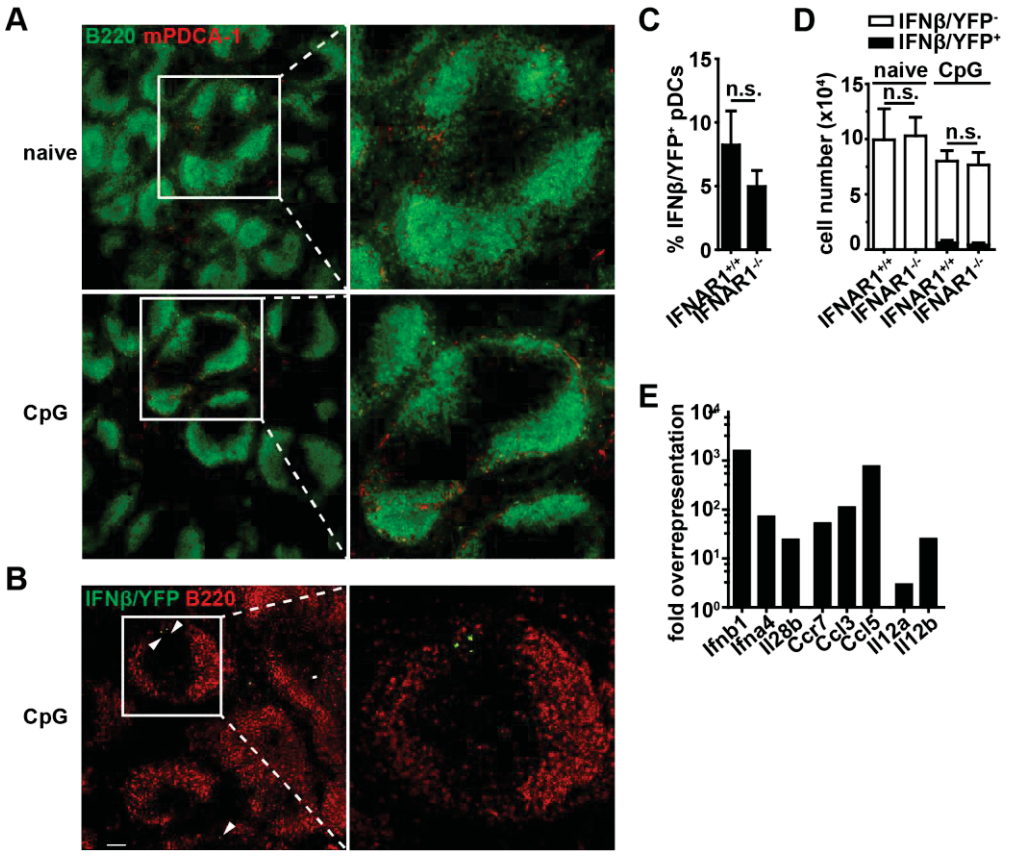

Fig. 3.1.4 IFNAR1-deficiency does not affect the functional properties of IFNβ-producing splenic pDCs after CpG stimulation.

(A,B) Immunofluorescence of the spleen of naïve and CpG stimulated IFNAR1$^{-/-}$IFNβ$^{mob/mob}$ mice. Arrows point to exemplary IFNβ/YFP^{+} cells. 4x original magnification (A). Bar, 100µm (B). (C) Percentages of IFNβ/YFP^{+} cells and (D) total numbers of IFNβ/YFP^{+} and IFNβ/YFP^{-} pDCs gated on CD11c^{int}mPDCA-1^{+} pDCs after CpG injection assayed by flow cytometry. (E) qRT-PCR shown as fold overrepresentation in IFNβ/YFP^{+} vs. IFNβ/YFP^{-} pDCs sorted from IFNAR1$^{-/-}$IFNβ$^{mob/mob}$ mice.

3.1.5 Enhanced chemotactic properties of IFNβ-producing pDCs

The gene expression profile of IFNβ/YFP^{+} pDCs indicated that this subset does not only produce large amounts of IFNβ and proinflammatory cytokines, but may also be involved in recruitment of NK cells or T cells given their high expression of CCL3 and CCL5. To analyse the function of CCL3 and CCL5 (and potentially other factors) produced by IFNβ/YFP^{+} pDCs we injected FACS sorted naïve pDCs or CpG-stimulated IFNβ/YFP^{-} or IFNβ/YFP^{+} pDCs into WT mice and analysed the cells recruited into the peritoneal cavity subsequently to the injection. As predicted by their gene expression profile, IFNβ/YFP^{+} pDCs but not IFNβ/YFP^{-} pDCs effectively promoted the influx of higher numbers of cells into the peritoneal cavity as compared to naïve pDCs (Fig. 3.1.5). Specifically,

IFNβ/YFP$^+$ pDCs predominantly recruited CD4$^+$ and CD8$^+$ T cells while there were no significant differences in the recruitment of NK cells by IFNβ/YFP$^-$ pDCs and IFNβ/YFP$^+$ pDCs (Fig. 3.1.5). This reveals that besides the production of IFNβ, this specific subset of pDCs also actively is involved in the recruitment of T cells thereby enabling further immune processes.

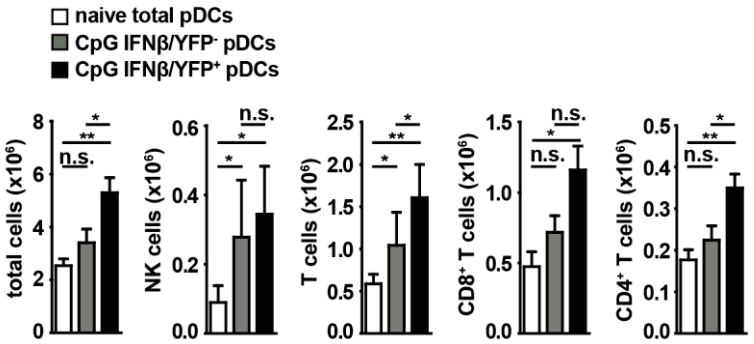

Fig. 3.1.5 Enhanced chemotactic properties of IFNβ-producing pDCs.
C57BL/6 mice were injected i.p. with BM-derived Flt3-L-differentiated untreated pDCs or CpG stimulated IFNβ/YFP$^+$ or IFNβ/YFP$^-$ pDCs. FACS analysis of peritoneal exudates 72 h p.i. from one representative of two independent experiments.

In this study, we identified a functionally distinct subset of IFNβ-producing splenic pDCs, after TLR9 stimulation, which is independent of the IFNAR and equipped with a unique gene expression profile that enables these pDCs to control leukocyte recruitment and coordinate early cellular immune responses.

3.1.6 Author Contributions

I am co-first author of the study presented in this thesis. I generated and analysed all FACS data for cell numbers, surface marker expression and activation analysis of IFNβ/YFP$^-$ vs. IFNβ/YFP$^+$ pDCs of CpG-stimulated or MCMV infected IFNβ$^{mob/mob}$ and IFNAR1$^{-/-}$xIFNβ$^{mob/mob}$ mice and of CpG-stimulated BM-Flt3-L-derived pDCs (Fig. 3.1.1, Fig. 3.1.4 and Supplementary Fig. 1 of the manuscript attached). I prepared and stained all spleen sections from naïve and CpG-stimulated IFNβ$^{mob/mob}$ and IFNAR1$^{-/-}$xIFNβ$^{mob/mob}$ mice for immunofluorescence analysis, took the images and analysed them (Fig. 3.1.2.

and Fig. 3.1.4). Blinded counting of pDC numbers in those immunofluorescence images was done by Sonja Kropp and Judith Alferink, statistical analyses of those counts were performed by myself. The microarray data was generated by Philipp Dresing. I prepared all spleen samples for FACS sorting of IFNβ/YFP^{-} vs. IFNβ/YFP^{+} pDCs from IFNβ$^{mob/mob}$ and IFNAR1$^{-/-}$xIFNβ$^{mob/mob}$ mice, Jens Bauer sorted the cells and I isolated the RNA and generated cDNA from those sorted cells for qRT-PCR analysis. Cytospin staining and qRT-PCRs of genes differentially upregulated in IFNβ/YFP^{-} vs. IFNβ/YFP^{+} pDCs was equally done by Jens Bauer and myself (Fig. 3.1.1, Fig. 3.1.3 and Supplementary Fig. 1 of the manuscript attached). Jens Bauer did the NK and T cell recruiting assay (Fig. 3.1.5) and he and Anja Schulze performed the transwell-migration (Fig. 3.1.3) and the re-stimulation assays (Supplementary Fig. 1 of the manuscript attached) for IFNβ/YFP^{-} and IFNβ/YFP^{+} pDCs. Jens Bauer, Stefanie Scheu, and I interpreted the data and wrote the paper. Stefanie Scheu supervised the study.

3.2 BATF as a potential negative feedback loop inducer in IFNβ producing pDCs after TLR9 stimulation

As described in chapter 3.1 we discovered that in the spleen only a very small subset of pDCs is able to produce IFNβ after TLR9 stimulation. This is quite surprising, since previous literature has suggested that pDCs are the main producers of type I IFN and that all pDCs should be equally able to produce large amounts of these cytokines (Colonna, 2004). In this study we could demonstrate that IFNβ-producing pDCs in the spleen are a distinct subset of pDCs with unique functions in orchestrating cellular immune responses and possessing a specialized gene expression profile as compared to non-IFNβ-producing pDCs, (Bauer, Dress et al., 2015, *in revision*). However, it remains unknown which specific features of these pDCs actually are responsible for their ability to produce large amounts of IFNβ while other pDCs remain incapable of producing this cytokine. A hint could be found in differential gene expression profiles. In the above described manuscript (3.1), in order to better understand the functional importance of this IFNβ-producing pDC subset, we performed a comprehensive analysis of several genes known to be involved in cellular immune processes,

including different chemokines and cytokines. However, among the highest differentially expressed genes in IFNβ/YFP$^-$ vs. IFNβ/YFP$^+$ pDCs are a few genes which have either been only minimally investigated previously, or remain entirely undescribed in the context of pDCs. The following two chapters will try to bring us closer to understand the functions of two such genes in IFNβ-producing pDCs: BATF and PSD-93.

BATF is one of the highest differentially regulated genes we found overrepresented in IFNβ-producing pDCs. Interestingly, a lot is now known about the function of this transcription factor in B and T cell development and in cDCs (Murphy et al., 2013). The function of BATF in pDCs remained to be uncovered. The following chapter aims to better understand the role of BATF in IFNβ production by pDCs.

3.2.1 IFNβ/YFP-producing pDCs highly upregulate BATF upon TLR9 stimulation

Before investigating if BATF has a function in IFNβ-producing pDCs we first verified its expression in these cells. Therefore, we FACS sorted CD11b$^-$ CD11c^{int}mPDCA-1$^+$IFNβ/YFP$^-$ and CD11b$^-$CD11c^{int}mPDCA-1$^+$IFNβ/YFP$^+$ pDCs from IFNβ$^{mob/mob}$ and IFNAR1$^{-/-}$xIFNβ$^{mob/mob}$ mice 6 h after stimulation with the TLR9 ligand CpG. qRT-PCR analysis of the sorted pDC populations confirmed that IFNβ/YFP$^+$ pDCs not only express IFNβ, but also BATF at significantly higher levels than IFNβ/YFP$^-$ pDCs (Fig. 3.2.1aA and B). In order to investigate the time course of BATF expression in pDCs, we generated BM-derived Flt3-L-derived pDCs, stimulated them with CpG for 0, 6, 12 or 24 h. FACS analysis of these cells revealed that most pDCs upregulate BATF upon stimulation, but only pDCs that were BATF^{hi} expressed IFNβ/YFP *in vitro* (Fig. 3.2.1aC). The highest expression of IFNβ/YFP$^+$ and BATF was observed at 12 h post stimulation (Fig. 3.2.1aD and E). Also IFNβ/YFP$^+$ pDCs showed considerably higher MFIs for BATF than IFNβ/YFP$^-$ pDCs (Fig. 3.2.1aF and G), indicating that this transcription factor is highly active in IFN/YFP$^+$ pDCs. In line with this, in immunofluorescence stainings of BM-Flt3-L-derived naive and stimulated pDCs we observed a high

expression of BATF in the nucleus of IFNβ/YFP^{+} pDCs 24 h after TLR9 stimulation (Fig. 3.2.1aH) These data confirm that BATF is highly differentially upregulated in IFNβ/YFP^{+} pDCs *in vitro*.

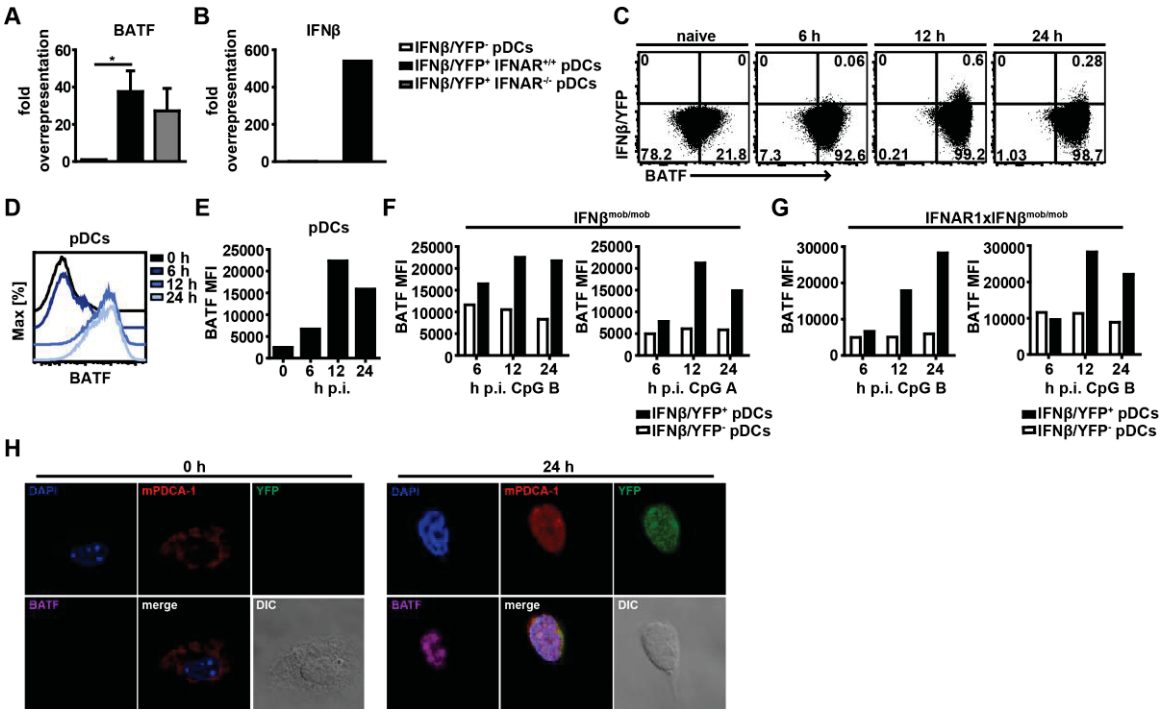

Fig. 3.2.1a Characterization of BATF expression in IFNβ/YFP producing pDCs upon TLR9 stimulation.
qRT-PCR analysis of sorted IFNβ/YFP^{-} vs. IFNβ/YFP^{+} splenic pDCs for expression of (A) *Batf* in IFNβ$^{mob/mob}$ and IFNAR1$^{-/-}$xIFNβ$^{mob/mob}$ mice and (B) *Ifnb* in IFNβ$^{mob/mob}$ mice 6 h after i.v. injection with CpG 1668/B complexed to DOTAP. (C) FACS analysis of BATF expression *in in vitro* generated BM-Flt3-L-derived IFNβ/YFP^{+} pDCs 0 h, 6 h, 12 h or 24 h after stimulation with CpG 1668/B complexed to DOTAP. (D-G) BATF MFI of BM-Flt3-L-derived (D-E) pDCs and (F-G) IFNβ/YFP^{-} vs. IFNβ/YFP^{+} pDCs 0 h, 6 h, 12 h or 24 h after stimulation with CpG 2216/A (F-G) or CpG 1668/B complexed to DOTAP (D-G). (H) Immunofluorescence images of BATF expression in BM-Flt3-L-derived IFNβ/YFP^{+} pDCs 0 h and 24 h after stimulation. (For (A) n=3 is shown (each sample is pooled from 12 mice). (B-H) One representative experiment out of three is shown.)

We next sought to confirm these findings *in vivo* and therefore injected IFNβ$^{mob/mob}$ mice with CpG. FACS analyses showed that only pDCs that were BATF^{hi} were co-positive for IFNβ/YFP *in vivo* (Fig. 3.2.1bA), and despite the fact that all pDCs upregulated BATF after stimulation (Fig. 3.2.1b.B), the MFI for BATF was significantly higher in IFNβ/YFP^{+} pDCs as compared to IFNβ/YFP^{-} pDCs (Fig. 3.2.1bC). Taken together, these data confirm that BATF is

significantly differentially expressed in IFNβ-producing pDCs vs. non-producing pDCs after TLR9 stimulation *in vitro* and *in vivo*.

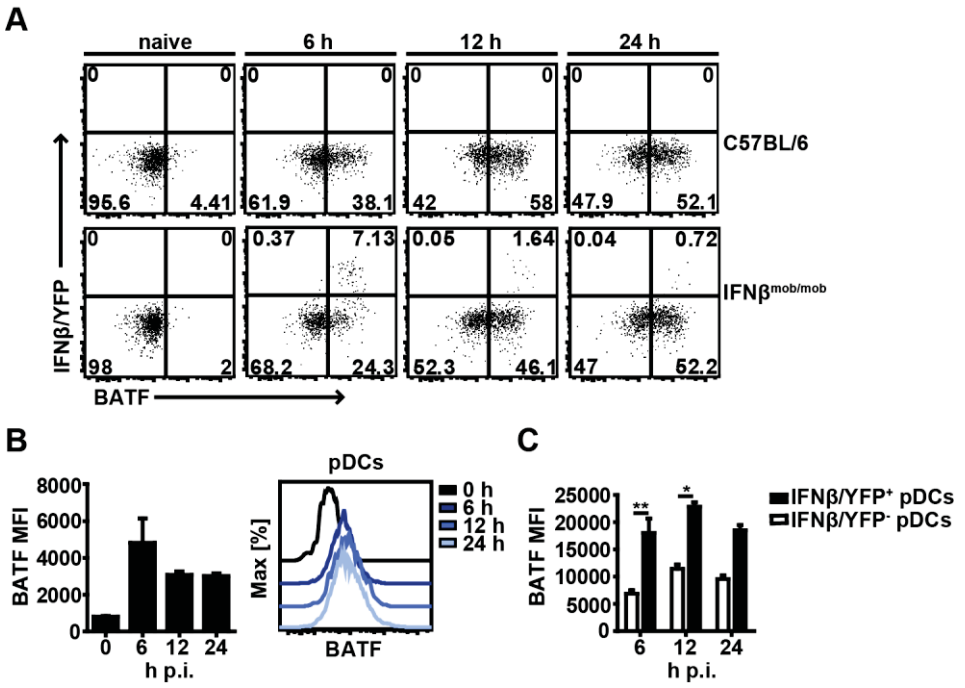

Fig. 3.2.1b Characterization of BATF expression in IFNβ/YFP producing pDCs upon TLR9 stimulation *in vivo*.
(A) FACS analysis of BATF expression in IFNβ/YFP^{+} pDCs in vivo 0 h, 6 h, 12 h or 24 h after i.v. injection of CpG 1668/B complexed to DOTAP. (B-C) BATF MFI of (B) pDCs and (C) IFNβ/YFP^{-} vs. IFNβ/YFP+ pDCs in the spleen of IFNβ$^{mob/mob}$ mice 0 h, 6 h, 12 h or 24 h after i.v. injection of CpG 1668/B complexed to DOTAP. ((A) One experiment out of three is shown and (B-C) n=3.)

3.2.2 BATF$^{-/-}$ mice have increased numbers of pDCs in the spleen

In order to investigate the role of BATF in IFNβ-producing pDCs we made use of BATF$^{-/-}$ mice (Schraml et al., 2009). Since pDC populations in BATF$^{-/-}$ mice have not been fully described, we performed a comprehensive analysis of pDCs in different tissues of naïve and CpG stimulated BATF$^{-/-}$ mice. Overall there was a higher percentage of CD11b^{-}CD11c^{int}mPDCA-1^{+} pDCs in mesenteric LNs (2.99 % in BATF$^{-/-}$ vs. 1.49 % in BATF$^{+/+}$) and liver (21.7 % in BATF$^{-/-}$ vs. 13.4 % in BATF$^{+/+}$) but not in spleen and lung in naïve BATF$^{-/-}$ mice compared to controls (Fig. 3.2.2aA). No obvious differences in pDC populations were observed between genotypes after CpG stimulation in most tissues, except a slightly increased percentage of pDCs (8.9% in BATF$^{+/+}$ and 14.1 % in BATF$^{-/-}$) in the liver of BATF$^{-/-}$ mice compared to BATF$^{+/+}$ mice (Fig. 3.2.2aA). Of note, overall

absolute cell numbers in spleens of BATF$^{+/+}$ and BATF$^{-/-}$ mice were comparable (Fig. 3.2.2aB) although absolute cell numbers of pDCs and cDCs were elevated in naïve and CpG stimulated BATF$^{-/-}$ mice (Fig. 3.2.2aC). There were no significant differences in activation of pDCs and cDCs evidenced by the MFIs for CD86 and MHC II expression (Fig. 3.2.2aD and E) and the frequencies of CD86 or MHCII expressing cells (Fig. 3.2.2aF) after stimulation with CpG between BATF$^{+/+}$ and BATF$^{-/-}$ mice.

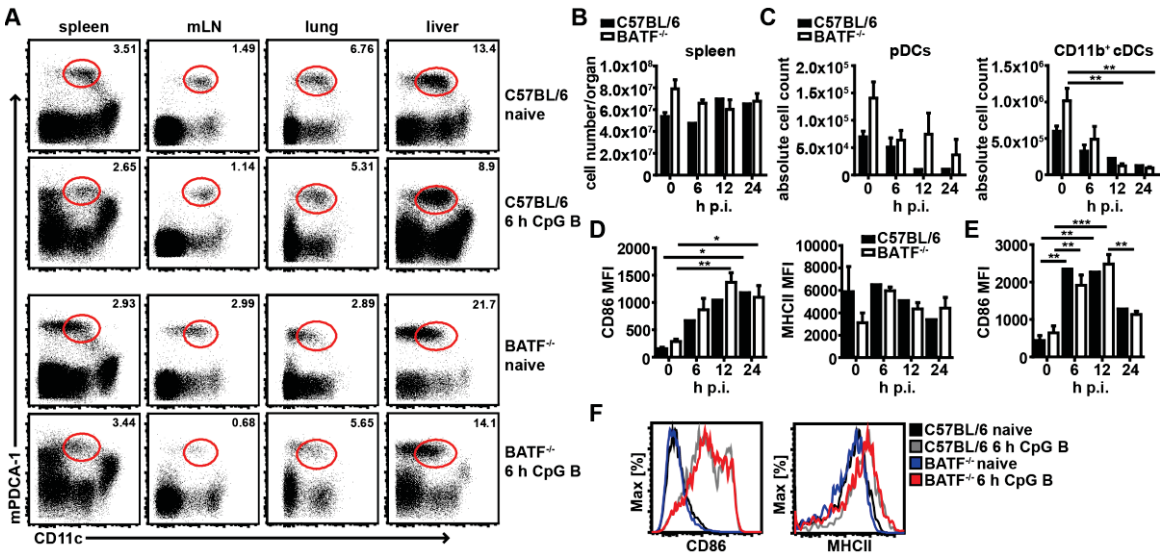

Fig. 3.2.2a Analysis of DC populations in BATF$^{-/-}$ mice after TLR9 stimulation.

(A) FACS analysis of pDC populations in spleen, mLN, lung and liver in WT and BATF$^{-/-}$ mice 0 h or 6 h after i.v. injection of CpG 1668/B complexed to DOTAP. (B) Absolute number of cells and (C) absolute numbers of pDCs and cDCs in the spleen of WT and BATF$^{-/-}$ mice 0 h, 6 h, 12 h and 24 h after stimulation. (D-F) Upregulation of activation markers on (D,F) pDCs and (E) cDCs after stimulation. For FACS analysis cells were pre-gated on living, CD3ε^{-}CD19^{-} cells, cDCs were gated as CD11c^{+}CD11b^{+}, pDCs were gated as CD11b^{-}CD11c^{int}mPCA-1^{+}. ((A and F) One experiment out of three is shown. (B-E) n=1-3.)

We observed a general trend of elevated numbers of cells in lung and LNs from BATF$^{-/-}$ mice (Fig. 3.2.2b.A). BATF$^{-/-}$ mice had no obvious differences in counts of CD11b^{-}CD11c^{int}mPDCA-1^{+} pDCs and CD11b^{+}CD11c^{+} cDCs in the liver (Fig. 3.2.2b.B). Slightly elevated numbers of pDCs were present in the lung of BATF$^{-/-}$ mice after 12 and 24 h of stimulation with CpG (Fig. 3.2.2b.C), and markedly higher numbers of CD11b^{+}CD11c^{+} cDCs were present in mesenteric 6 h after stimulation and in peripheral and cervical LNs at 12 h and 24 h after stimulation

relative to control animals (Fig. 3.2.2b.D-F). Additionally, we found higher levels of NK cells in the liver of BATF$^{-/-}$ mice at 12 and 24 h post stimulation with CpG (Fig. 3.2.2b.B). In summary, BATF$^{-/-}$ mice have slightly higher absolute numbers of pDCs compared to BATF$^{+/+}$ mice across different tissues and show differences to varying degrees in certain myeloid cell populations after CpG stimulation.

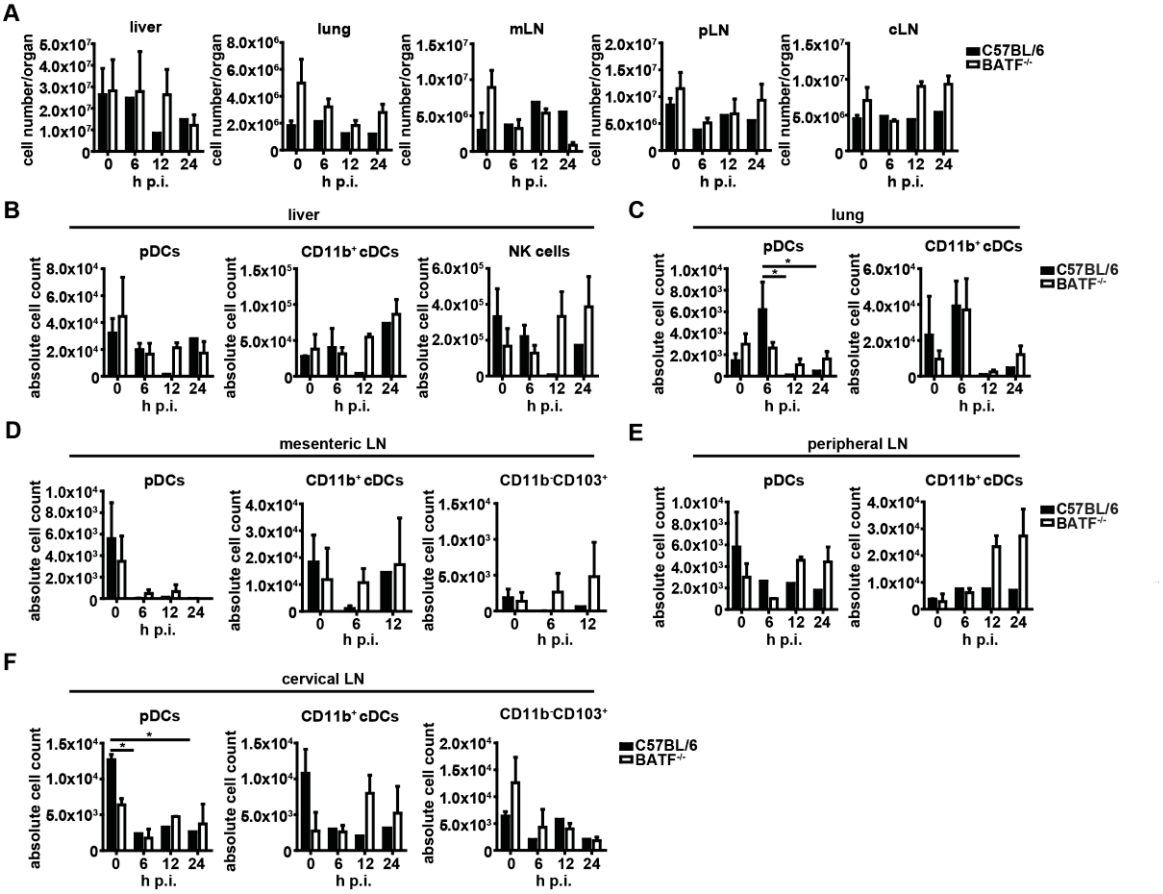

Fig. 3.2.2b Analysis of myeloid populations in different tissues in BATF$^{-/-}$ mice after TLR9 stimulation.
(A) Absolute number of cells in liver, lung and LNs. FACS analysis of absolute cell numbers of myeloid populations in (B) liver, (C) lung, (D) mesenteric LN, (E) peripheral LN and (F) cervical LN. For (B-E) cells were pre-gated on living, non B/T cells: cDCs were gated on CD11b^{+}CD11c^{+} cells, pDCs on CD11b^{-}CD11c^{int}mPDCA-1^{+} cells, NK cells on CD11c$^{+/-}$NK1.1^{+} cells, migratory DCs on CD11b^{-}CD11c^{+}CD103^{+} cells. ((A-F) n=1-3.)

We wondered if different types of CpG stimuli might have a specific impact on pDC numbers and activation in BATF$^{-/-}$ mice. It is known, that A-type CpGs like CpG 2216 induce a stronger type I IFN response than B-type CpGs like CpG 1668 used in the previous experiments (Waibler et al., 2008). Therefore, we repeated the experiments shown in 3.2 and 3.3 with CpG 2216/A instead of CpG

1668/B to compare both data sets. We could not observe any differences in absolute cell counts in spleen, liver, lung or LNs (Fig. 3.2.2cA) nor in numbers and activation of splenic DCs between the two types of CpG we tested (Fig. 3.2.2cB-E). In addition to this, DC and NK cell numbers in liver (Fig. 3.2.2cF), and DC numbers in lung and LNs (Fig. 3.2.2cG-J) were comparable to those observed after stimulation with CpG 1668/B. These results clearly demonstrate that phenotype of quantity and activation status of DCs we have observed in BATF$^{-/-}$ mice is consistent across different types of CpG-stimuli.

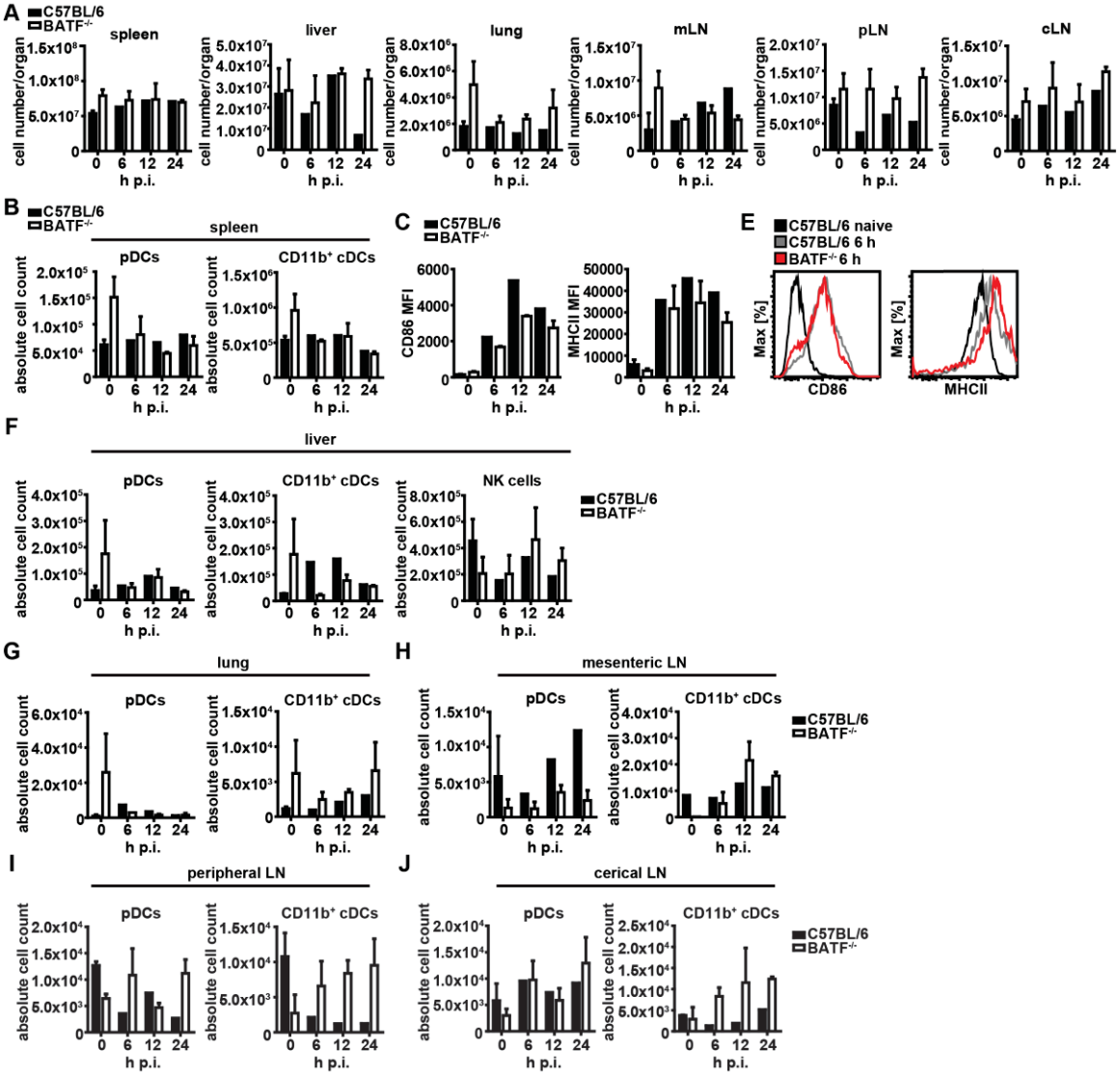

Fig. 3.2.2c Analysis of DC populations in BATF$^{-/-}$ mice after TLR9 stimulation with an A-type CpG.

(A) Absolute numbers of cells in spleen, liver, lung and LNs after i.v. injection of CpG 2216/A complexed to DOTAP. (B) Absolute cell numbers of pDCs and cDCs in the spleen and (C,E) upregulation of activation markers on splenic pDCs 0 h, 6 h, 12 h and 24 h after stimulation with CpG 2216/A complexed to DOTAP. Absolute cell

numbers of myeloid populations in (F) liver, (G) lung, (H) mesenteric LNs, (I) peripheral LNs and (J) cervical LNs in WT and BATF$^{-/-}$ mice 0 h, 6 h, 12 h and 24 h after stimulation. For FACS analysis cells were pre-gated on living, CD3ε^{-}CD19^{-} cells, cDCs were gated as CD11b^{+}CD11c^{+}, pDCs were gated as CD11b^{-}CD11c^{int}mPDCA-1^{+}. ((A-J) =1-3.)

3.2.3 Classical pDC markers are expressed at lower levels on splenic BATF-deficient pDCs

Since we found, that BATF$^{-/-}$ mice have higher numbers of pDCs, we next investigated whether BATF-deficient pDCs express the same surface markers as BATF$^{+/+}$ pDCs. To this end we injected BATF$^{-/-}$ mice with CpG and analysed the expression of classical pDC surface markers after 0, 6, 12 and 24 h. While BATF$^{+/+}$ pDCs showed the classical pDC surface marker phenotype, CD11b^{-} CD11c^{int}mPDCA-1^{+}B220^{+}SiglecH^{+}CCR9^{+}, and also highly expressed MHC II even in the steady state (see Fig. 3.1.1.), pDCs from BATF$^{-/-}$ mice appeared to have a lower expression of most of these markers. Naïve BATF$^{-/-}$ pDCs were also CD11b^{-}CD11c^{int}mPDCA-1^{+}B220^{+}SiglecH^{+}CCR9^{+} and MHCII^{+} but within the CD11b^{-}CD11c^{int}mPDCA-1^{+} pDC population only ~77 % of pDCs were positive for B220 (versus >95 % in BATF$^{+/+}$), ~88 % of pDCs were positive for CCR9 (versus >99 % in BATF$^{+/+}$) and just ~36% expressed SiglecH (versus >60 % in BATF$^{+/+}$) (shown as comparative histograms in Fig.3.2.3A). Of note, this marker profile changed little over time after CpG stimulation. Furthermore, after stimulation, up to ~53 % of the cells within the CD11b^{-}CD11c^{int}mPDCA-1^{+} population in BATF$^{-/-}$ mice were negative for the classical pDC marker B220 (versus <95 % in BATF$^{+/+}$) and showed a significantly lower expression of CCR9 (Fig.3.2.3B). Taken together, BATF$^{-/-}$ pDCs have a qualitatively similar surface marker profile as BATF$^{+/+}$ pDCs but seem to have quantitatively lower expression of some classical pDC markers, which might reflect a developmental defect in these cells *in vivo*. To date, we have not observed any defects in pDC development in bone marrow-derived Flt3-L pDC cultures from BATF$^{-/-}$ mice vs. BATF$^{+/+}$ mice *in vitro* (data not shown).

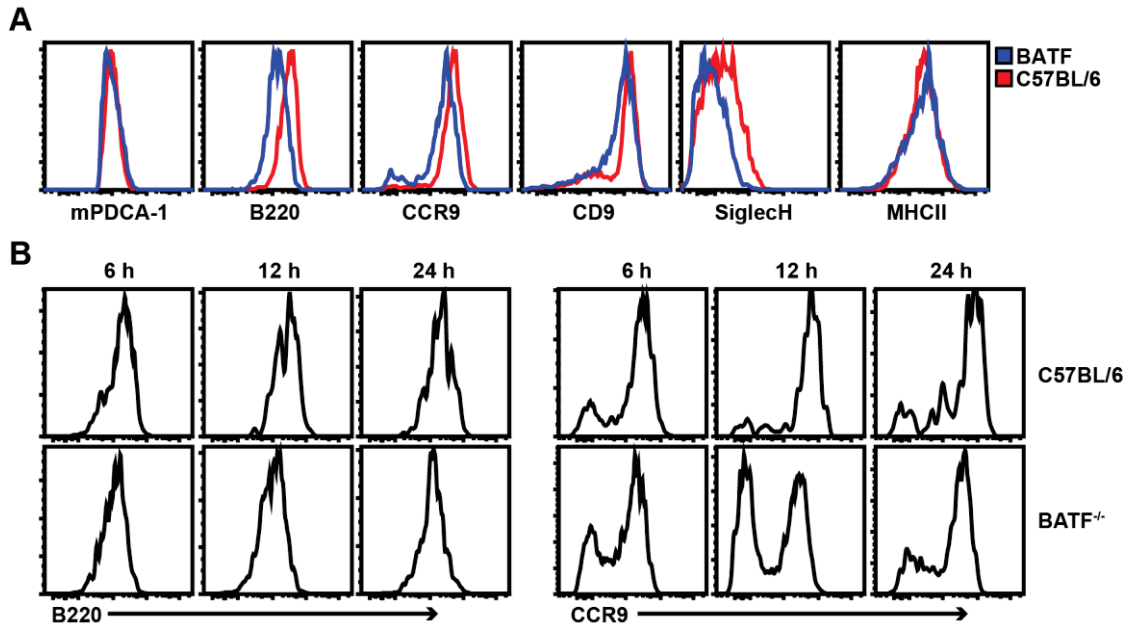

Fig. 3.2.3 Characterization of pDC surface marker expression in BATF$^{-/-}$ mice.

FACS analysis of surface marker expression on splenic pDCs after (A) 0 h, (B) 6 h, 12 h or 24 h i.v. stimulation with CpG 1668/B from C57BL/6 and BATF$^{-/-}$ mice. pDCs are gated on living, CD3ε$^-$CD19$^-$CD11b$^-$CD11c^{int}mPDCA-1$^+$ cells. (One representative experiment out of three is shown.)

3.2.4 BATF$^{-/-}$ mice produce higher amounts of IFNβ in different organ compartments after stimulation with the A-type CpG 2216 compared to control mice

Next we sought to determine if BATF deficiency has an effect on type I IFN production *in vivo.* To address this question, we first performed whole organ ELISAs for IFNα and IFNβ on spleen, liver, lung, mesenteric and peripheral LN tissues from BATF$^{+/+}$ and BATF$^{-/-}$ mice following stimulation with either CpG 1668/B or CpG 2216/A. After stimulation with CpG 1668/B IFNα levels in spleen, liver and lung of BATF$^{-/-}$ mice were slightly reduced whereas IFNα in the LNs was increased compared to BATF$^{+/+}$ mice at certain timepoints (Fig. 3.2.4A). Despite the fact that there were no differences in absolute DC numbers in BATF$^{-/-}$ mice after stimulation with CpG 1668/B or CpG 2216/A (3.2.2), there was a strong impact on IFNβ production depending on the CpG stimulus used. CpG 1668/B induced high levels of IFNβ in the spleen of BATF$^{+/+}$ but not BATF$^{-/-}$ mice (Fig. 3.2.4B) while interestingly CpG 2216/A had the opposite effect (Fig. 3.2.4C). Overall CpG 2216/A induced much higher levels of IFNβ than CpG 1668/B in all tested tissues, with significantly higher expression in BATF$^{-/-}$ as compared to

BATF$^{+/+}$ mice (Fig. 3.2.4C). CpG 1668/B on the other hand induced more IFNβ production in BATF$^{+/+}$ mice than BATF$^{-/-}$ mice with one exception: In the liver more IFNβ was detected in BATF$^{-/-}$ than in BATF$^{+/+}$ mice (Fig. 3.2.4B). Intriguingly, BATF-deficiency does not have a negative effect on the production of type I IFN as we initially hypothesized but rather leads to increased production of IFNβ at least after stimulation with CpG 2216/A.

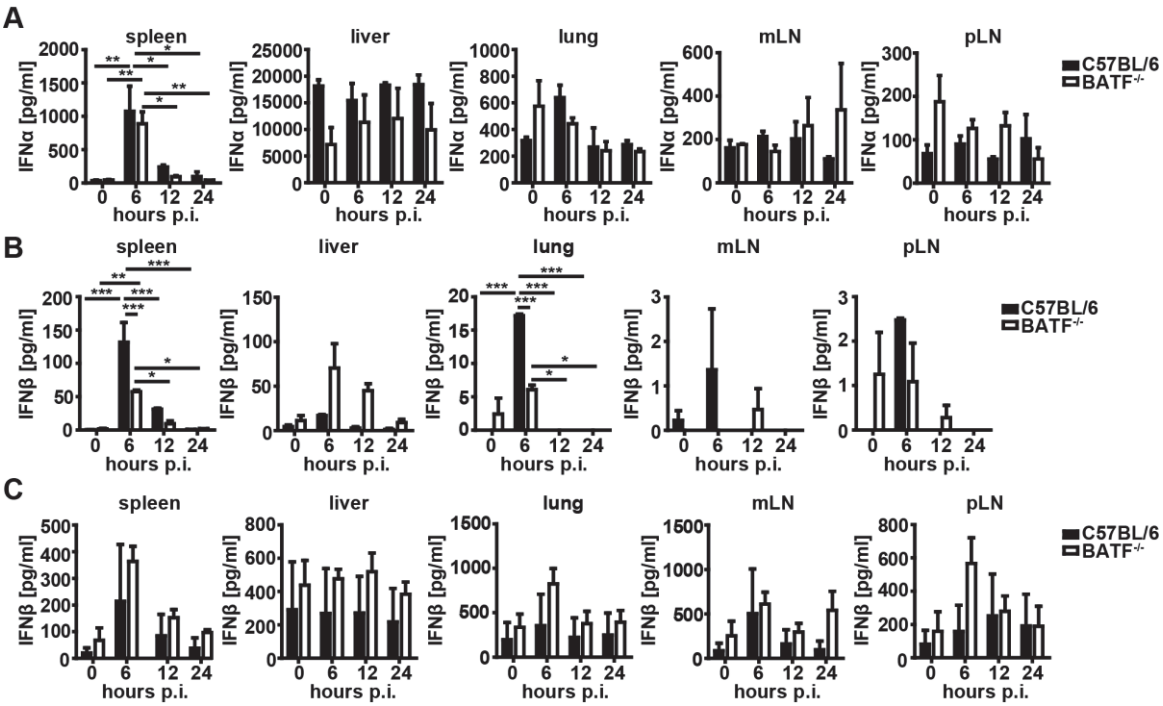

Fig. 3.2.4 Type I IFN production by BATF$^{-/-}$ mice.

Whole organ ELISA for (A) IFNα and (B,C) IFNβ levels in spleen, liver, lung and LNs of WT and BATF$^{-/-}$ mice 0 h, 6 h ,12 h and 24 h after i.v. injection of CpG 1668/B (A,C) or CpG 2216/A (B) complexed to DOTAP. ((A-C) n=3.)

3.2.5 BM-Flt3-L-derived BATF$^{-/-}$ DCs produce large amounts of IFNβ after challenge with CpG B or MCMV *in vitro*

After discovering that BATF$^{-/-}$ mice have increased levels of IFNβ we wondered if this is due to the increased number of pDCs in these mice, or an increased capacity to produce type I interferon. Therefore we further analysed the characteristics of and IFNβ production by BATF$^{-/-}$ pDCs. To this end we crossed our IFNβ-reporter mice (IFNβ$^{mob/mob}$) with the BATF$^{-/-}$ mice and generated a new strain of BATF$^{-/-}$xIFNβ$^{mob/mob}$ mice. For initial *in vitro* analysis we generated BM-derived Flt3-L-differentiated pDCs from BATF$^{+/+}$xIFNβ$^{mob/mob}$, BATF$^{+/-}$xIFNβ$^{mob/mob}$

and BATF$^{-/-}$x IFNβ$^{mob/mob}$ mice and stimulated these cells with CpG 1668/B or CpG 2216/A or Poly(I:C) to assess their responsiveness to different TLR stimuli. Upon treatment with the B type CpG 1668/B >2 % of BATF$^{-/-}$ pDCs produced IFNβ/YFP while only ~0.5 % of the BATF$^{+/+}$ pDCs and <0.5 % of BATF$^{+/-}$ pDCs were IFNβ/YFP^{+} 6 h after stimulation (Fig. 3.2.5A). Percentages of IFNβ/YFP^{+} cells decreased in all genotypes at 12 and 24 h after stimulation. In contrast, stimulation with the A type CpG 2216/A led to higher percentages of IFNβ/YFP^{+} pDCs in all genotypes, increasing between 6 h and 24 h after stimulation (Fig. 3.2.6.B). Stimulation with Poly(I:C) led to a maximum of ~5 % IFNβ/YFP^{+} BATF$^{+/+}$xIFNβ$^{mob/mob}$ pDCs at 12 h after stimulation but only a maximum of 1 % of IFNβ/YFP^{+} BATF$^{+/-}$xIFNβ$^{mob/mob}$ and 1% of BATF$^{-/-}$xIFNβ$^{mob/mob}$ pDCs (Fig. 3.2.5C). Interestingly, both CpGs comparably activated BATF$^{+/+}$ and BATF$^{-/-}$ pDCs till 12 h after stimulation while 24 h after CpG 1668/B stimulation the MFI for CD86 was lower in BATF$^{+/-}$ and BATF$^{-/-}$ pDCs than in WT mice. Also, after stimulation with Poly(I:C) the MFI for CD86 was lower in *in vitro* generated BATF$^{-/-}$ pDCs hinting at a stronger responsiveness after TLR9 than TLR3 stimulation (Fig. 3.2.5D). After these initial experiments, we infected BATF$^{+/+}$ and BATF$^{-/-}$ pDCs with MCMV C3X (MOI 1) in order to test a more physiologically relevant TLR9 stimulus. To our surprise, BATF$^{-/-}$ pDCs were obviously less activated than BATF$^{+/-}$ or BATF$^{+/+}$ pDCs based on surface markers, but had the highest percentage of IFNβ/YFP^{+} cells (~7 % after 6 h and ~6 % after 24 h as compared to ~3 % after 6 h and ~3.5 % after 24 h in the control BATF$^{+/+}$ pDC population) (Fig.3.2.5E and F). Of note, IFNβ/YFP^{-} and IFNβ/YFP^{+} pDCs were equally activated with respect to CD86 expression after infection with MCMV, whereas after stimulation with CpG 2216/A or Poly(I:C) IFNβ/YFP^{+} pDCs were more highly activated than IFNβ/YFP^{-} pDCs in all genotypes (Fig. 2.3.5G). Accordingly, the higher percentage of IFNβ/YFP^{+} pDCs from BATF$^{-/-}$ cells after CpG 2216/A stimulation correlated with significantly higher levels of type I IFN, especially IFNβ, in supernatants from cultures of these cells (Fig. 3.2.5H and I).

In summary, BATF$^{-/-}$ pDCs have a greater capacity to produce IFNβ *in vitro* compared to BATF$^{+/+}$ pDCs after stimulation with CpG or MCMV.

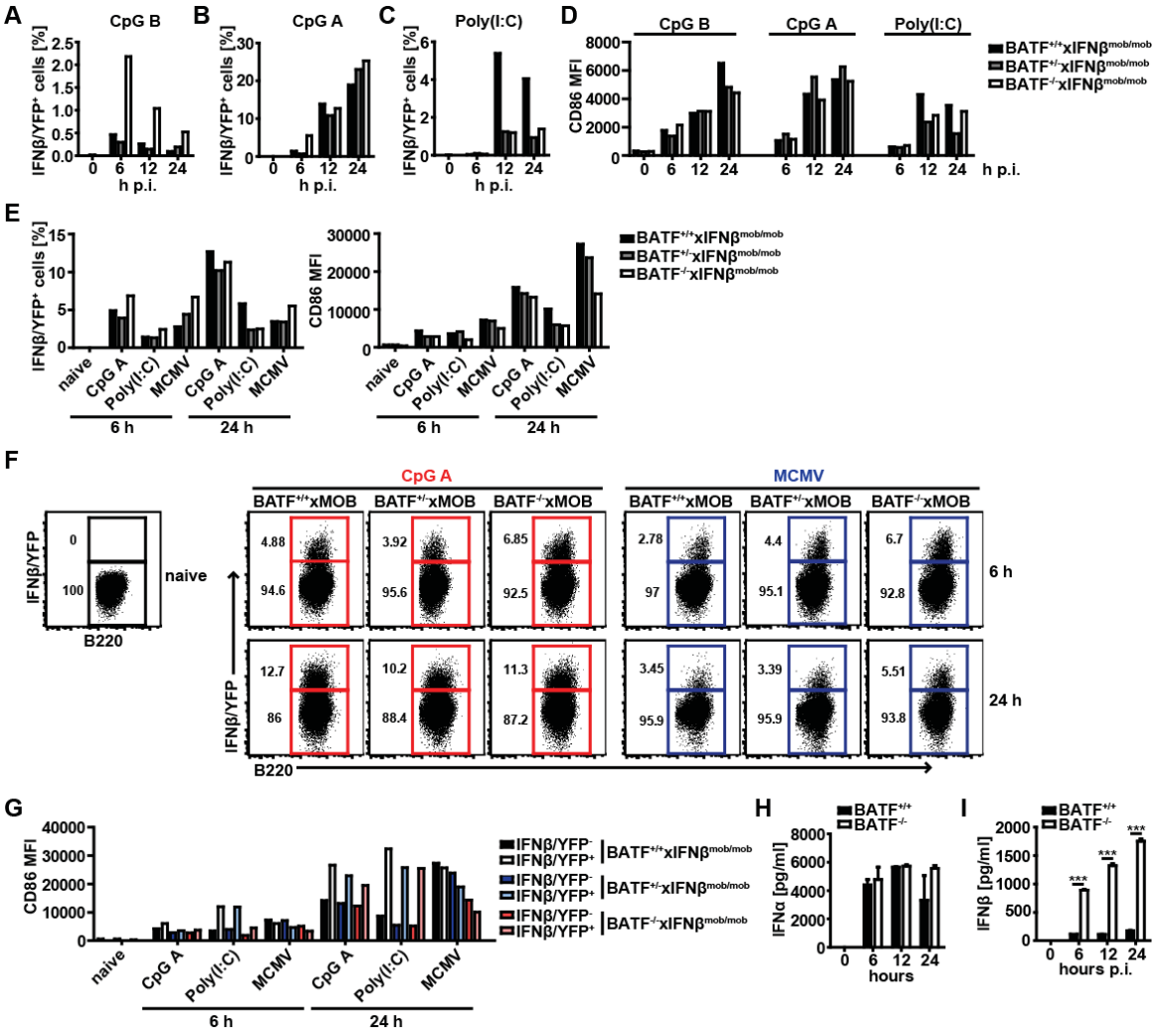

Fig. 3.2.5 Expression of type I IFN and IFNβ/YFP by BATF$^{-/-}$ mice *in vitro*.

BM-derived Flt3-L cultured pDCs were stimulated with CpG 1668/B complexed to DOTAP, CpG 2216/A or Poly(I:C) for 0 h, 6 h, 12 h or 24 h. Cells are pre-gated on living, CD11b^{-}CD11c^{+}B220^{+} pDCs. Percentage of IFNβ/YFP^{+} pDCs after stimulation with (A) CpG 1668/B, (B) CpG 2216/A and (C) Poly(I:C). (D) Upregulation of the activation marker CD86 on pDCs upon TLR stimulation. (E) Percentage and activation of pDCs after infection with MCMV C3X in comparison to stimulation with CpG 2216/A or Poly(I:C). (F) FACS analysis of IFNβ/YFP^{+} pDCs after infection with MCMV C3X or stimulation with CpG 2216/A and (G) activation status of IFNβ/YFP^{-} vs. IFNβ/YFP^{+} pDCs. (H and I) ELISA for levels of (H) IFNα and (I) IFNβ in the supernatant of CpG-stimulated pDCs. ((A-D) One representative experiment out of three is shown, (E-G) n=1, (H,I) n=3.)

3.2.6. Splenic BATF$^{-/-}$ IFNβ-producing pDCs are highly activated but produce only low amounts of IFNβ early after stimulation with CpG *in vivo*

Next we analysed whether the observed elevated production of IFNβ by BM-derived BATF$^{-/-}$ pDCs also holds true in an *in vivo* model. Therefore we injected BATF$^{+/+-}$xIFNβ$^{mob/mob}$, BATF$^{+/-}$xIFNβ$^{mob/mob}$ and BATF$^{-/-}$xIFNβ$^{mob/mob}$ mice with CpG 1668/B or CpG 2216/A. Surprisingly, upon injection with either CpG 1668/B or

CpG 2216/A more IFNβ/YFP^{+} pDCs were found in BATF$^{+/-}$xIFNβ$^{mob/mob}$ mice than in BATF$^{+/+}$xIFNβ$^{mob/mob}$ or BATF$^{-/-}$xIFNβ$^{mob/mob}$ mice. Indeed, BATF$^{-/-}$ mice exhibited the lowest percentage of IFNβ/YFP^{+} pDCs of all mice tested (Fig. 3.2.6a A, E and H). This correlated with a significant higher MFI for YFP in BATF$^{+/-}$ pDCs as compared to BATF$^{+/+}$ and BATF$^{-/-}$ pDCs (Fig. 3.2.6aB and F). Despite this, pDC activation markers CD86 and MHCII were equally upregulated in BATF$^{+/-}$ and BATF$^{-/-}$ pDCs following stimulation (Fig. 3.2.6aC, G and K). Interestingly, IFNβ/YFP^{+} pDCs from BATF$^{+/-}$ mice had a higher MFI for CD86 but not MHCII compared to IFNβ/YFP^{-} pDCs after stimulation with CpG 1668/B or CpG 2216/A, while IFNβ/YFP^{+} pDCs from BATF$^{-/-}$ mice had a higher MFI for both, CD86 and MHCII as compared to IFNβ/YFP^{-} pDCs for the same stimuli (Fig. 3.2.6aI and J). In contrast to our *in vitro* findings, these data show that after *in vivo* stimulation with CpG BATF$^{-/-}$ mice have a reduced number of IFNβ-producing pDCs in the spleen.

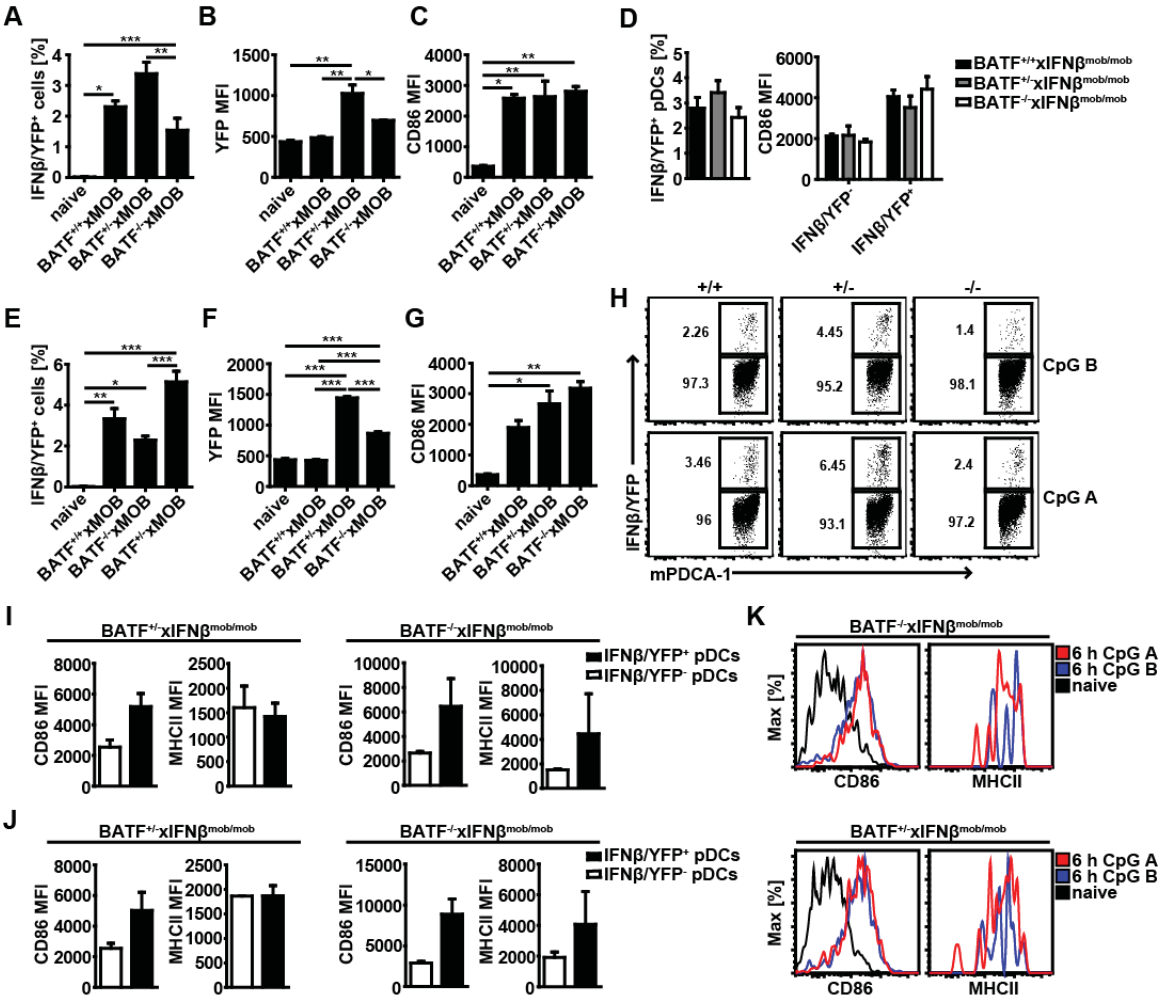

Fig. 3.2.6a Expression of IFNβ/YFP by splenic pDCs of BATF$^{+/+}$, BATF$^{+/-}$ and BATF$^{-/-}$ mice *in vivo*.
(A) Percentage, (B) YFP MFI and (C) CD86 MFI of IFNβ/YFP expressing pDCs 6 h and (D) 24 h after i.v. injection with CpG 1668/B complexed to DOATP. (E) Percentage, (F) YFP MFI and (G) CD86 MFI of IFNβ/YFP expressing pDCs 6 h after i.v. injection with CpG 2216/A complexed to DOATP. (H) FACS analysis of IFNβ/YFP production by pDCs. (I-K) Upregulation of CD86 (I and K) or MHCII (J, K) on BATF$^{+/-}$ and BATF$^{-/-}$ pDCs upon stimulation with CpG 1668/B (I,K) or CpG 2216/A (J, K). (n=3; H and K one representative experiment is shown.)

In order to explain this discrepancy, we next analysed the *in vivo* surface marker phenotype of IFNβ/YFP$^+$ pDCs in BATF$^{+/+}$xIFNβ$^{mob/mob}$, BATF$^{+/-}$xIFNβ$^{mob/mob}$ and BATF$^{-/-}$xIFNβ$^{mob/mob}$ mice after stimulation with CpG 1668/B or CpG 2216/A for 6 h. In previous studies we could show that after TLR9 activation, splenic IFNβ/YFP$^+$ pDCs are CD11c^{int} mPDCA-1$^+$ B220$^+$ SiglecH$^+$ CCR9$^+$ but CD9$^-$ (Bauer, Dress et al., 2015 *in revision*). In general this phenotype for IFNβ/YFP$^+$ pDCs also holds true in BATF$^{+/-}$ and BATF$^{-/-}$ mice, except for lower expression of B220 on BATF$^{-/-}$ pDCs (Fig. 3.2.6bA and B). Thus, the surface marker phenotype

of IFNβ/YFP^{+} pDCs is stable and independent of the expression of the transcription factor BATF. Furthermore, in line with the lower number of IFNβ/YFP^{+} pDCs observed following stimulation, BATF$^{-/-}$ mice have significantly reduced serum IFNβ levels after CpG treatment *in vivo* (Fig. 3.2.6cA and B). Taken together, despite increased IFNβ production *in vitro*, BATF$^{-/-}$ mice show a lower IFNβ production *in vivo* after stimulation with CpG.

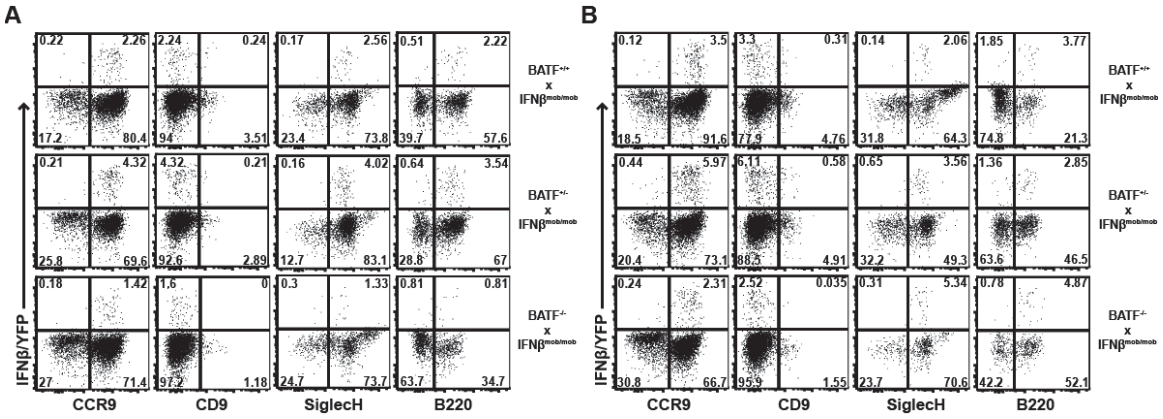

Fig. 3.2.6b Surface marker profile of IFNβ/YFP-producing pDCs of BATF$^{+/+}$, BATF$^{+/-}$ and BATF$^{-/-}$ mice *in vivo*.
(A,B) FACS analysis of surface marker expression of IFNβ/YFP producing pDCs in BATF$^{+/+}$, BATF$^{+/-}$ and BATF$^{-/-}$ mice upon stimulation with CpG 1668/B (A) or CpG 2216/A (B). (One representative experiment is shown).

Furthermore, in line with the lower number of IFNβ/YFP^{+} pDCs observed following stimulation, BATF$^{-/-}$ mice have significantly reduced serum IFNβ levels after CpG treatment *in vivo* (Fig. 3.2.6cA and B). Taken together, despite increased IFNβ production *in vitro*, BATF$^{-/-}$ mice show a lower IFNβ production *in vivo* after stimulation with CpG.

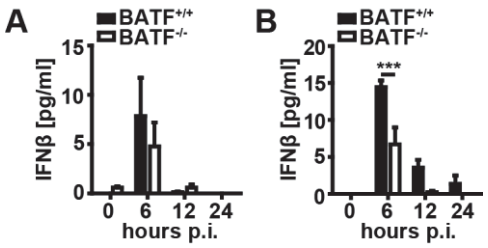

Fig. 3.2.6c Type I IFN production in BATF$^{+/+}$ and BATF$^{-/-}$ mice.
Serum ELISA for IFNβ after stimulation with CpG 1668/B (A) or CpG 2216/A (B). (n=3-6)

3.2.7 BATF$^{-/-}$ mice show increased numbers of highly activated pDCs and increased type I IFN production in later phases of infection with LCMV

Since our previous results seemed contradictory, we tried another *in vivo* stimulation approach using a more complex viral stimulus. Therefore BATF$^{-/-}$ and WT mice were infected with a low dose of the LCMV Armstrong strain (PFU 200) and spleen samples were analysed on day 3, 4 or 8 post infection. We found that, BATF$^{-/-}$ mice had a significantly lower percentage of splenic pDCs on day 3 p.i. but similar percentages of splenic cDCs early p.i. as compared to BATF$^{+/+}$ mice (Fig. 3.2.7A). Upregulation of the activation markers CD86 (Fig. 3.2.7B and C) and MHCII (Fig. 3.2.7D) was similar. Interestingly, BATF$^{-/-}$ mice had elevated serum levels of IFNα and IFNβ early after infection compared to BATF$^{+/+}$ mice (Fig. 3.2.7E). In both, BATF$^{-/-}$ and BATF$^{+/+}$ mice NK cells were normally recruited and activated after infection with LCMV (Fig. 3.2.7F and G). Surprisingly, this picture changed drastically on day 8 after LCMV infection. While the splenic pDC population had almost completely vanished in BATF$^{+/+}$ mice 8 days after infection, splenic pDCs continued to increase and were significantly higher in BATF$^{-/-}$ mice at this time point (Fig. 3.2.7H and I). This splenic BATF$^{-/-}$ pDC population was found to downregulate the surface markers B220 and CCR9 upon LCMV stimulation (Fig. 3.2.7H). Furthermore, pDCs and cDCs were more highly activated in BATF$^{-/-}$ mice relative to controls. MHCII was highly expressed and CD86 was significantly upregulated on these cell types on day 8 after infection in BATF$^{-/-}$ but was barely detectable in BATF$^{+/+}$ mice (Fig. 3.2.7J-L). Furthermore we found genes involved in type I IFN signalling to be more highly expressed in BATF$^{-/-}$ than in BATF$^{+/+}$ mice e.g. IRF7 was 3-fold higher induced in BATF$^{-/-}$ mice 8 days post infection (Fig. 3.2.7M).

In summary, after infection with LCMV BATF$^{-/-}$ mice maintain higher numbers of pDCs which are highly activated. Likely the increased DC numbers and activation state is a result of increased viral titer on day 8 (Grusdat et al., 2014) and this could be due either to defects in DC function and/or defects in T-cell activity known to occur in BATF$^{-/-}$ mice (Murphy et al., 2013). This appears to result in increased production of type I IFN in BATF$^{-/-}$ mice in the early and late phase of infection with LCMV.

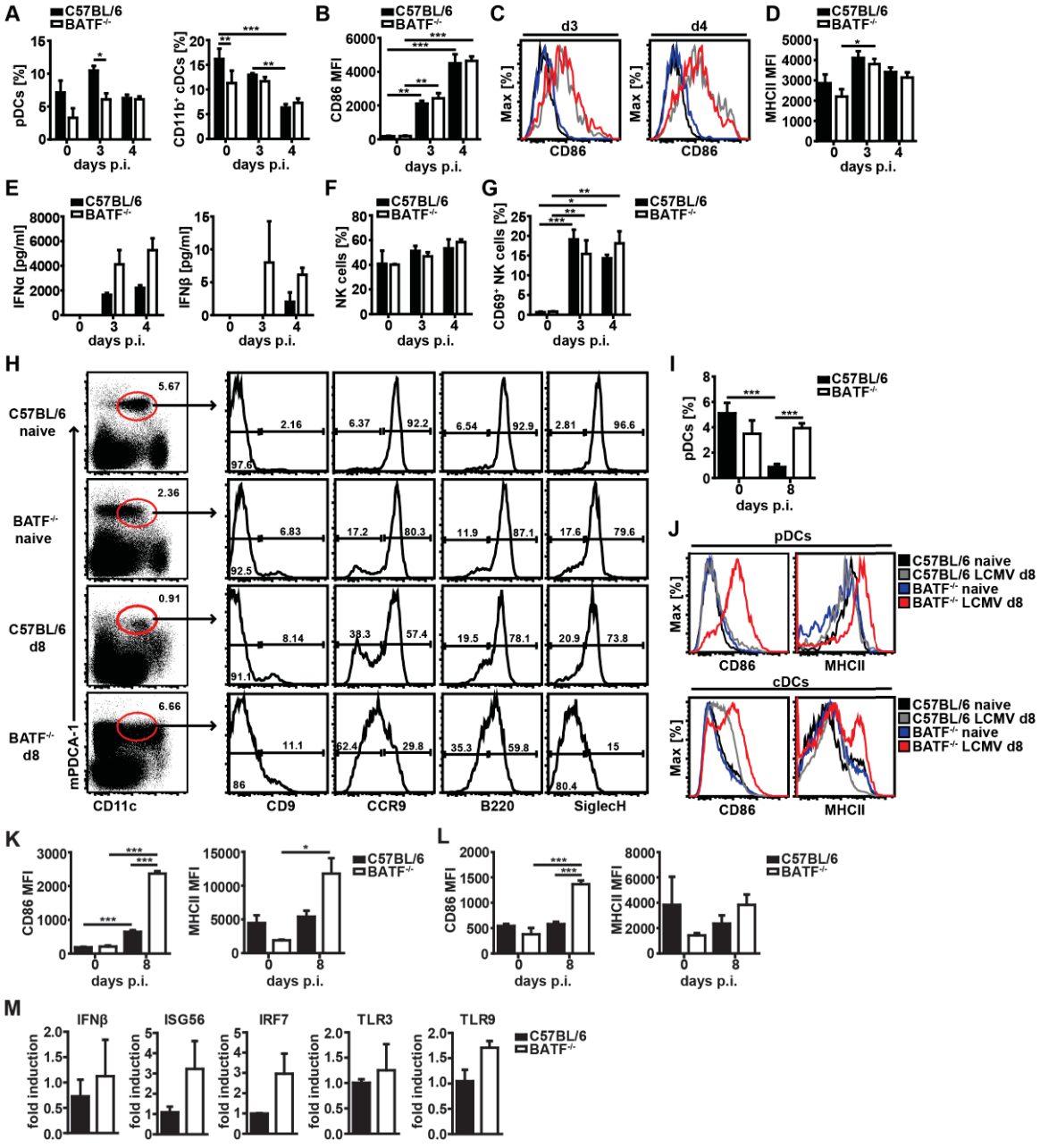

Fig. 3.2.7 The impact of BATF in DCs during infection with LCMV *in vivo*.

Percentage of pDCs (A) and cDCs (B), MFIs of the activation markers CD86 (B and C) and MHCII (D) on pDCs, serum level for type I IFN (E) and percentage of NK cells (F) and activated NK cells (G) in BATF$^{+/+}$ and BATF$^{-/-}$ mice after i.p. infection with 200 PFU LCMV Armstrong for 3 or 4 d. (H) FACS analysis of pDC surface markers in BATF$^{+/+}$ and BATF$^{-/-}$ mice after i.p. infection with 200 PFU LCMV Armstrong for 8 d. (I) Percentage of pDCs and (J and K) activation of pDCs and (J and L) cDCs after 8 d of infection. (M) qRT-PCR analysis of genes involved in type I IFN signaling by pDCs and cDCs in the liver of BATF$^{+/+}$ and BATF$^{-/-}$ mice after i.p. infection with 200 PFU LCMV Armstrong for 8 d. ((A-G) n=6, (H-M) n=9.)

3.2.8 Potential interaction of BATF with the *Ifnβ*-promoter

Since BATF is a transcription factor highly expressed in the nucleus of IFNβ-producing pDCs (see Fig. 3.2.1aH), we hypothesized that it may directly or indirectly influence the promoter activity of the IFNβ gene. To test this hypothesis, we performed a dual *Ifnβ*-luciferase assay where the interferon promoter is upstream of the luciferase (Luthra et al., 2011) with or without overexpression of *Batf* in HEK293T cells. Indeed, with increasing BATF concentrations we could observe increasing luciferase induction (Fig. 3.2.8). This hints at a possible interaction of BATF with the *Ifnβ*-promoter, and provides a potential explanation for the involvement of BATF in IFNβ production by pDCs.

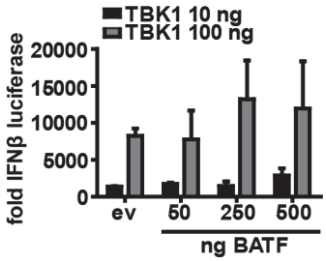

Fig. 3.2.8 Luciferase assay for BATF-Ifnβ-promoter interactions.
(ev = empty vector) (n=1, triplicates)

3.2.9 BATF$^{-/-}$ mice are protected in the early phase of infection with *T. gondii*

As described in chapter 3.4 we are interested in the influence of type I IFN during infection with the protozoan parasite *T. gondii*. Our results described above have shown that BATF has an impact on IFNβ production by pDCs after TLR9 stimulation with CpG or CMV. Therefore we were interested in the outcome of *T. gondii* infection in BATF$^{-/-}$ mice. Surprisingly, relative to BATF$^{+/+}$, BATF$^{-/-}$ mice seem to be partially protected in the early phase of infection but then unlike BATF$^{+/+}$, rapidly succumb the *T. gondii* infection in the chronic phase (after 30 days) of infection (Fig. 3.2.10). We suspect that early increase in IFNβ production in BATF$^{-/-}$ mice might offer a survival advantage during the early phases of infection, whereas additional defects may impair survival during long term infection.

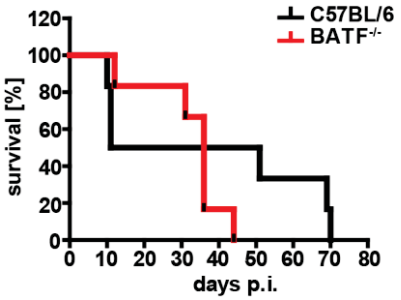

Fig. 3.2.9 Survival of BATF$^{-/-}$ vs. C57BL/6 mice after infection with *T. gondii*. (n=6)

3.3 PSD-93 and its role in IFNβ producing splenic pDCs

PSD-93 is well described as a postsynaptic neuronal protein with functions including involvement in assembly of the N-methyl-D-aspartate receptor (Brenman et al., 1996; Carlisle et al., 2008; Kim et al., 1996). However, a function for this protein in immune cells has not yet been described. Interestingly, we found PSD-93 to be the highest differentially expressed gene in splenic IFNβ-producing pDCs vs. non-IFNβ-producing pDCs after TLR9 stimulation (3.1). Therefore, we hypothesize that this gene might have an important impact on induction of *Ifnb* and in the function of IFNβ-producing pDCs. The following chapter aims to gain insight into the possible role of PSD-93 in IFNβ-producing pDCs.

3.3.1 IFNβ/YFP-producing pDCs highly upregulate PSD-93 upon TLR9 stimulation

First we sought to verify the expression of PSD-93 in IFNβ-producing pDCs in an independent experimental approach. To this end we FACS sorted CD11b^{-} CD11c^{int}mPDCA-1^{+}IFNβ/YFP^{-} and CD11b^{-}CD11c^{int}mPDCA-1^{+}IFNβ/YFP^{+} pDCs from IFNβ$^{mob/mob}$ and IFNAR1$^{-/-}$xIFNβ$^{mob/mob}$ mice 6 h after stimulation with the TLR9 ligand CpG 1668 (B type CpG). qRT-PCR analysis on cDNA from the sorted pDC populations confirmed that IFNβ/YFP^{+} pDCs differentially upregulate PSD-93, up to 150-fold in WT mice and up to 20-fold in IFNAR1$^{-/-}$ mice, as compared to IFNβ/YFP^{-} pDCs (Fig. 3.3.1A and B). Furthermore, immunofluorescence analysis of BM-derived Flt3-L-differentiated pDCs revealed that upon stimulation with CpG 1668/B for 24 h, PSD-93 appeared to be

expressed within the membrane structure of IFNβ/YFP^{+} pDCs while it was undetectable in unstimulated pDCs (Fig. 3.3.1C) or IFNβ/YFP^{-} pDCs (data not shown). These data confirm that PSD-93 is significantly differentially expressed in IFNβ-producing pDCs vs. non-producing pDCs after TLR9 stimulation.

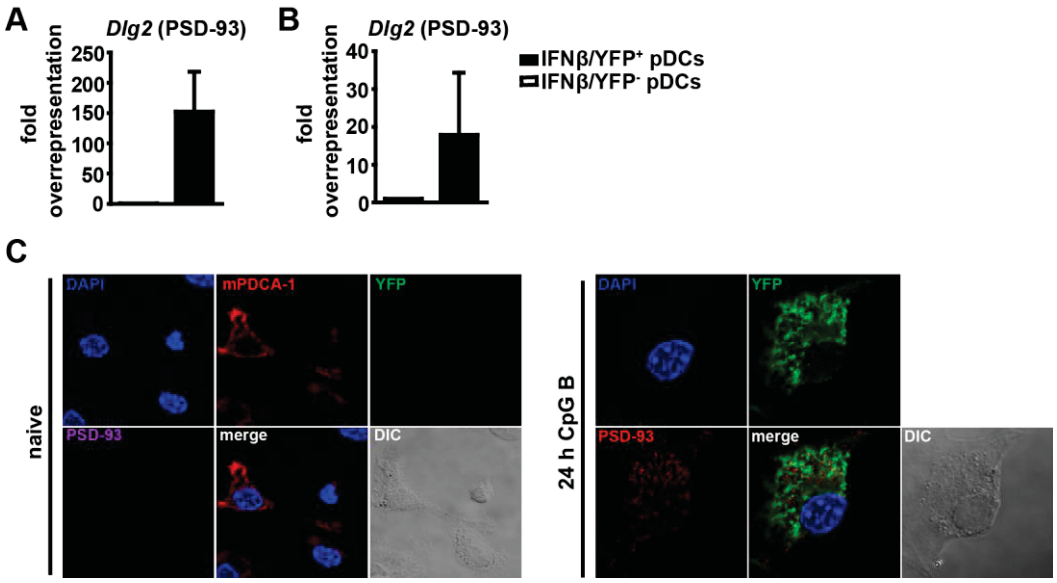

Fig. 3.3.1 PSD-93 expression in IFNβ-producing pDCs.
(A, B) qRT-PCR analysis of sorted IFNβ/YFP^{-} vs. IFNβ/YFP^{+} splenic pDCs for expression of (A) Dlg2 (PSD-93) in IFNβ$^{mob/mob}$ mice (B) Dlg2 (PSD-93) in IFNAR1$^{-/-}$xIFNβ$^{mob/mob}$ mice 6 h after i.v. injection with CpG 1668/B complexed to DOTAP. (C) Immunofluorescence images of PSD-93 expression in BM-Flt3-L-derived IFNβ/YFP^{+} pDCs 0 h and 24 h after stimulation. (For (A,B) n=3 is shown (each sample is pooled from 12 mice). (C) One representative experiment out of three is shown.)

3.3.2 PSD-93$^{-/-}$ BM-Flt3-L-derived DCs develop normally

PSD-93 is a membrane protein known to be involved in receptor signalling pathways in neurons (Brenman et al., 1996; Carlisle et al., 2008; Kim et al., 1996). It can be speculated that a lack of this protein in pDCs might be accompanied by either developmental defects of these cells, altered expression of surface markers, or lack of response to natural or synthetic stimuli triggering membrane receptor signal transduction pathways. To investigate these possibilities we made use of PSD-93$^{-/-}$ mice (McGee et al., 2001). First we sought to analyse potential differentiation defects in BM-derived pDCs. We therefore generated BM-derived-Flt3-L-differentiated DCs *in vitro*. We could not observe

differences in percentages of pDCs (e.g. ~26 % without stimulation) and cDCs (e.g. ~22-25 % without stimulation) in both wildtype and PSD-93$^{-/-}$ cultures. No significant differences were detected in expression of specific surface markers on pDCs between the two genotypes, and PSD-93$^{-/-}$ pDCs showed normal expression of classic BM-derived pDC markers such as CD11b, B220, mPDCA-1, CD8α, CD9, or CCR9 (Fig. 3.3.2A). Furthermore, we could not detect any significant differences in the expression of CD86 or MHCII on CD11b^{-} CD11c^{+}B220^{+} pDCs or CD11b^{+}CD11c^{+}B220^{-} cDCs from these cultures upon stimulation with the TLR9 ligands CpG 1668/B or CpG 2216/A or the TLR3 ligand Poly(I:C) (Fig. 3.3.2B and C). Taken together, PSD-93$^{-/-}$ mice appear to have normal differentiation capacities of cDCs and pDCs in the bone marrow derived cultures.

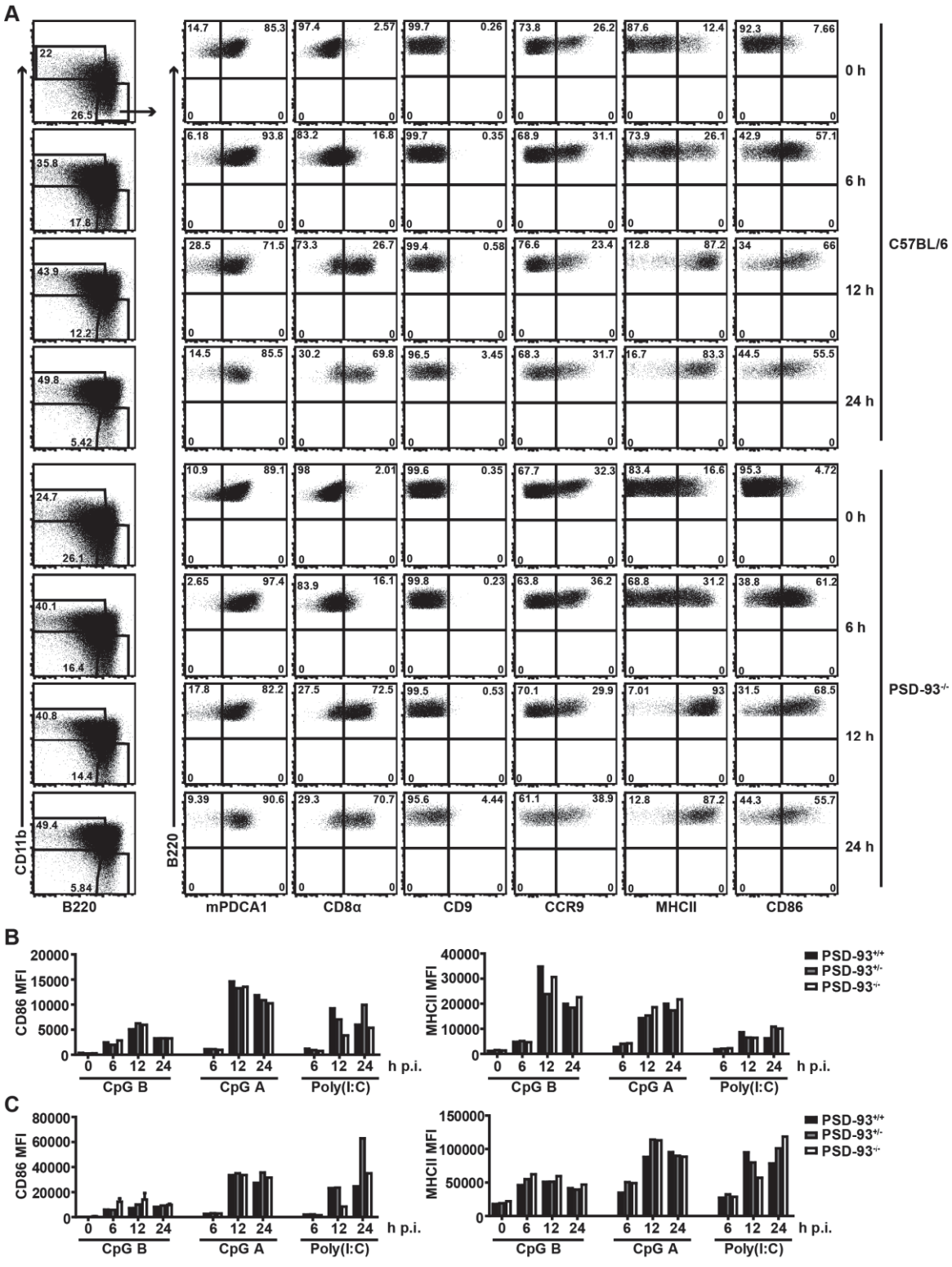

Fig. 3.3.2 Differentiation capacity and activation status of PSD-93$^{-/-}$ Flt3-L-derived DCs after TLR stimulation *in vitro*.

(A) FACS analysis of BM-Flt3-L-derived pDC surface marker expression 0 h, 6 h, 12 h and 24 h after stimulation with CpG 1668/B complexed to DOTAP. MFI for CD86 and MHCII after stimulation with either CpG 1668/B complexed to DOTAP, CpG 2216/A or Poly(I:C) on (B) pDCs and (C) cDCs. (Shown is one representative experiment out of three).

3.3.3 PSD-93$^{-/-}$ mice have increased numbers of pDCs

Next we wanted to know, if this normal development of DCs observed in an *in vitro* BM-cell culture system reflects the *in vivo* situation. Therefore we analysed the DC populations from different tissues from naïve and CpG-stimulated PSD-93$^{-/-}$ mice. Overall, there was a significant increase in the absolute number of cells in the spleen and a decrease in absolute cell counts in the liver of naïve PSD-93$^{-/-}$ mice as compared to PSD-93$^{+/-}$ and PSD-93$^{+/+}$ mice (Fig. 3.3.3A). Interestingly, this was mirrored by significantly increased numbers of splenic cDCs (2-fold higher) in naïve PSD-93$^{-/-}$ mice and splenic pDCs (2-3-fold higher) in naïve and CpG-stimulated PSD-93$^{-/-}$ mice as compared to WT mice (Fig. 3.3.3B and C). Overall, PSD-93$^{-/-}$ mice had higher absolute numbers of pDCs in liver, lung and LNs before and/or after 24 h stimulation with CpG (Fig. 3.3.3C). Also, percentages for CD11b^{-}CD11c^{int}mPDCA-1^{+} pDCs were higher in PSD-93$^{-/-}$ mice than WT or PSD-93-heterozygous mice e.g. 3.25 % pDCs in the spleen of PSD-93$^{+/+}$ mice and 5.31 % pDCs in the spleen of PSD-93$^{-/-}$ mice (Fig. 3.3.3D and E). We could not observe any obvious differences in the expression of activation markers such as CD86 and MHCII on naïve or CpG stimulated pDCs from PSD-93$^{+/+}$, PSD-93$^{+/-}$ or PSD-93$^{-/-}$ mice (Fig. 3.3.3E). Furthermore, in line with the *in vitro* data, naïve PSD-93$^{-/-}$ pDCs exhibited the same surface marker profile as PSD-93$^{+/+}$ mice as shown in Fig. 3.3.3.F. An exception to this is a slight upregulation of CD9 from ~2.6 % CD9^{+} cells for PSD-93$^{+/+}$ pDCs to ~7 % for PSD-93$^{-/-}$ pDCs.

Taken together, our data show, that PSD-93$^{-/-}$ mice have elevated numbers of pDCs and that these pDCs are able develop and express the classic pDCs surface marker profile.

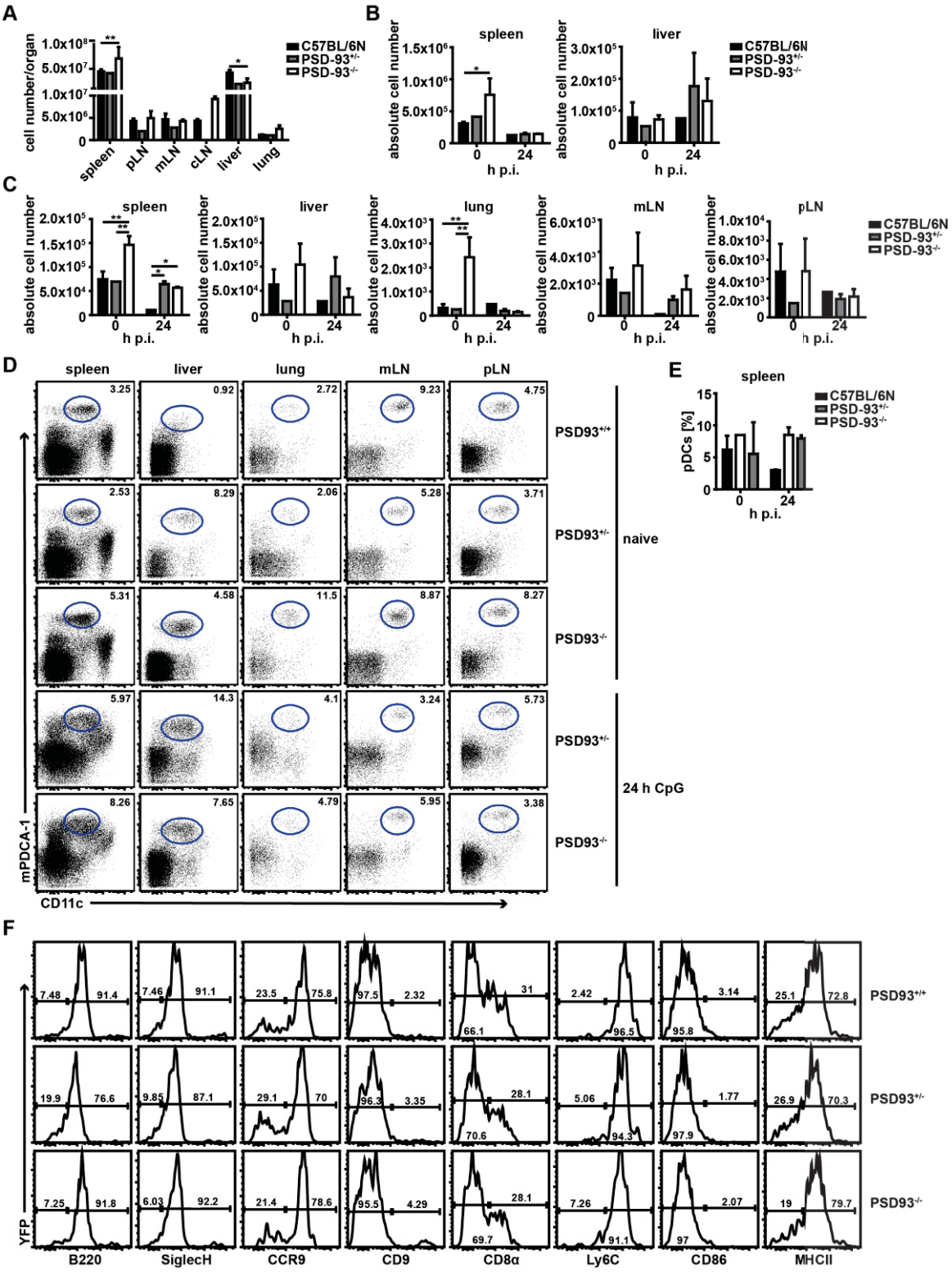

Fig. 3.3.3 Analysis of DC population in PSD-93$^{-/-}$ mice *in vivo*.

(A) Total number of cells in spleen, liver, lung and LNs in naive PSD-93$^{-/-}$ mice. Absolute numbers of (B) cDCs in spleen and liver and (C) pDCs spleen, liver, lung and LNs in naive PSD-93$^{-/-}$ mice whole organ cell numbers. (D, E) FACS analysis and percentage of pDC populations in spleen, liver, lung and LNs in PSD-93$^{-/-}$ mice 0 h and 24 h after i.v. injection of CpG 1668/B complexed to DOTAP. (F) FACS analysis of surface marker expression on naive

WT and PSD-93$^{-/-}$ pDCs. For FACS analysis cells were gated on living, non B/T cells; pDCs were gated on CD11b^{-} CD11c^{int}mPDCA-1^{+}; cDCs were gated on CD11b^{+}CD11c^{+}. ((A-C) n=3, (D-F) n=1-2.)

3.3.4 PSD-93$^{-/-}$ BM-Flt3-L-derived pDCs produce higher amounts of IFNβ after infection with MCMV but not stimulation with CpG *in vitro*

Our previous data raised the question as to whether PSD-93$^{-/-}$ mice would express higher levels of type I IFN since they have more pDCs and cDCs able to produce these cytokines. In order to test this hypothesis we crossed IFNβ-reporter mice (IFNβ$^{mob/mob}$) with PSD-93$^{-/-}$ mice and generated a new PSD-93$^{-/-}$ xIFNβ$^{mob/mob}$ mouse strain. Our first experiment after generating these mice was to analyse BM-derived Flt3-L-differentiated pDCs from PSD-93$^{-/-}$xIFNβ$^{mob/mob}$ mice to investigate the IFNβ production by PSD-93$^{-/-}$ pDCs. We found, that after 6 h or 24 h of stimulation with CpG 2216/A or Poly(I:C) there are no significant differences in the percentage of IFNβ/YFP^{+} pDCs: ~15 % with CpG and ~0.5-1.5 % with Poly(I:C) in PSD-93$^{+/+}$ as well as PSD-93$^{-/-}$ pDCs (Fig. 3.3.4A, B and C). In line with this, IFNα and IFNβ levels in the supernatant of CpG stimulated pDCs were comparable for PSD-93$^{+/+}$ and PSD-93$^{-/-}$ (Fig. 3.3.4D). However, upon infection of cell cultures with MCMV, PSD-93$^{-/-}$ pDCs produced more IFNβ/YFP after 6 h and 24 h of infection: e.g. ~15 % of the PSD-93$^{-/-}$ pDCs were IFNβ/YFP^{+} and only ~9 % of the PSD-93$^{+/+}$ pDCs after 24 h of infection (Fig. 3.3.4E and A). There were neither significant differences in the activation of the overall pDC population after infection with MCMV nor between the activation status of IFNβ/YFP^{-} and IFNβ/YFP^{+} pDCs of PSD-93$^{+/+}$, PSD-93$^{+/-}$ and PSD-93$^{-/-}$ pDCs after 6 h or 24 h stimulation with CpG or infection with MCMV (data not shown). These data confirm our hypothesis that PSD-93$^{-/-}$ pDCs are able to produce larger amounts of IFNβ, at least *in vitro* and after infection with MCMV.

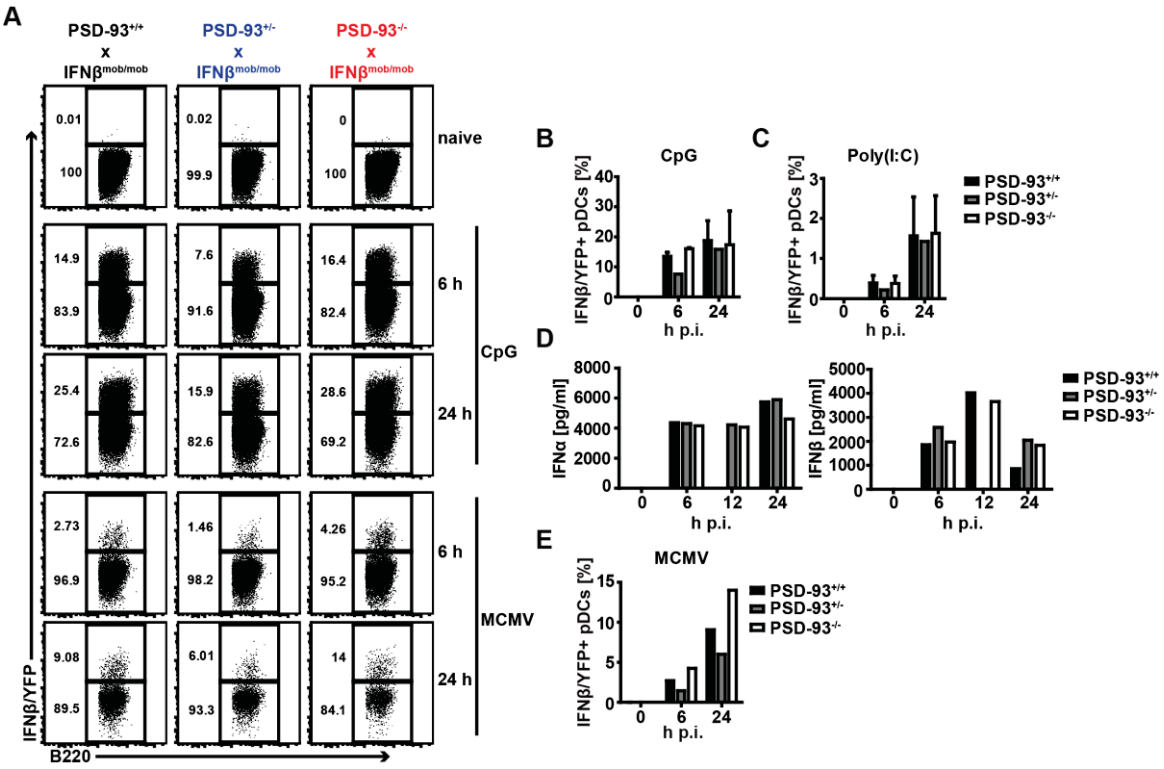

Fig. 3.3.4 Analysis of IFNβ/YFP production by PSD-93$^{-/-}$ pDCs *in vitro* upon TLR stimulation.

(A) FACS analysis of IFNβ/YFP production by pDCs from WT and PSD-93$^{-/-}$ mice after stimulation with CpG 2216/A or MCMV C3X (MOI 1) for 0 h, 6h or 24 h. Percentage of IFNβ/YFP producing BM-Flt3-L-derived pDCs after stimulation with (B) CpG 2216/A or (C) Poly(I:C) for 0 h, 6h and 24 h. (D) IFNα and IFNβ levels in the supernatant after stimulation with CpG 2216/A. (E) Percentage of IFNβ/YFP producing BM-Flt3-L-derived pDCs after infection with MCMV C3X (MOI 1) for 0 h, 6 h and 24 h. ((A) One representative out of two experiments; (B) n=2; (C-E) n=1.)

3.3.5 PSD-93$^{-/-}$ mice possess a lower percentage but increased absolute number of IFNβ producing pDCs after TLR9 stimulation *in vivo*

We next investigated the production of IFNβ by PSD-93$^{-/-}$ mice *in vivo*. Therefore we injected PSD-93$^{-/-}$xIFNβ$^{mob/mob}$ mice with CpG 1668/B for 6 h. PSD-93$^{-/-}$ mice had overall higher numbers of pDCs. In line with this absolute numbers of IFNβ/YFP^{+} cells and IFNβ/YFP^{+} pDCs were significantly higher (~2-fold) in PSD-93$^{-/-}$ mice compared to PSD-93$^{+/+}$ mice (Fig. 3.3.5aA) in spite a lower percentage of IFNβ/YFP^{+} pDCs in PSD-93$^{-/-}$ mice (Fig. 3.3.5aB and C). Compared to controls, the MFI of YFP was also elevated in the PSD deficient context (Fig. 3.3.5aD) while the activation status of pDCs was comparable: Both PSD-93$^{-/-}$ and PSD-93$^{+/+}$ pDCs equally upregulated CD86 upon CpG stimulation (Fig. 3.3.5aE and G). Also, there was no difference between the activation status of IFNβ/YFP^{+} pDCs from PSD-93$^{-/-}$ and PSD-93$^{+/+}$ mice while IFNβ/YFP^{+} pDCs from PSD-93$^{-/-}$

mice showed a slightly lower expression of MHCII as compared to IFNβ/YFP^{+} pDCs from PSD-93$^{+/+}$ mice (Fig. 3.3.5aF and G). The surface marker expression profile of IFNβ/YFP^{+} pDCs from PSD-93$^{+/+}$, PSD-93$^{+/-}$ and PSD-93$^{-/-}$ mice 6 h after stimulation with CpG was comparable and exhibited no obvious differences in surface marker expression (Fig. 3.3.5aH).

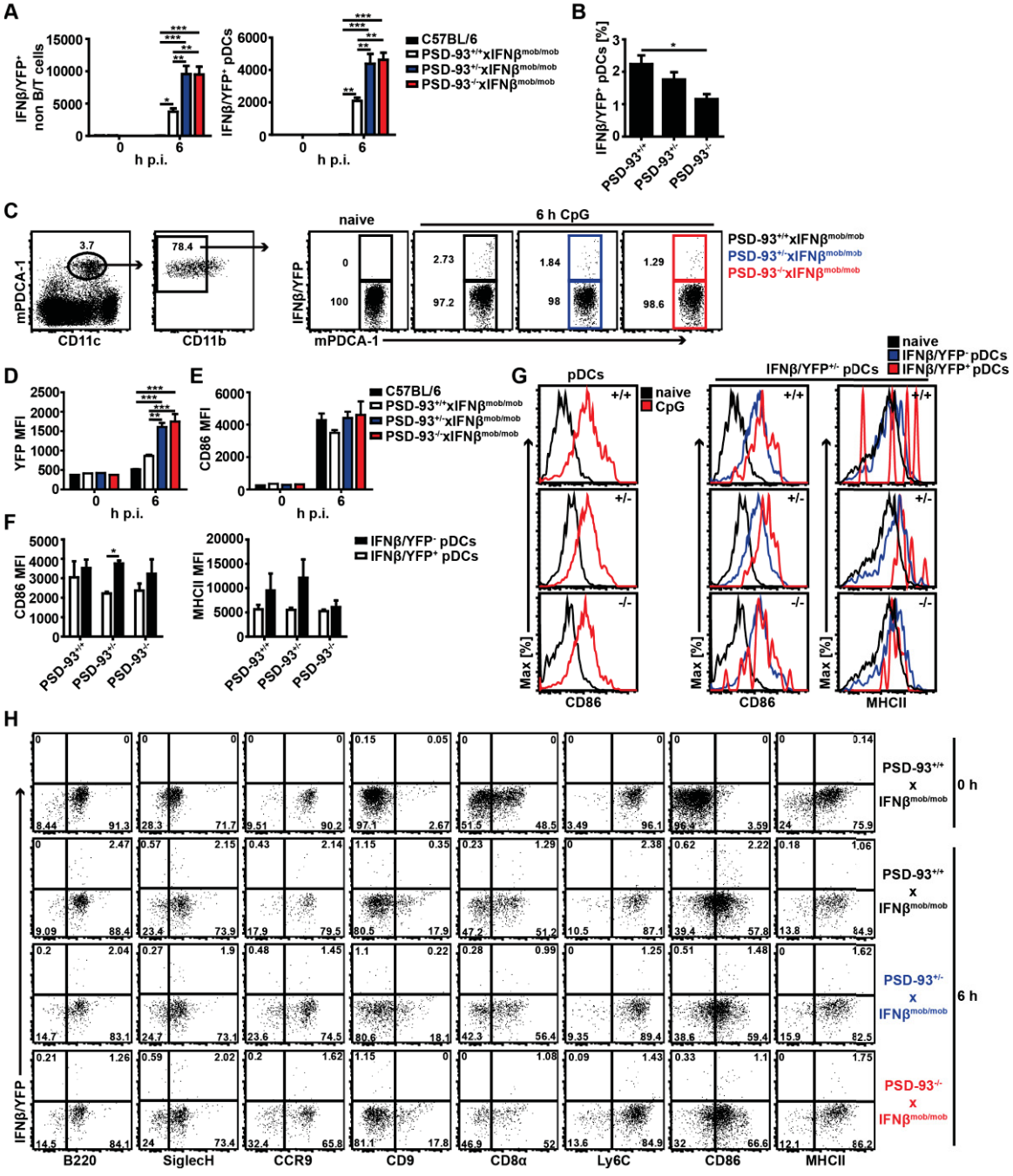

Fig. 3.3.5a IFNβ production by PSD-93$^{-/-}$ pDCs after TLR9 stimulation *in vivo*.

(A) Absolute cell number and (B, C) percentage of IFNβ-producing non B/T cells and pDCs 0 h and 6 h after stimulation with CpG 1668/B. (D) YFP MFI and (E) CD86 MFI of pDCs and (F) CD86 MFI and MHCII MFI of IFNβ/YFP^{-}

vs. IFNβ/YFP$^+$ pDCs in WT and PSD-93$^{-/-}$ mice after i.v. injection of CpG 1668/B complexed to DOTAP for 0 h or 6 h. (G) MFI for CD86 on pDCs, CD86 and MHCII on IFNβ/YFP$^-$ vs. IFNβ/YFP$^+$ pDCs and (H) FACS analysis of expression of surface markers on IFNβ/YFP-producing pDCs from WT and PSD-93$^{-/-}$ mice after i.v. injection of CpG 1668/B complexed to DOTAP for 0 h or 6 h. Cells are pregated on living, CD3ε$^-$CD19$^-$, gating strategy for CD11b$^-$CD11c^{int}mPDCA-1$^+$ pDCs is shown in (C). (n=3; (C,G,H) One representative is shown.)

Furthermore, we could detect significantly increased levels for IFNα, not for IFNβ, in spleen and liver of PSD-93$^{-/-}$ mice 6 h after stimulation with CpG (Fig. 3.3.5b). These effects were not seen in the serum of these mice (data not shown).
In summary, despite lower percentages of IFNβ/YFP$^+$ pDCs PSD-93$^{-/-}$ mice have significantly increased absolute numbers of IFNβ/YFP$^+$ pDCs and IFNα organ levels after TLR9 stimulation with CpG *in vivo*.

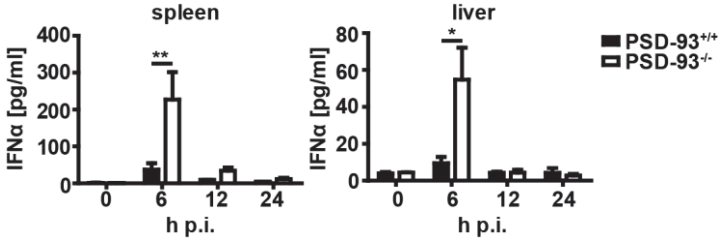

Fig. 3.3.5b Serum type I IFN level after stimulation with CpG 2216/A *in vivo*. (n=3)

3.3.6 PSD-93$^{-/-}$ mice display an increased susceptibility towards infection with *T. gondii*

We have shown that PSD-93 is highly upregulated in IFNβ-producing pDCs and might play a role in inducing IFNβ production by these pDCs after TLR9 stimulation. Therefore, we were interested in the impact of PSD-93-deficiency during infection. As a model we chose the infection with the intracellular parasite *T. gondii*. Surprisingly, PSD-93$^{+/+}$ and PSD-93$^{+/-}$ mice mice were protected in the early phase of infection with *T. gondii* but started to succumb the infection starting around day 35 p.i., while PSD-93$^{-/-}$ mice showed higher susceptibility already in the early phase of infection around day 5. Almost 40 % of the PSD-93$^{-/-}$ mice died by day 10 post infection while 100 % of PSD-93$^{+/+}$ and PSD-93$^{+/-}$ mice were still alive (Fig. 3.3.3.6). This is an interesting outcome, raising the possibility that PSD-93 might be essential for proper signalling downstream of TLR9 to

induce production of IFNβ. Also PSD-93$^{-/-}$ mice produce lower amounts of IFNβ a key factor during host response to *T. gondii.*

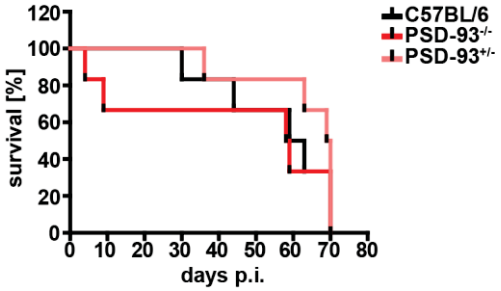

Fig. 3.3.6 Survival of PSD-93$^{-/-}$ mice after infection with 40 cysts *T. gondii.* (n=6)

3.4 Type I IFN play a crucial role in host defence against T. gondii

The protozoan parasite *Toxoplasma gondii* is one of the most prevalent human parasites worldwide. While rather harmless in healthy individuals, an infection with *T. gondii* in immunosuppressed patients can be quite dangerous, and during pregnancy can lead to deformation of the embryo or even abortion. While the essential importance of IFNγ in host response to infection with *T. gondii* is well established the impact of type I IFN is, so far, poorly described. Therefore we were interested to test whether type I IFNs have a function in host protection against *T. gondii*.

3.4.1 IFNβ$^{-/-}$ and IFNAR1$^{-/-}$ mice are highly susceptible towards infection with *T. gondii*

In order to investigate, if type I IFN, namely IFNα and IFNβ, play a role in infection with *T. gondii*, we first infected WT and IFNβ$^{-/-}$ mice with a low dose of 20 cysts of the *T. gondii* strain ME49 and analysed their survival after infection. While in the early phase of infection WT and IFNβ$^{-/-}$ mice were able to handle the infection, IFNβ$^{-/-}$ mice succumbed to the infection significantly more rapidly in the chronic phase starting around day 35 p.i. (Fig. 3.4.1A). This outcome indicates that IFNβ has an important role in host protection against *T. gondii.* Next we

included IFNAR1$^{-/-}$ mice into our studies and infected all three genotypes with a dose of 40 cysts of *T. gondii* ME49. Following this, up to 30 % of the IFNβ$^{-/-}$ and IFNAR1$^{-/-}$ mice died around day 10 after infection, followed by a plateau phase of survival till day 25 when almost all IFNβ$^{-/-}$ and IFNAR1$^{-/-}$ mice started to succumb the infection. In contrast to this, WT mice survived at least till the chronic phase and at the end of our survival analysis >50 % of WT mice were still alive compared to less than 20 % of IFNAR1$^{-/-}$ mice and <10 % of IFNβ$^{-/-}$ mice (Fig. 3.4.1B). We found, that after infection with *T. gondii* the survival of IFNβ$^{-/-}$ and IFNAR1$^{-/-}$ mice was significantly decreased as compared to WT mice while no differences in loss of weight were detected between the three genotypes tested (Fig .3.4.1C). In line with this IFNβ$^{-/-}$ mice had significantly higher brain cyst loads on day 25 p.i. as compared to WT mice. On day 35 p.i. cyst loads in both IFNβ$^{-/-}$ and IFNAR1$^{-/-}$ mice were significantly increased while they remained unchanged in WT mice (Fig. 3.4.1D). Of note, absolute cell numbers in most tissues did not differ between the genotypes. Solely, in the spleen and mesenteric LN we could observe significant changes in the recruitment or proliferation of absolute cells around day 7 and 12 post infection. Cell numbers in IFNβ$^{-/-}$ mice were already significantly increased on day 7 p.i. and decreased again on day 12 p.i. while splenic cell numbers in WT mice peaked on day 12 p.i.. Interestingly, IFNAR1$^{-/-}$ mice failed to increase cell numbers in the mesenteric LNs as efficiently as WT or IFNβ$^{-/-}$ mice on day 7 p.i. (Fig. 3.4.1E). Our data demonstrate that IFNβ$^{-/-}$ mice as well as IFNAR1$^{-/-}$ mice are highly susceptible towards infection with *T. gondii*, as they show decreased survival and increased brain cyst loads after i.p. infection of 40 cysts *T. gondii* ME49.

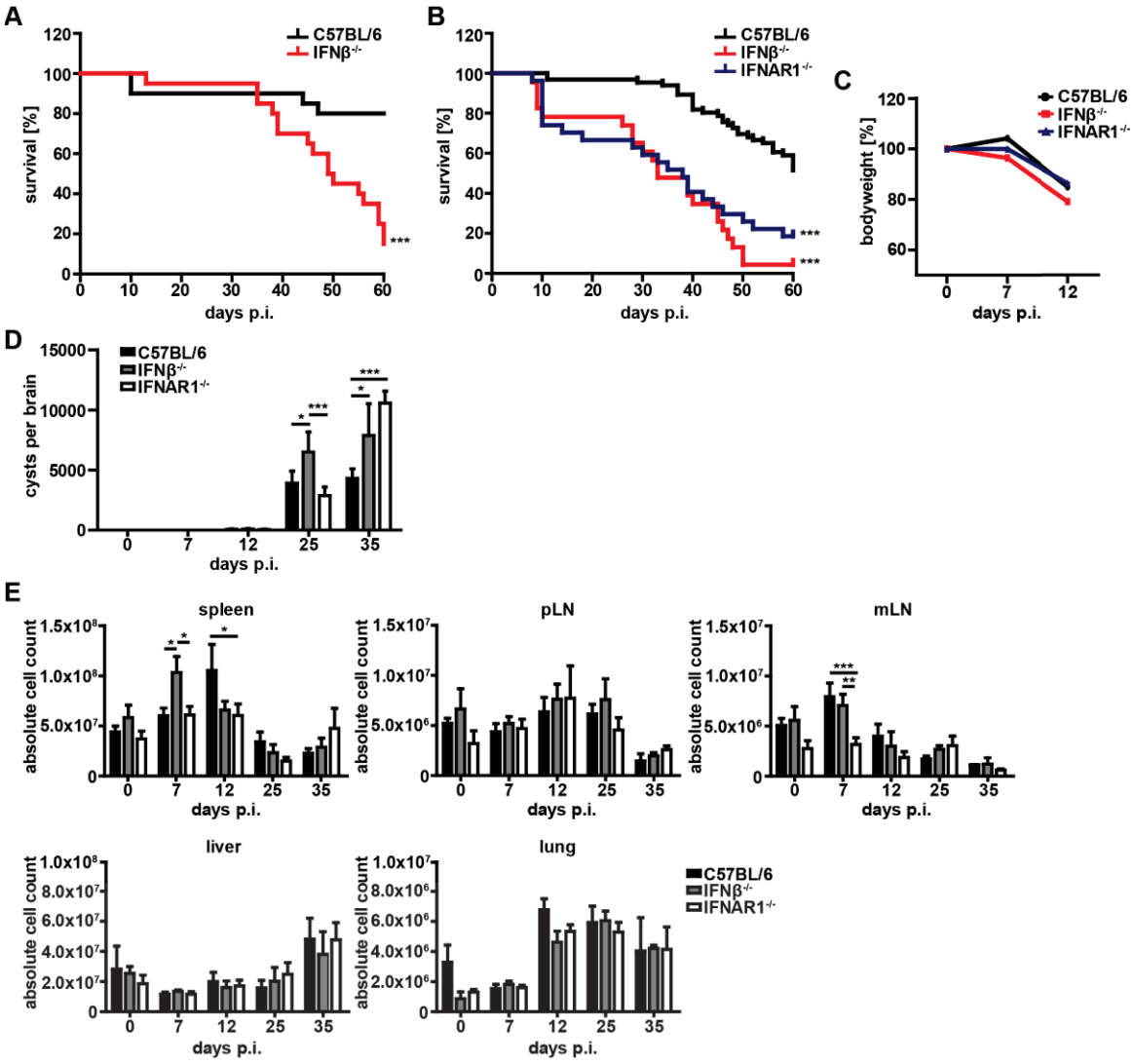

Fig. 3.4.1 Decreased survival of IFNβ$^{-/-}$ and IFNAR1$^{-/-}$ mice after infection with *T. gondii*.

Survival after i.p. infection with (A) 20 cysts or (B) 40 cysts of *T. gondii* ME49. (C) Bodyweight and (D) cyst load in the brain of WT and IFNβ$^{-/-}$ and IFNAR1$^{-/-}$ mice after i.p. infection with 40 cysts *T. gondii* ME49. (E) Analysis of organ cell numbers after i.p. infection with 40 cysts *T. gondii* ME49.

3.4.2 IFNβ$^{-/-}$ and IFNAR1$^{-/-}$ mice fail to induce efficient IFNγ response after infection with *T. gondii*

IFNγ and IL-12 are crucial cytokines for induction of a successful host defence against *T. gondii.* Therefore we wondered if the increased susceptibility of IFNβ$^{-/-}$ and IFNAR1$^{-/-}$ mice towards this infection is due to a lack of these cytokines. In order to investigate this we analysed protein and RNA levels of IFNγ and IL-12 and genes involved in type I IFN signalling in WT, IFNβ$^{-/-}$ and IFNAR1$^{-/-}$ mice up to 25 days after infection. We found that WT mice had a significant increase in

serum IFNγ in the first days after infection with a sudden peak of ~400 pg/µl on day 7 (Fig.3.4.2A). While this IFNγ level stayed high in WT mice at least till day 12 p.i. IFNβ$^{-/-}$ and IFNAR1$^{-/-}$ mice failed to mount a stable IFNγ response. Both knockouts had elevated IFNγ levels on day 7 p.i.. In contrast to WT levels, these amounts were decreased to basal levels again on day 12 p.i. (Fig.3.4.2B). Interestingly, serum IFNβ levels in WT mice were slowly increasing with time of infection, while IFNAR$^{-/-}$ had significantly increased levels of IFNβ on day 7 p.i., just before the first drop in survival, and lower levels after this point (Fig. 3.4.2C). We could not detect any IFNβ levels in the serum of IFNβ$^{-/-}$ mice (data not shown). Of note, serum IL-12 levels showed similar increases over the course of infection in WT, IFNβ$^{-/-}$ and IFNAR1$^{-/-}$ mice (Fig. 3.4.2D). Obviously, there was no defect in IL-12 production by IFNβ$^{-/-}$ and IFNAR1$^{-/-}$ mice. We also compared the expression of *Ifnγ* and *Il-12* on RNA level in spleen and liver. Surprisingly, there were no differences at all in IFNγ expression in the spleen but marked differences in the liver. At day 7 p.i. WT mice had an almost 10-fold higher induction of IFNγ than IFNβ$^{-/-}$ and IFNAR1$^{-/-}$ mice and exhibited also higher levels of *Ifnγ* mRNA throughout the course of infection. (Fig. 3.4.2E). Furthermore, despite the comparable protein levels of IL-12, on mRNA expression level there were massive differences in the induction of this cytokine in WT and IFNβ$^{-/-}$ and IFNAR1$^{-/-}$ mice in the spleen but not in the liver. Both, IFNβ$^{-/-}$ as well as IFNAR1$^{-/-}$ mice displayed an increased induction of *Il-12* message as compared to WT mice in the spleen. Of note, while *Il-12* induction peaked on day 7 p.i. in IFNβ$^{-/-}$ mice, IFNAR1$^{-/-}$ mice showed the highest expression levels for *Il-12* in the chronic phase of infection around day 25 p.i. (Fig. 3.4.2F).

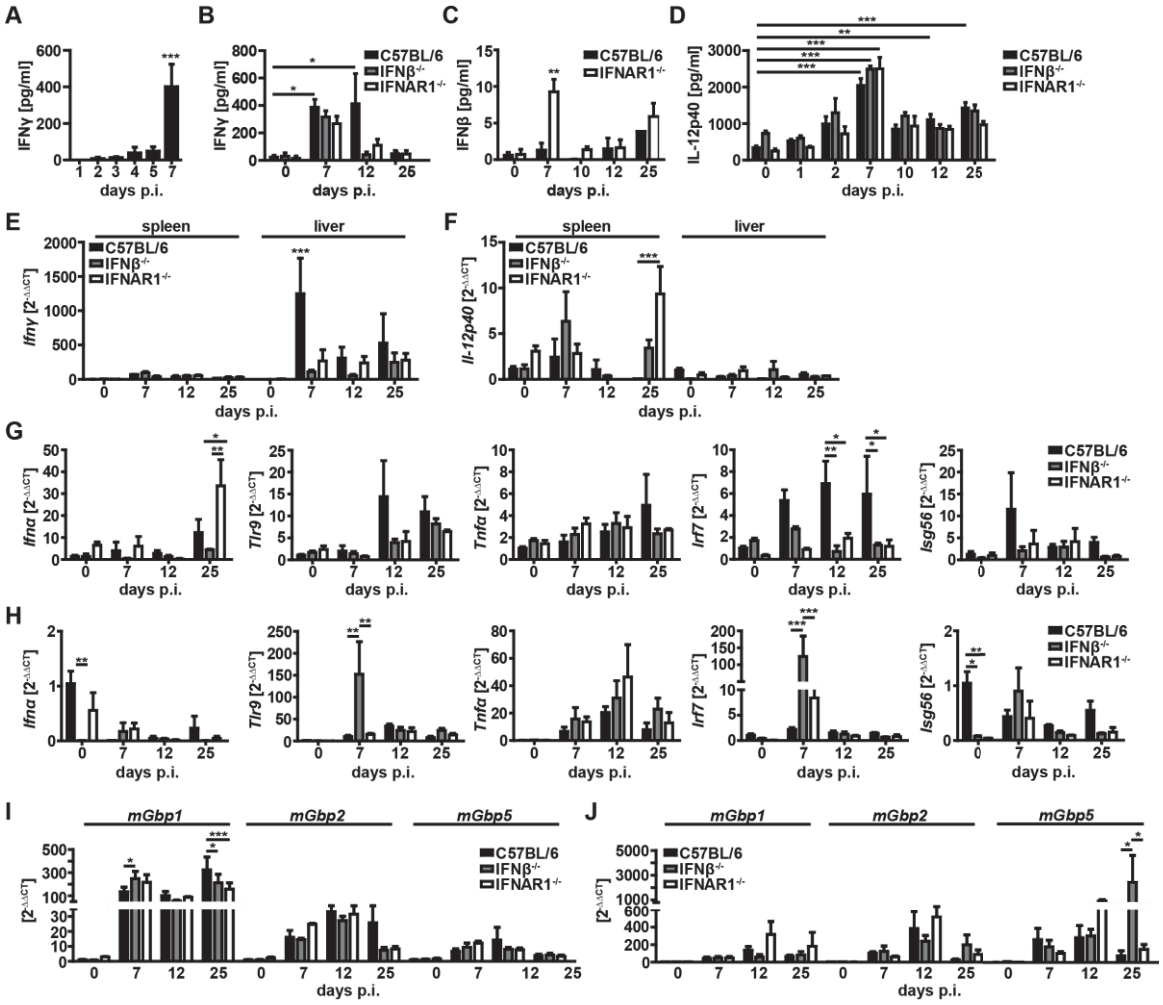

Fig. 3.4.2 IFNβ$^{-/-}$ and IFNAR1$^{-/-}$ mice fail to induce a proper type I IFN and IFNγ response as compared to WT mice after infection with *T. gondii*.
Serum levels of (A and B) IFNγ, (C) IFNβ and (D) IL-12p40 in WT, IFNβ$^{-/-}$ and IFNAR1$^{-/-}$ mice after i.p. infection with 40 cysts of *T. gondii* ME49. qRT-PCR analysis of expression of (E) *Ifnγ* and (F) *Il12* in spleen and liver, (G-H) *Ifnα* and genes involved in type I IFN pathways in (G) spleen and (H) liver and of IFNγ stimulated genes in (I) spleen and (J) liver in WT, IFNβ$^{-/-}$ and IFNAR1$^{-/-}$ mice after i.p. infection with 40 cysts of *T. gondii* ME49. ((A-C) n=3-6, (D-J) n=4)

We also compared the induction of *Ifnα* and type I IFN related genes in WT and IFNβ$^{-/-}$ and IFNAR1$^{-/-}$ mice upon infection with *T. gondii*. Interestingly, most of these genes were reciprocally regulated between spleen and liver. E.g. there was almost no induction of *Ifnα* in the liver in all genotypes but a significant increase in the spleen only in IFNAR1$^{-/-}$ mice peaking on day 25 p.i. (Fig. 3.4.2G and H). Further, genes directly involved in type I IFN signalling like *Tlr9* and *Irf7* were highly and significantly induced in the spleen of WT but not IFNβ$^{-/-}$ and IFNAR1$^{-/-}$ mice (up to 3-fold higher in WT mice). Whereas, in the liver *Tlr9* and *Irf7* were

strongly and significantly induced in IFNβ$^{-/-}$ mice as compared to IFNAR1$^{-/-}$ and WT mice hinting to a dysregulation of type I IFN related genes. Also *Isg56* was higher, but not significantly, induced in the spleen of WT mice and in the liver of IFNβ$^{-/-}$ mice on day 7 p.i.. We could not observe any significant differences in the induction of TNFα on a transcriptional level in WT, IFNβ$^{-/-}$ or IFNAR1$^{-/-}$ mice (Fig. 3.4.2G and H). Furthermore, since there is an obvious lack of IFNγ induction and production in WT IFNβ$^{-/-}$ and IFNAR1$^{-/-}$ mice we were wondering if this affected the induction of mGBPs. MGBPs are IFNγ-induced proteins directly involved in recognition and clearing of *T. gondii* tachyzoites. Therefore induction of these genes and proteins was shown to be important for a proper host defence during infection with *T. gondii* (Degrandi et al., 2007; Degrandi et al., 2013; Howard et al., 2011). We could not detect any defects in upregulation of *mGbp2* or *mGbp5* in the spleen of IFNβ$^{-/-}$ or IFNAR1$^{-/-}$ mice as compared to WT mice. Solely, *mGbp1* was higher induced in IFNβ$^{-/-}$ and IFNAR1$^{-/-}$ mice on day 7 p.i. and in WT mice on day 25 p.i. (Fig. 3.4.2I). In the liver no significant differences were detectable for expression of *mGbp1* and *mGbp2* in WT, IFNβ$^{-/-}$ and IFNAR1$^{-/-}$ mice. Only *mGbp5* was significantly higher expressed in IFNβ$^{-/-}$ mice on day 25 p.i. (Fig. 3.4.2J). These results indicate that WT mice as well as IFNβ$^{-/-}$ and IFNAR1$^{-/-}$ mice are clearly able to induce sufficient amounts of mGBPs despite the lower levels of IFNγ in IFNβ$^{-/-}$ and IFNAR1$^{-/-}$ mice. In summary, IFNβ$^{-/-}$ and IFNAR1$^{-/-}$ mice have a strong defect in IFNγ production and a significantly dysregulated induction of important genes within the type I IFN signalling pathway upon infection with *T. gondii*. Despite this, all genotypes were equally able to induce IL-12 and mGBPs in response to infection with *T. gondii*.

3.4.3 Recruitment of DCs into responding tissues is dysregulated in IFNβ$^{-/-}$ and IFNAR1$^{-/-}$ mice after infection with *T. gondii*

We next wondered if the observed differences in induction of type I IFN related genes in spleen and liver were a result of a differential recruitment of myeloid cells like DCs and macrophages in WT and knockout mice. Therefore we did a comprehensive analysis on recruitment of DCs and granulocytes into spleen, liver, lung, and mesenteric and peripheral LNs in all three genotypes after

infection with *T. gondii*. To our surprise, IFNβ$^{-/-}$ mice had significantly increased absolute numbers of splenic pDCs and CD11b^{+}CD11c^{+} cDCs in contrast to WT and IFNAR1$^{-/-}$ mice (Fig. 3.4.3A). This fits with the observed overall higher absolute numbers in the spleen of IFNβ$^{-/-}$ mice on day 7 p.i. (Fig. 3.4.1E). Also, IFNβ$^{-/-}$ mice had significantly higher numbers of CD8α^{+} cDCs into the peripheral LNs on day 12 and day 25 p.i. as compared to WT and IFNAR1$^{-/-}$ mice. pDC and CD11b^{+}CD11c^{+} cDC numbers in the peripheral LNs were comparable between all genotypes (Fig. 3.4.3A). Interestingly, WT mice already had two times higher numbers of pDCs in the naïve mesenteric LNs than IFNβ$^{-/-}$ and IFNAR1$^{-/-}$ mice. In general, also after infection with *T. gondii* WT mice had higher pDC and cDC numbers in the mesenteric LNs than IFNβ$^{-/-}$ and IFNAR1$^{-/-}$ mice. The only exception to this was a comparable number of CD11b^{+}CD11c^{+} cDCs in IFNβ$^{-/-}$ mice on day 7 p.i. (Fig. 3.4.3A). In the liver, IFNβ$^{-/-}$ mice had significantly higher absolute numbers of pDCs and CD11b^{+}CD11c^{+} cDCs on day 7 p.i. and CD8α^{+} cDCs on day 12 p.i. (Fig. 3.4.3A). In the lung, WT and IFNβ$^{-/-}$ mice had significantly higher numbers of pDCs and cDCs than IFNAR1$^{-/-}$ mice (Fig. 3.4.3A). Taken together, IFNβ$^{-/-}$ mice had significantly increased DC numbers over all tissues, except the mesenteric LNs while in contrast to that IFNAR1$^{-/-}$ mice had normal or significantly reduced DC numbers. Also, upon infection WT mice also had higher numbers of migratory CD11b^{-}CD103^{+} cDCs as compared to IFNβ$^{-/-}$ and IFNAR1$^{-/-}$ mice (Fig. 3.4.3B) while IFNAR1$^{-/-}$ mice had significantly increased numbers of CD11b^{+}Ly6C^{hi} inflammatory monocytes on day 12 p.i. (Fig. 3.4.3C). Interestingly, in WT and IFNAR1$^{-/-}$ mice but not IFNβ$^{-/-}$ mice we found very high numbers of CD11b^{+}Gr-1^{hi} granulocytes on day 12 p.i. in the spleen, while these cells were comparable in the lung and increased in the peripheral and mesenteric LNs of WT and IFNβ$^{-/-}$ but decreased in IFNAR1$^{-/-}$ mice (Fig. 3.4.3D-G).

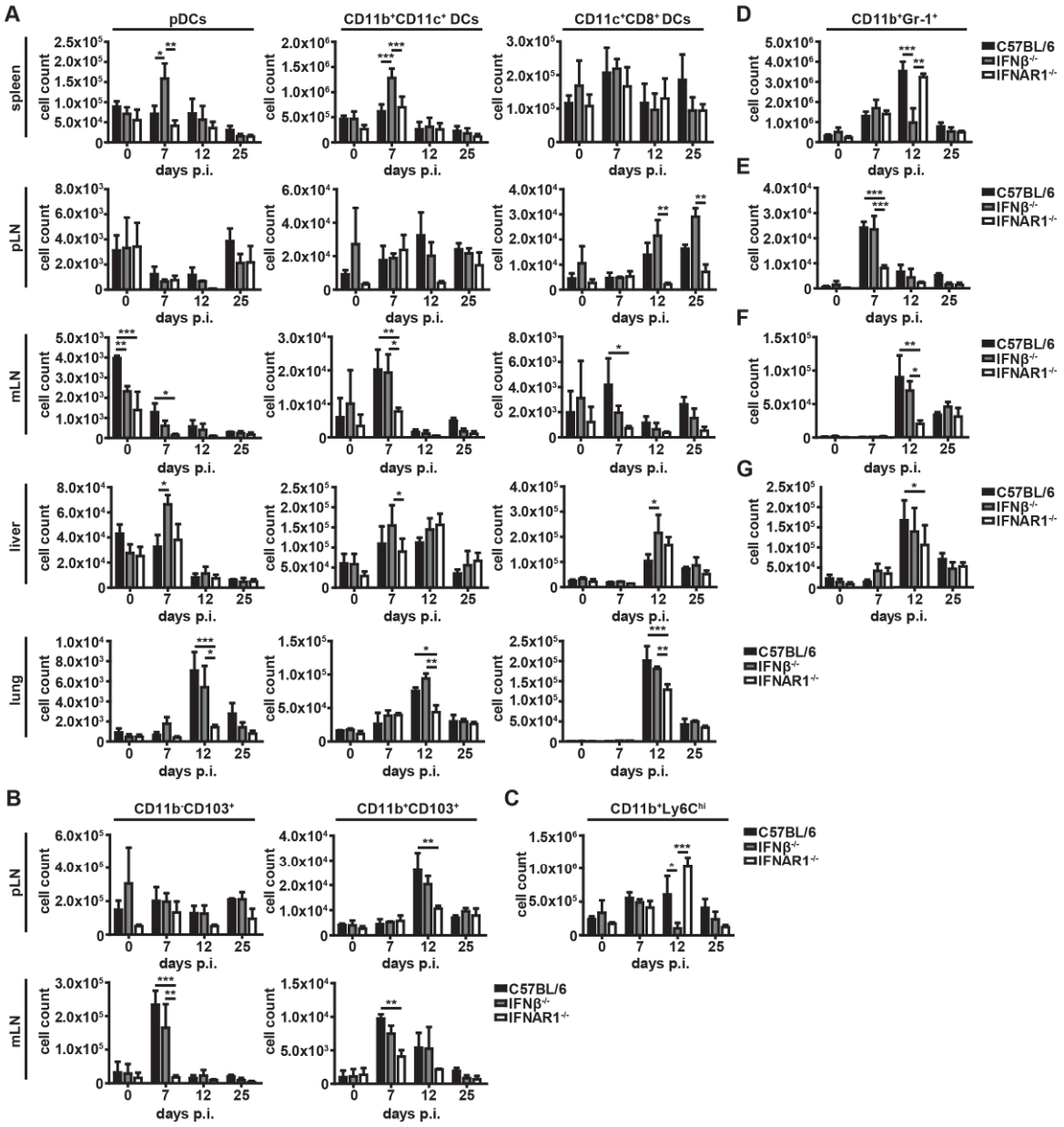

Fig. 3.4.3 Comparison of myeloid cell populations in WT, IFNβ$^{-/-}$ IFNAR1$^{-/-}$ mice after infection with *T. gondii*. **WT, IFNβ$^{-/-}$ IFNAR1$^{-/-}$ mice were i.p. infected with 40 cysts of *T. gondii* ME49. (A) Analysis of pDC and cDC populations in spleen, liver, lung and LNs. (B) Analysis of migratory DCs in pLN and mLN and (C) splenic inflammatory monocytes. (D-G) Cell counts of granulocytes in (D) spleen, (E) pLN, (F) mLN and (G) lung. FACS data were pre-gated on living, CD3ε^{-}CD19^{-} cells; pDCs gated on CD11b^{-}CD11c^{int}mPDCA-1^{+}; other cell types as indicated. (n=6)**

Our results show, that after infection with *T. gondii* there is an obvious and complex deregulation in cellularity in the responding tissues in IFNβ$^{-/-}$ and IFNAR1$^{-/-}$ mice.

3.4.4 DCs are the main producers of IFNβ after infection with *T. gondii in vitro*.

So far we have shown that mice deficient for IFNβ or the IFNAR are highly susceptible towards infection with *T. gondii*, that they have an impaired production of IFNγ but not IL-12 and obvious differences in absolute numbers of DCs in the infected tissues. This led us to the assumption that DCs must be important in host response and protection against *T. gondii*. Therefore we were interested to define, which cells actually produce IFNβ in response to *T. gondii*. To study this we first used an *in vitro* approach and generated BM-derived Flt3-L-differentiated DCs or M-CSF-differentiated macrophages from WT, IFNβ$^{-/-}$, IFNAR1$^{-/-}$ and IFNβ$^{mob/mob}$ mice. Fully differentiated DCs and macrophages then were challenged either with CpG or Poly(I:C) as positive controls for IFNβ production or viable or heatkilled *T. gondii* ME49 tachyzoites for 0 h or 24 h. IFNβ/YFP expression and activation of pDCs, cDCs and macrophages was analysed by FACS. Our data revealed that after infection with *T. gondii* pDCs, cDCs, and macrophages are able to produce IFNβ. Though, pDCs and cDCs showed higher percentages of IFNβ/YFP^{+} cells after infection with *T. gondii* than macrophages. Also the DCs had a higher response to heatkilled tachyzoites than to viable ones. E.g. pDCs had up to 2 % IFNβ/YFP^{+} cells after challenge with heatkilled tachyzoites (cDCs ~0.5 %) and only up to 1 % after infection with viable tachyzoites (cDCs ~0.25 %) (Fig. 3.4.4A and B). In contrast, macrophages had a higher IFNβ response to viable tachyzoites (~0.2 % IFNβ/YFP^{+} cells) than to heatkilled tachyzoites (~0.1 % IFNβ/YFP^{+} cells) (Fig. 3.4.4B). Also, MFIs for YFP were lower in DCs after infection with *T. gondii* as compared to CpG stimulation (Fig. 3.4.4C). Further, we found that cDCs as well as pDCs from WT mice were equally and highly activated after infection with either viable or heatkilled tachyzoites (Fig. 3.4.4D, E and F). IFNβ$^{-/-}$ cDCs also were equally activated after infection with either viable or heatkilled tachyzoites (Fig. 3.4.4D and F) while IFNβ$^{-/-}$ pDCs were activated by heatkilled but barely by viable tachyzoites (Fig. 3.4.4E and G). Surprisingly IFNAR1$^{-/-}$ pDCs were not found to be activated upon infection with either viable or heatkilled tachyzoites (Fig. 3.4.4E and G) and IFNAR1$^{-/-}$ cDCs also barely responded to the parasites (Fig. 3.4.4D and F). In general, BMDMs also barely upregulated CD69 across all three

genotypes (Fig. 3.4.4H) or CD40 (Fig. 3.4.4I) after infection with viable or heat-killed tachyzoites, which is in line with their very low production of IFNβ/YFP.

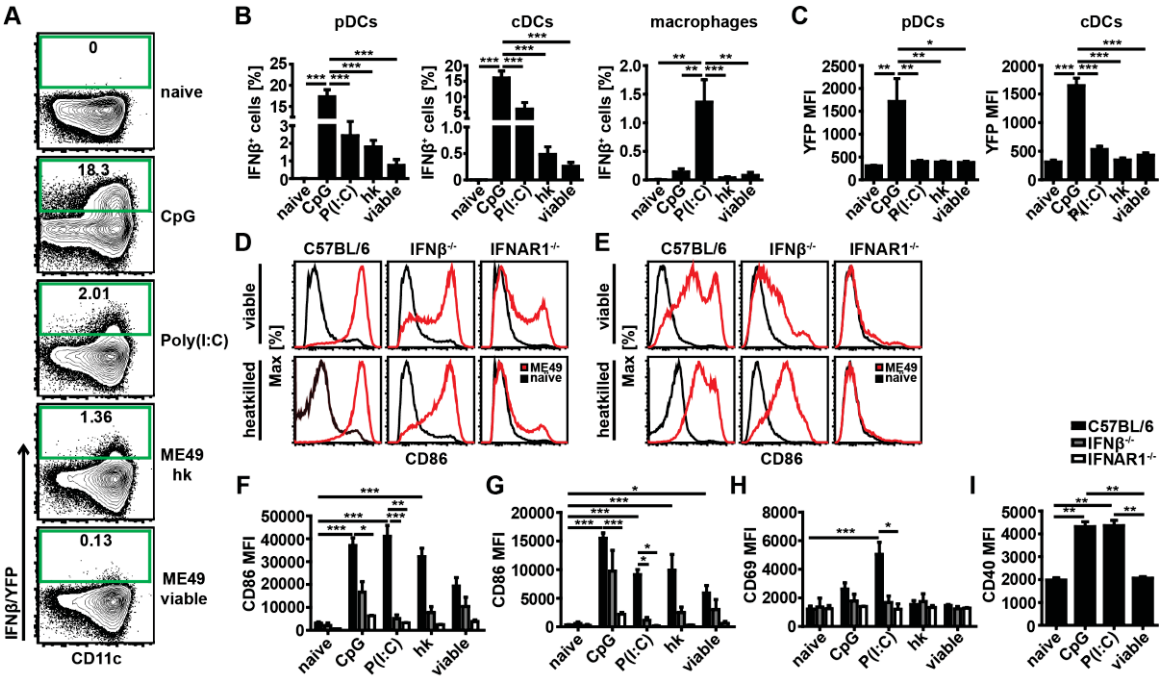

Fig. 3.4.4 IFNβ production by DCs and macrophages after infection with *T. gondii in vitro*.
Analysis of IFNβ producing BMDMs and BM-Flt3-L-derived DCs upon stimulation with CpG or Poly(:) or infection with viable or heatkilled tachyzoites of *T. gondii* ME49 (15 tachyzoites per cell) for 0 h or 24 h. (A) FACS analysis of IFNβ/YFP production, (B) percentage of IFNβ/YFP producing cells and (C) YFP MFI of stimulated and infected pDCs and cDCs in IFNβ$^{mob/mob}$ mice. (D-G) Comparison of CD86 MFIs in WT, IFNβ$^{-/-}$ and IFNAR1$^{-/-}$ (D, F) cDCs and (E,G) pDCs. (H) Comparison of CD69 MFIs WT, IFNβ$^{-/-}$ and IFNAR1$^{-/-}$ macrophages and (I) CD40 MFI in WT macrophages. pDCs and cDCs from the same culture were pre-gated on living, CD11b^{-}CD11c^{+}B220^{+} pDCs or CD11b^{+}CD11c^{+}B220^{-} cDCs; macrophages are gated on living CD11b^{+}F4/80^{+} cells. (n=3; (A,D,E) One representative experiment out of three is shown.)

These results suggest that after infection with *T. gondii* IFNβ is mostly produced by DCs, predominantly pDCs. Also we found that pDCs from IFNβ$^{-/-}$ or IFNAR1$^{-/-}$ mice are barely or not activated by *T. gondii in vitro* which could have a decisive impact on the outcome of infection if this holds true in the *in vivo* situation.

3.4.5 DCs and macrophages are able to produce IFNβ in various tissues after infection with *T. gondii in vivo*

Next we wanted to see if we could confirm our *in vitro* data on IFNβ producing cells *in vivo*. Therefore we infected IFNβ$^{mob/mob}$ mice with 40 cysts of *T. gondii* ME49 and analysed the IFNβ/YFP production in different tissues over the first

days of infection up to day 7. We found that ~1 % cells produced IFNβ after infection with *T. gondii*. But surprisingly this low IFNβ/YFP production was stable at least till day 7 p.i. and occurred in spleen, liver, lung, mesenteric LNs, peripheral LNs and cervical LNs and therefore basically throughout the whole body (Fig. 3.4.5A). Also we found that IFNβ/YFP$^+$ cells were mostly CD11c^{int} or CD11c$^+$ with just a few CD11c$^-$ cells hinting towards IFNβ/YFP production mostly by DCs (pregated on living, non B and T cells; Fig. 3.4.5A). Most IFNβ/YFP$^+$ cells were found in the liver (~1.5 % on day 3), followed by the spleen with ~0.6 % IFNβ/YFP$^+$ cells on day 3 and the lung with ~0.2 % IFNβ/YFP$^+$ cells on day 7 (Fig. 3.4.5B and C). These results confirm our *in vitro* data that upon infection with *T. gondii* DCs are the most important producers of IFNβ. Also we could show, that at least till day 7 p.i. there is a low albeit constant production of IFNβ throughout all tissues tested.

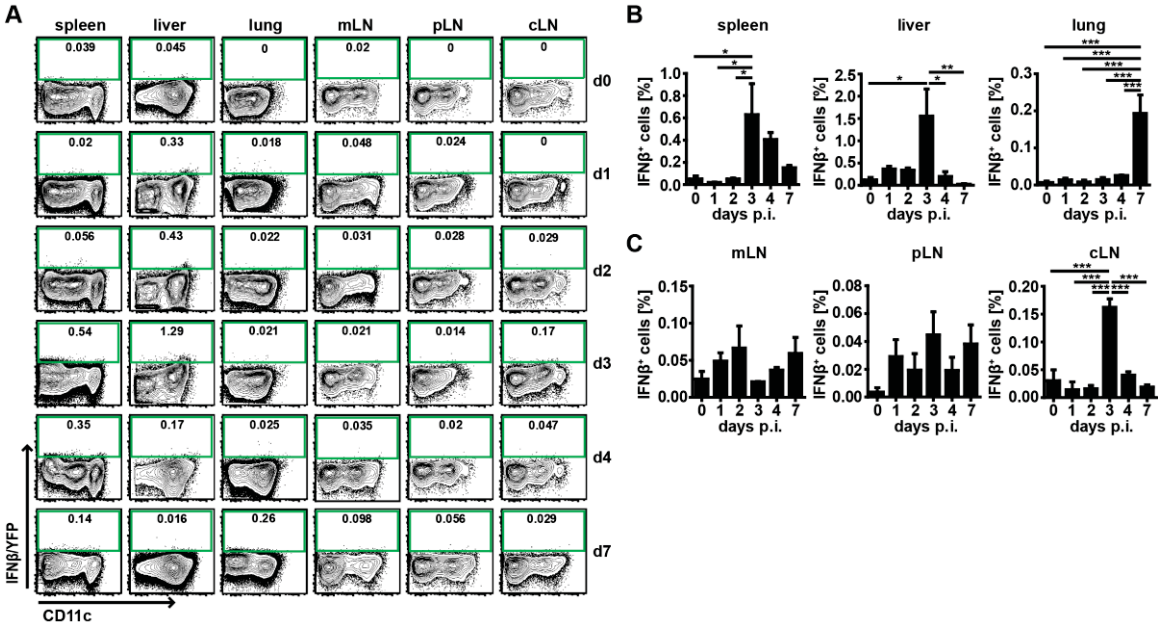

Fig. 3.4.5 IFNβ production by DCs and macrophages after infection with *T. gondii in vivo*.
IFNβ$^{mob/mob}$ mice were i.p. infected with 40 cysts of *T. gondii* ME49. (A) FACS analysis of IFNβ/YFP producing cells in spleen, liver, lung and LNs up to 7 d after infection. Percentage of IFNβ/YFP-producing cells in (B) spleen, liver, lung and (C) LNs up to 7 d after infection. (n=3; (A) One representative is shown.)

3.4.6 Dysregulated IFNγ production by NK and T cells in IFNβ$^{-/-}$ and IFNAR1$^{-/-}$ mice after infection with *T. gondii*

Since IFNβ$^{-/-}$ and IFNAR1$^{-/-}$ mice fail to induce a strong IFNγ response during the infection with *T. gondii* we wanted to investigate the cellular source of IFNγ during infection. To this end we infected all three genotypes with 40 cysts *T. gondii* ME49 and performed intracellular FACS staining and analysis for IFNγ but also IL-12 and TNFα in spleen, liver, lung, mesenteric LNs and peritoneal lavage. We included the peritoneal lavage since after i.p. infection the peritoneal cavity is the first potential location for a cellular host response towards *T. gondii*. Confirming our ELISA and qRT-PCR data the general IL-12 production by living, CD3ε^{-}CD19^{-} cells was comparable in WT, IFNβ$^{-/-}$ and IFNAR1$^{-/-}$ mice 7, 10 and 12 days p.i. in spleen, lavage, and mesenteric LNs. Only, the absolute number, not percentage, of IL-12^{+} cells was significantly higher in the liver of IFNβ$^{-/-}$ mice on day 10 p.i. as well as the percentage, but not absolute number, of IL-12^{+} cells in the lung of IFNAR1$^{-/-}$ mice as compared to the other genotypes (Fig. 3.4.6aA). Surprisingly, in contrast to our qRT-PCR data, the percentage and absolute cell number of TNFα^{+} cells in the spleen of IFNAR1$^{-/-}$ mice was significantly decreased as compared to WT and IFNβ$^{-/-}$ mice (Fig. 3.4.6aB).

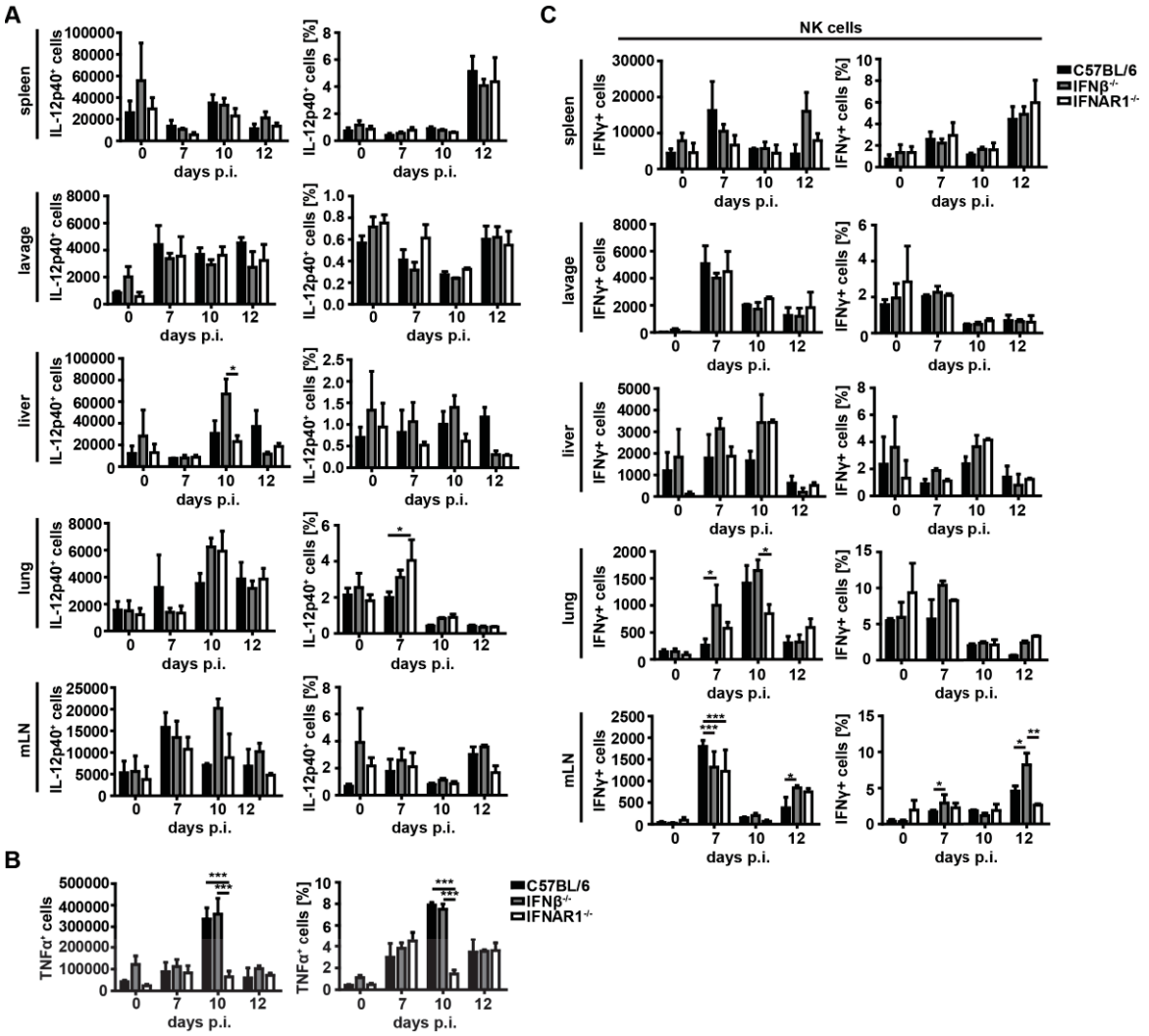

Fig. 3.4.6a Analysis of IL-12p40, TNFα and IFNγ production in WT, IFNβ$^{-/-}$ and IFNAR1$^{-/-}$ mice after infection with *T. gondii*.

Mice were i.p. infected with 40 cysts *T. gondii* ME49. Absolute numbers and percentage of (A) IL-12p40, TNFα (B only spleen) producing cells and (C) IFNγ producing NK cells in spleen, lavage, liver, lung and mLN, as determined by intracellular cytokine staining and FACS analysis. (A,B) Pre-gated on CD3ε^{-}CD19^{-}NK1.1^{-}CD11c$^{+/-}$ cells. (C) Pre-gated on CD3ε^{-}CD19^{-}NK1.1^{+}CD11c$^{+/-}$ cells. (n=3)

Next, we focused on the IFNγ production by NK cells and CD4^{+} or CD8^{+} T cells. We found that in the spleen IFNγ was mainly produced by WT NK cells and to a lesser extent by IFNβ$^{-/-}$ and IFNAR1$^{-/-}$ NK cells on day 7 p.i., just before the critical time around day 10 when the first IFNβ$^{-/-}$ and IFNAR1$^{-/-}$ mice die. Interestingly, NK as well as T cells in both knockouts produced high amounts of IFNγ on day 12 p.i. (Fig. 3.4.6aC and Fig. 3.4.6b). Regarding IFNγ production by NK cells there were no significant differences in the lavage or liver of WT, IFNβ$^{-/-}$ and IFNAR1$^{-/-}$ mice after infection. Whereas there was more IFNγ produced by

CD4$^+$ and CD8$^+$ T cells in WT and IFNβ$^{-/-}$ but not IFNAR1$^{-/-}$ mice in the lavage and in the liver IFNβ$^{-/-}$ and IFNAR1$^{-/-}$ mice in general seemed to have higher IFNγ-T cell responses (Fig. 3.4.6aC and Fig. 3.46b). Interestingly, in the lung the picture was quite controversial since there was a significant higher production of IFNγ by NK cells from IFNβ$^{-/-}$ mice but significant more IFNγ$^+$ CD4$^+$ T cells in IFNAR1$^{-/-}$ mice and higher numbers of IFNγ$^+$ CD8$^+$ T cells in WT mice as compared to the other genotypes (Fig. 3.4.6aC and Fig. 3.4.6b). In the mesenteric LNs we found that NK cells from WT produced significant higher amounts of IFNγ on day 7 p.i., whereas the IFNγ-NK cell response by IFNβ$^{-/-}$ and IFNAR1$^{-/-}$ mice came delayed and less intense on day 12 p.i. In WT mice also both CD4$^+$ and CD8$^+$ T cells produced elevated amounts of IFNγ on day 7 and 10 after infection as compared to IFNβ$^{-/-}$ and IFNAR1$^{-/-}$ mice (Fig. 3.4.6aC and Fig. 3.4.6b).

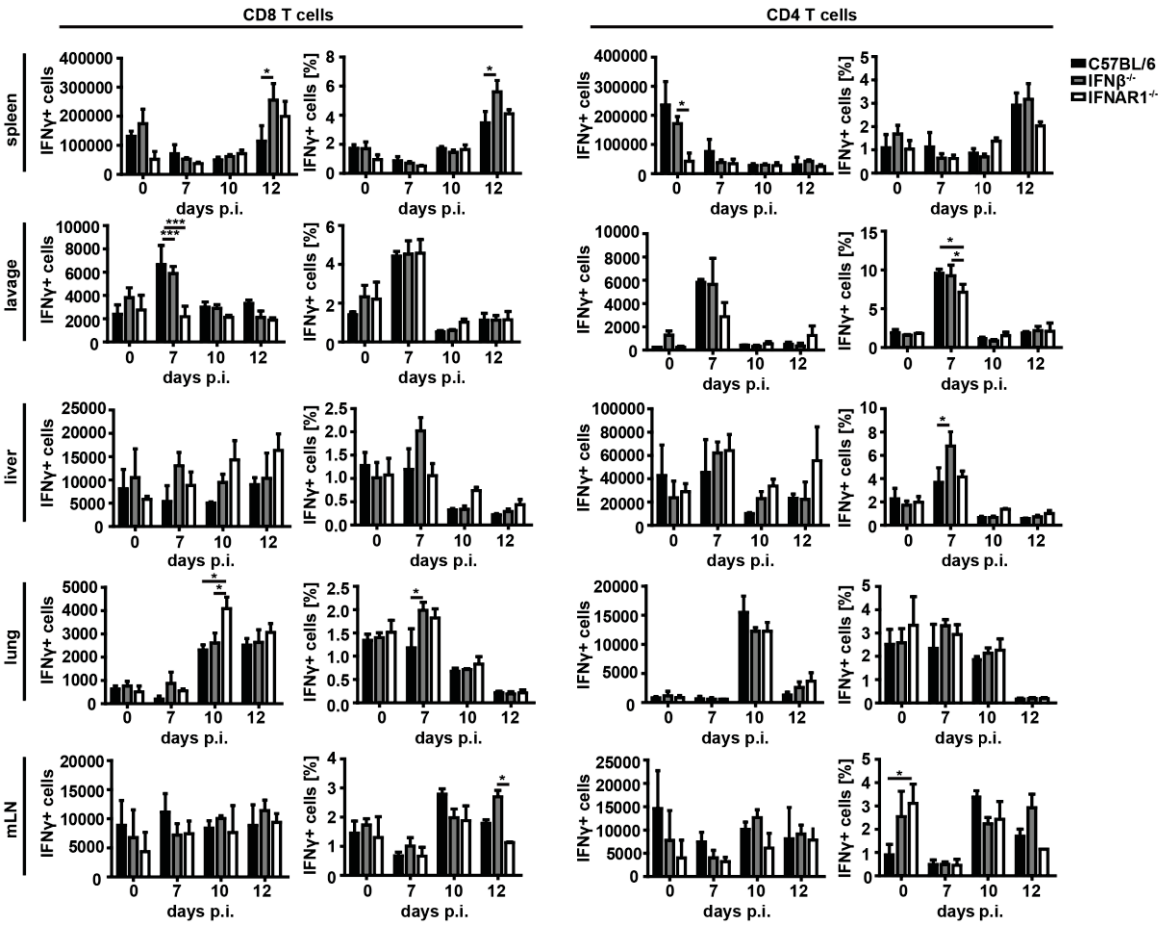

Fig. 3.4.6b Analysis of IFNγ production in WT, IFNβ$^{-/-}$ and IFNAR1$^{-/-}$ mice after infection with *T. gondii*.

Mice were i.p. infected with 40 cysts *T. gondii* ME49. Absolute numbers and percentage of IFNγ producing $CD4^+$ and $CD8^+$ T cells in spleen, lavage, liver, lung and mLN, as determined by intracellular cytokine staining and FACS analysis. T cells are pre-gated on $CD3\varepsilon^+CD19^-NK1.1^-$ and $CD4^+$ or $CD8^+$ cells. (n=3)

Overall, we found that NK and T cells in WT, IFNβ$^{-/-}$ and IFNAR1$^{-/-}$ mice are able to produce IFNγ but there are significant differences around day 7 p.i. with regard to what cell types produce this cytokine and in which tissue. This different distribution of IFNγ production could be critical in survival of an infection with *T. gondii*.

3.4.7 Highly activated DCs are essential for proper activation of NK cells during infection with *T. gondii*

We found NK cells to be important in IFNγ production after infection with *T. gondii*, especially in the spleen and mesenteric LN. These are probably the first places for parasite recognition by DCs and macrophages after i.p. infection with *T. gondii*. Therefore we were interested in the DC-NK cell interactions. In order to investigate these, we generated BM-derived Flt3-L-differentiated pDCs and cDCs from WT and IFNAR1$^{-/-}$ mice. After 7 days of culture we activated those DCs with CpG for 12 h in order to generate IFNβ-producing DCs or left them untreated. Activated or untreated WT or IFNAR1$^{-/-}$ DCs or recombinant IFNβ were added to cultured, MACS purified splenic NK cells from WT or IFNAR1$^{-/-}$ mice overnight. Subsequently, NK cells were analysed for upregulation of the activation markers NKp46 and CD69, as a very early activation marker. Upon treatment of NK cells with untreated WT or IFNAR$^{-/-}$ DCs there was no change in the activation status of NK cells. We found NKp46 to be barely induced upon any our tested stimuli (Fig. 3.4.7A-C). However, CD69 was strongly upregulated, up to ~70 %, on WT NK cells that were cocultured with activated WT DCs but only ~17 % if they were cocultured with IFNAR1$^{-/-}$ DCs and ~12 % if they were treated with rIFNβ (Fig. 3.4.7A). IFNAR1$^{-/-}$ NK cells stimulated with activated WT DCs also highly upregulated CD69, ~57 %, but only ~14 % after stimulation with IFNAR1$^{-/-}$ DCs and there was no activation at all after stimulation with rIFNβ (Fig. 3.4.7A). Statistically, induction of CD69 expression on WT NK cells with WT DCs or rIFNβ was significantly higher than the activation of IFNAR1$^{-/-}$ NK cells (Fig. 3.4.7B and C). Additionally, WT cDCs and pDCs used for stimulation of NK cells were

significantly higher activated upon stimulation with CpG or rIFNβ (Fig. 3.4.7D and E). Therefore, our data show that properly activated DCs that are able to produce type I IFN, but not IFNβ alone, are crucial for proper activation of NK cells.

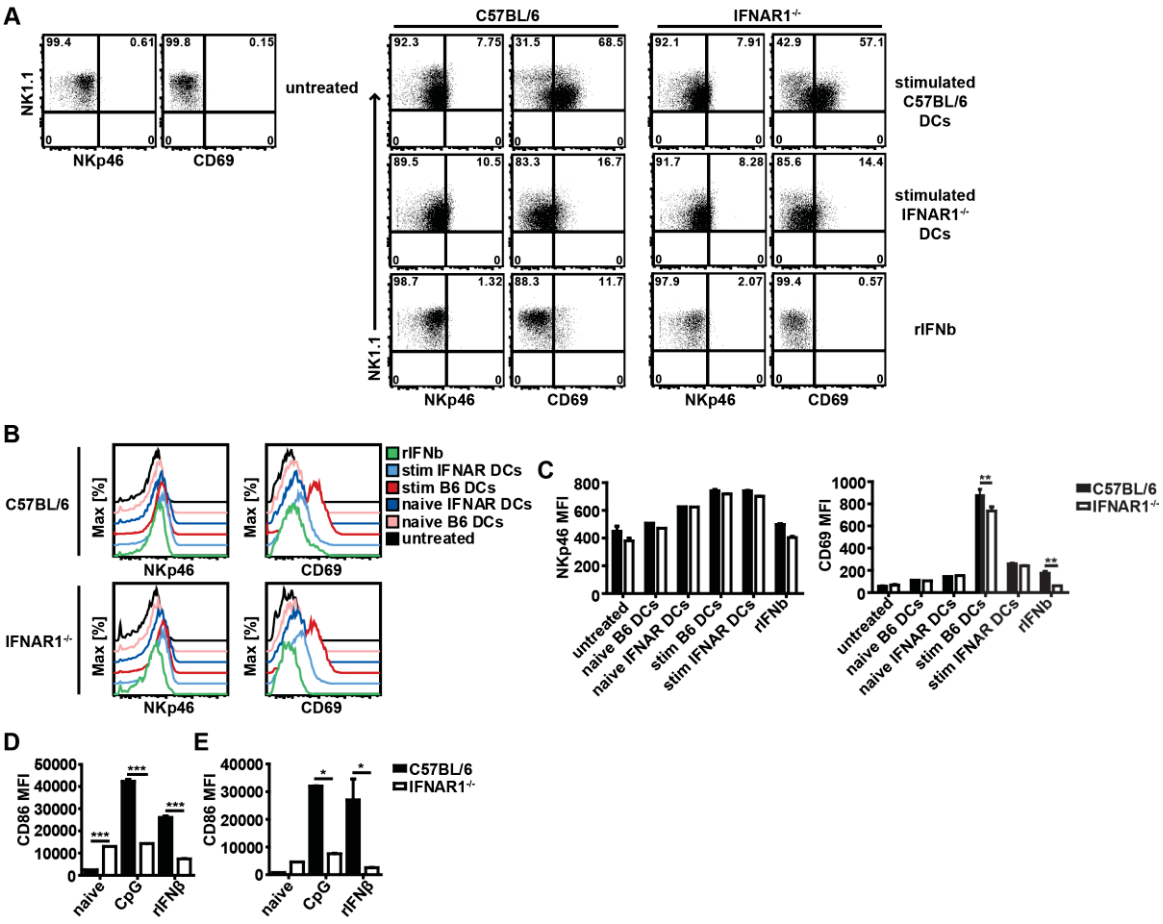

Fig. 3.4.7 Fully activated DCs are essential for proper activation of NK cells during infection with *T. gondii*. **Splenic naive WT and IFNAR1$^{-/-}$ NK cells were isolated via MACS depletion, cultured and stimulated with naive or CpG-stimulated BM-Flt3-L-derived WT or IFNAR1$^{-/-}$ DCs or rIFNβ. (A, B) FACS analysis of NK cell activation and (C) NKp46 and CD69 MFIs of WT and IFNAR1$^{-/-}$ NK cells after stimulation. Analysis of activation of BM-Flt3-L-derived (D) CD11b^{+}CD11c^{+}B220^{-} cDCs and (E) CD11b^{-}CD11c^{+}B220^{+} pDCs that were used to stimulate the NK cells. (n=2)**

To further analyse the function of NK cells during infection wit*h T. gondii* in WT and IFNβ$^{-/-}$ and IFNAR1$^{-/-}$ mice we tried an *in vivo* NK cell depletion approach. NK cells were selectively depleted *in vivo* using a mAb against NK1.1. The strategy for NK cell depletion is shown in Fig. 3.4.8aA. In brief, mice were injected with 100 µg/mouse αNK1.1 or IgG2a as control every 3 days and 1 day prior infection with 40 cysts of *T. gondii* ME49. NK cell depletion, though, was successful as analysed in blood samples on day -1, 1, 2, 3.5 and 5 p.i. by FACS (Fig. 3.4.8aB).

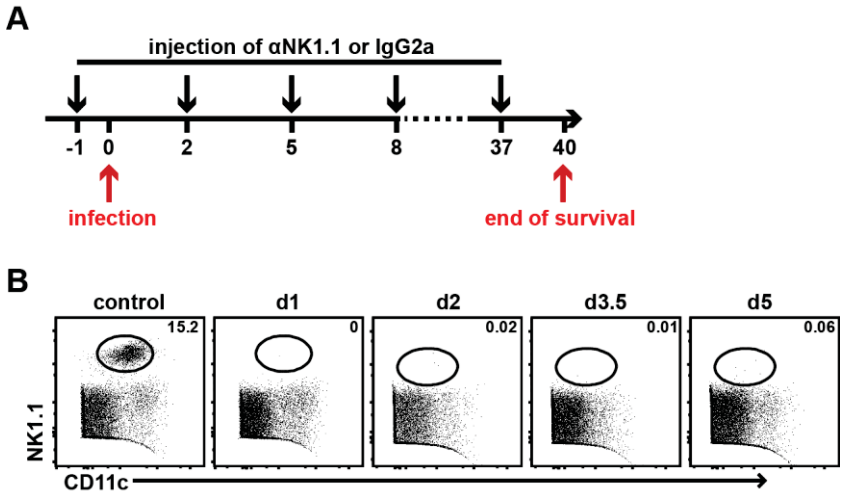

Fig. 3.4.8a NK cell depletion.

(A) Scheme of NK cell depletion and (B) blood FACS analysis of NK cell depletion. Cells were pre-gated on living CD3ε^{-}CD19^{-}NK1.1^{+}CD11c$^{+/-}$ cells. (n=3 per timepoint)

Survival was monitored till day 40 p.i.. Surprisingly, IFNβ$^{-/-}$ mice showed an improved survival upon injection with IgG2a (Fig. 3.4.8bA) and there was barely any difference in the outcome of survival after NK cell depletion as compared to not depleted mice (Fig. 3.4.8bB and Fig. 3.4.1B).

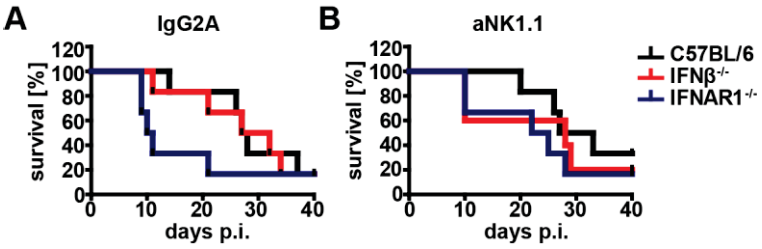

Fig. 3.4.8b Survival of WT, IFNβ$^{-/-}$ and IFNAR1$^{-/-}$ mice after NK cell depletion and infection with 40 cysts of *T. gondii*.

Survival after injection of (A) IgG2a or (B) αNK1.1 every three days. (n=6)

Obviously, depletion of NK cells had no impact on survival after infection with *T. gondii.* A possible explanation for the increased survival of IFNβ$^{-/-}$ mice in this depletion experiment is that the injection of 200 µl PBS (with antibody) thrice a week could have positively affected the survival of the different genotypes.

4. Discussion

Type I IFN are crucial mediators of cellular responses of the innate and adaptive immune system. A previous study from our lab showed that IFNβ is produced by splenic pDCs after TLR9 stimulation (Scheu et al., 2008). The specific characteristics of these IFNβ-producing pDCs are the subject of this thesis. In this study we show that IFNβ is mostly produced by pDCs upon TLR9 stimulation in the spleen and that these pDCs are a unique subset defined by a specific surface marker profile, localization, gene expression, and ability to actively recruit T cells. We further sought to investigate functions of genes highly differentially expressed in IFNβ-producing pDCs and to define the role of type I IFN during infection with the protozoan parasite *Toxoplasma gondii*.

4.1 After TLR9 stimulation IFNβ expression is restricted to a distinct subset of splenic pDCs (Bauer and Dress et al., *in revision*)

In this study, using an IFNβ-reporter mouse model ($IFN\beta^{mob/mob}$), we could demonstrate that type I IFN is almost exclusively produced by pDCs in the spleen after TLR stimulation with the synthetic ligand CpG or infection with MCMV. Although pDCs are frequently thought to constitute a homogenous population implying that all pDCs are equally able to produce large amounts of IFNα and IFNβ (Colonna, 2004), in this study we were able to show that upon TLR9 stimulation only ~5% of all splenic pDCs were able to produce IFNβ. This indicates that in contrast to previous assumptions, the vast majority of pDCs (~95%) were not able to produce this cytokine upon this stimulation. We could show that this was not due to a lack of stimulation in non-producing cells since both subsets, IFNβ-producing as well as non-producing pDCs, were comparably activated. Further, a subsequent second stimulation of non-producing or IFNβ-producing pDCs had no impact on IFN production by these cells. Our data demonstrate that in spite of commonly held assumptions, pDCs appear to constitute a heterogeneous population. In the larger picture, this is perhaps not surprising since for cDCs various functional subpopulations are described

already, such as $CD8\alpha^+CD11b^-$, $CD8\alpha^-CD11b^+$ resident cDCs or $CD103^+$ migratory cDCs and many others (Lambrecht and Hammad, 2009; Merad et al., 2008; Niess et al., 2005; Shortman and Liu, 2002), and given that there is evidence for multiple pre-cursors of both pDCs and cDCs (Perie and Naik, 2015). Different pre-cursors might give rise to distinct pDC subsets, as it has been shown in the case of cDCs (Schlitzer et al., 2015a; Schlitzer et al., 2015b). Future work will help us to gain a better understanding of development and functions not only of distinct cDC but also pDC subsets. Also, it has been shown that an insufficient control of type I IFN production by pDCs is involved pathology of auto-immune diseases e.g. psoriasis (Nestle et al., 2005), Sjögren's syndrome (Gottenberg et al., 2006) or systemic lupus erythematosus (Sisirak et al., 2014). Therefore, a tight restriction of type I IFN production in order to limit auto-immunity pathology due to deregulated type I IFN production is of great importance and offers another explanation why IFNβ production is restricted to a low frequency subset of pDCs in the spleen.

We found IFNβ-producing pDCs to be $CD11b^-$ $CD11c^{int}$ $mPDCA\text{-}1^+$ $B220^+$ $SiglecH^+$ $Ly6C^+$ and $CCR9^+$ but $CD9^-$. This is interesting, since reports on CCR9 and/or CD9 expression by overall pDCs and type I IFN producing pDCs have been controversial. It was reported that bone marrow-derived IFNα-producing pDCs highly express CD9 but can be either positive or negative for CCR9 (Hadeiba et al., 2008; Schlitzer et al., 2011; Segura et al., 2009), while pDCs in the periphery rather downregulate expression of CD9 (Bjorck et al., 2011) and CCR9 upon stimulation (Hadeiba et al., 2008). These observations point to organ specific differences in pDC populations. Also, our data are supported by earlier findings demonstrating that $CCR9^-$ pDCs rather represent pre-cursors of cDCs than functional bona-fide pDCs (Segura et al., 2009). Alternatively, the capacity to produce type I IFN might be differentially regulated depending on the developmental stage of pDCs (Schlitzer et al., 2011).

In order, to understand the differences between IFNβ-producing and non-producing pDCs we performed microarray analysis on sorted IFNβ-producing and non-producing pDCs and analysed their differential gene expression as early as 6 h after TLR9 stimulation. We found almost 1500 genes differentially expressed between these two pDC subsets of which most are involved in immune effector

processes and regulation of immune cell localization as predicted by gene ontology analyses. Among these genes we found CCR7, a chemokine receptor that is lowly expressed on pDCs in the steady state but becomes highly upregulated after TLR9 stimulation to enable homing of pDCs e.g. into lymph nodes (Seth et al., 2011). Differences in CCR7 expression levels in distinct pDC subsets have not yet been described. In this study we show that IFNβ-producing pDCs exhibit higher expression levels of CCR7 than non-producing pDCs. Furthermore, in a transwell-migration assay IFNβ-producing pDCs had a higher capacity to migrate towards CCL19 and CCL21, ligands of CCR7. Interestingly, within the splenic white pulp CCL19 and CCL21 are constitutively expressed by stromal cells (Luther et al., 2000; Gunn et al., 1998). This data is consistent with the localisation patterns of IFNβ-producing pDCs within the spleen. In the naïve situation most pDCs are found around the marginal zone. However, we found that upon TLR9 stimulation pDCs in general were predominantly located within the B and T cell zone of the spleen, and few of them clustered at the marginal sinus. This result is in accordance with previous data on splenic pDC distribution by Asselin-Paturel et al. (2005). We observed that IFNβ-producing pDCs were exclusively located at the B and T cell area, which is in line with their high upregulation of CCR7 and their enhanced migration capacity. This specific localisation pattern might be strategic importance since it brings these pDCs closer to B and T cells which might provide an advantage in T cell priming and/or induction of subsequent immune responses. In support of this hypothesis we found the chemokines CCL3 and CCL5 to be highly differentially upregulated in IFNβ-producing pDCs vs. non-producing pDCs. To test whether IFNβ-producing pDCs recruit T cells or are involved in immune modulatory processes we performed an *in vivo* inflammation assay where we injected sorted IFNβ-producing pDCs or non-producing pDCs following TLR stimulation or naïve pDCs into the peritoneum of wildtype mice. This resulted in massive recruitment of immune cells into the peritoneal cavity of these mice, mostly NK and T cells, by both IFNβ-producing and non-producing pDCs, but not by naïve pDCs. However, IFNβ-producing pDCs were the only cells able to recruit significantly higher numbers of $CD4^+$ T cells which express CCR1 and CCR5, the corresponding receptors for CCL3 and CCL5.

Type I IFN production and expression of type I IFN stimulated genes (ISGs) can be enhanced and influenced by a positive feedback loop via the IFNAR. Here, secreted IFNα or IFNβ binds to the IFNAR which is expressed either by the producing cell itself or neighbouring cells resulting in induction of IRF7 and other ISGs and more type I IFN (Barchet et al., 2002; Ivashkiv and Donlin, 2014; Platanias, 2005). Interestingly, we found that IFNβ production as well as localisation of IFNβ-producing pDCs and their gene expression profile after TLR9 stimulation where independent of this positive feedback loop via the IFNAR. Therefore, this specific transcriptional program might represent cell intrinsic properties of IFNβ-producing pDCs within the overall heterogeneous pDC population. These results are also in accordance with a previous studies showing that IFNα production by pDCs occurred independently of the IFNAR-mediated feedback loop (Barchet et al., 2002). Another recent study suggested that the IFNAR1 subunit rather than the IFNAR2 subunit is important for IFNβ signalling and that IFNβ preferentially binds with greater affinity to this subunit leading to induction of distinct sets of ISGs (de Weerd et al., 2013). Our IFNAR-deficient IFNβ-reporter mice have a deletion for the IFNAR1 subunit and therefore should be functionally deficient in IFNβ-IFNAR interactions according to this paper. This serves to further support our finding that IFNβ production by the subset of pDCs we examined is independent of the IFNAR.

A model by Apostolou et al. suggested that expression of the gene for IFNβ is a stochastic event dependent on interchromosomal association of three different gene loci leading to binding of the scaffold transcription factor NF-κB to the enhancer region of *ifnb* (Apostolou et al., 2008). Another model, offered by Zhao et al. states that IFNβ production is influenced by cell-to-cell differences in components important for gene induction such as differential levels of the key transcription factor IRF7 (Zhao et al., 2012). In general, both of these models imply a random expression of IFNβ as mechanism to regulate production and avoid overabundance of this cytokine. However, these studies were carried out in fibroblasts not in DCs, and our findings of a specific localisation and differential gene expression profile of IFNβ-producing pDCs strongly contradict the model of stochastic expression of IFNβ. Of note, we could not observe any differences in expression of IRF7 between IFNβ-producing and non-producing pDCs. Rather,

these findings suggest that production of IFNβ is specifically regulated among different tissues and cell types. Another potential explanation for restricted expression of IFNβ by only ~5% of pDCs could be an epigenetic blockade of the *ifnb* promoter in the non-producing pDC subset. So far, this has only been described for murine embryonic fibroblasts (Fang et al., 2012), and should be investigated in DCs or other cell types in future studies.

In summary, using and IFNβ-reporter mouse model we were able to characterise for the first time a distinct subset of IFNβ-producing pDCs within the spleen after TLR9 stimulation. Here we describe IFNβ-producing pDCs as a low frequency subset of splenic $CCR9^{+}$ $CD9^{-}$ pDCs with specific a localisation, gene expression profile and function independent of the type I IFN mediated feedback loop.

4.2 The ability of a distinct subset of pDCs to produce IFNβ is associated with their gene expression profile

In the work described in chapters 3.1 and 4.1 we were able to show that IFNβ-producing pDCs in the spleen are a distinct subset of pDCs with unique functions and a distinct gene expression profile as compared to non-IFNβ-producing pDCs (Bauer, Dress et al., *in revision*). However, since our data contradict existing models of a stochastic expression of the IFNβ gene (Apostolou et al., 2008; Zhao et al., 2012) it was important to determine if we could identify additional factors which drive pDCs to become either IFNβ-producing or non-producing cells. In order to achieve this goal, we analysed our microarray data from the work described in 3.1 and 4.1 for genes highly and differentially expressed in IFNβ-producing vs. non-producing pDCs, including genes with no known functions in pDCs. This resulted in a few candidate genes with annotated functions in cell signalling, development or cell maintenance processes. We picked two of these genes for subsequent analysis based a combination of being among the top ten genes most overrepresented in IFNβ-producing vs. non-producing pDCs, on potentially relevant functions described in other cell types, and on the availability of existing knock-out mice. The chosen genes encode the transcription factor BATF and the membrane protein PSD-93.

4.3 BATF is involved in regulation of IFNβ production by pDCs after TLR9 stimulation

BATF family members reportedly play a role in development and function of immune cell types such as T and B cells (Edelson et al., 2010; Ise et al., 2011; Schraml et al., 2009). The transcription factor BATF3 is crucial for the development of $CD8\alpha^+$ cDCs (Hildner et al., 2008). However, no impact of BATF on development of pDCs has been observed (Tussiwand et al., 2012), nor has a role for this transcription factor in pDC functions like type I IFN production been described. In this study, we show that BATF is highly expressed in IFNβ-producing pDCs, and may be directly involved in IFNβ production by these cells.

In previous findings we could demonstrate that IFNβ-producing pDCs have a distinct gene expression profile compared to non-IFNβ-producing pDCs, with various genes involved in immune regulation processes highly differentially expressed. Among these genes we found BATF to be highly upregulated. In accordance with our microarray data, we were able to verify this distinct higher expression of BATF in *ex vivo* sorted IFNβ-producing pDCs by qRT-PCR. Furthermore, using IFNβ-reporter mice in combination with FACS analysis and confocal microscopy, we could show that splenic and bone marrow-derived pDCs expressing IFNβ also had a high intracellular (nuclear) expression of BATF. These data confirm that IFNβ-producing pDCs upregulate the transcription factor BATF *in vitro* and *in vivo* after TLR9 stimulation.

Tussiwand et al. have reported that pDC development is unaffected by a loss of BATF (Tussiwand et al., 2012). Effects on type I IFN production of these cells were also not previously reported. However, since we know that IFNβ-producing pDCs represent only ~5% of the overall splenic pDC population, we hypothesized that developmental defects and/or a loss of this very low frequency population could have gone unnoticed in previous studies. In order to investigate development, function and type I IFN production in pDCs lacking BATF we made use of $BATF^{-/-}$ mice (Schraml et al., 2010). In accordance with Tussiwand et al. we found bone marrow-derived Flt3-L-differentiated pDCs to develop normally and capable of upregulating activation markers upon TLR stimulation (Tussiwand et al., 2012). Furthermore, percentages of pDCs in most tissues in naïve or

stimulated BATF-deficient mice were comparable to wildtype mice. However, we found that absolute numbers of splenic pDCs were increased in naïve and stimulated BATF-deficient mice relative to controls, and that BATF-deficient mice overall have slightly higher absolute numbers of pDCs across all analysed tissues. This was true for absolute cell count but not in terms of percentage and has not been described before. In some tissues this was accompanied by an increased overall cell number. Another explanation could be that due to the developmental defect of $CD8\alpha^+$ cDCs, DC-progenitors might be driven towards commitment to the pDC rather than cDC lineage. Furthermore, it is possible, that these immature pDCs might convert to cDCs later as a compensatory effect (Schlitzer et al., 2011; Segura et al., 2009). This latter explanation could be strengthened by the observation that BATF-deficient pDCs show a lower expression of the classical pDC surface markers B220 and CCR9, even though they expressed normal levels of other classical pDC surface markers such as CD11c, mPDCA-1, SiglecH and MHC class II. This could be a hint, that these cells are either not yet functional or fully developed pDCs or, as shown for $CCR9^-$ pDCs might have the capacity to convert to cDCs (Segura et al., 2009). Therefore, BATF might not be involved in pDC ontogeny in the bone marrow rather than in final development or maturation of these cells in the periphery. We were wondering if this had an impact on type I IFN production by pDCs and especially IFNβ production since IFNβ-producing wildtype pDCs strongly upregulate BATF suggesting a potential role for this transcription factor in pDC transcriptional induction of IFNβ. We found that stimulation with A and B type CpGs generally resulted in comparable numbers of comparably activated pDCs, as shown by the upregulation of CD86, in BATF-deficient mice with no obvious CpG-specific effects. In contrast, using whole tissue ELISA we observed overall higher levels of IFNβ in the analysed tissues (e.g. spleen) in BATF-deficient mice after stimulation with an A type CpG while stimulation with B type CpG resulted in higher levels of IFNβ in wildtype and lower levels in BATF-deficient mice. It has been shown, that A type CpG potentially induces stronger type I IFN responses than B type CpG (Waibler et al., 2008). Therefore it might be possible, that BATF-deficient pDCs are less responsive in that they need a stronger stimulus to produce high amounts of IFNβ. Alternatively, CpG A and CpG B, both of which

trigger TLR9, might induce slightly different signalling pathways downstream from TLR9, which might be altered due to the lack of the transcription factor BATF. We sought to determine if increased production of IFNβ following CpG A is due to the increased numbers of pDCs in BATF-deficient mice or altered signalling pathways and therefore altered capacities to produce this cytokine per cell. To this end, we generated a new mouse strain of $BATF^{-/-}$x$IFN\beta^{mob/mob}$ by crossing $BATF^{-/-}$ mice with IFNβ-reporter mice. Bone marrow-derived Flt3-L-differentiated pDCs from these $BATF^{-/-}$x$IFN\beta^{mob/mob}$ mice show higher percentages of IFNβ/YFP^{+} cells 6 h after stimulation with CpG A or B compared to their heterozygous or wildtype counterparts. Furthermore, B type CpG stimulation also led to increased percentages of IFNβ/YFP^{+} cells after 12 and 24 h stimulation of BATF-deficient cells while this difference was not apparent for CpG A stimulation. These effects were not influenced by a different activation status of wildtype and knock out cells since upregulation of activation markers such as CD86 was comparable between the genotypes after stimulation with CpG. However, after infection with MCMV pDCs deficient for BATF expressed significantly lower levels of CD86 but significantly higher levels of IFNβ/YFP than BATF-heterozygous or -wildtype mice. Furthermore, we found significantly increased levels of IFNβ in the supernatant of BATF-deficient BMDCs. This is in line with the tissue ELISA data for IFNβ, and again hints to a facilitation of IFNβ expression upon a very strong TLR9 stimulus in BATF-deficient cells and a greater capacity for BATF-deficient pDCs to produce large amounts of IFNβ *in vitro* compared to $BATF^{+/+}$ pDCs. To our surprise, we could not confirm these data *in vivo*. In contrast to our *in vitro* findings, upon *in vivo* stimulation with CpG (A or B) $BATF^{-/-}$ mice have a reduced number of IFNβ-producing pDCs in the spleen. Analysis of the surface marker profile of IFNβ/YFP-producing BATF-deficient pDCs revealed a lower expression of B220 on these cells, in line with the lower expression of B220 overall in the BATF-deficient pDC population. These decreased numbers of IFNβ-producing pDCs are in line with reduced serum levels for IFNβ in BATF-deficient mice upon CpG stimulation. In summary, despite increased IFNβ production *in vitro*, $BATF^{-/-}$ mice show reduced production of IFNβ *in vivo* after stimulation with CpG. These results seem quite contradictory at a first glance. But, we have to consider that the population we define here as pDCs, shows a lower expression of key-pDC

surface markers such as B220 and CCR9 in BATF-deficient mice and might therefore not be true or fully differentiated pDCs, but could be immature pDCs with a potential to convert into cDCs. This could explain why in a BATF-deficient situation only few pDCs respond with IFNβ production *in vivo*. *In vitro*, we create an artificial situation where we enrich fully differentiated pDCs by using the growth and differentiation factor Flt3-L and further facilitate maturation of these pDCs with a directed TLR stimulation e.g. with CpG. This might skew more BATF-deficient pDCs to become fully differentiated and mature pDCs able to produce IFNβ than it is likely to happen in the *in vivo* situation. Also, it is possible that only a very strong TLR stimulus is able to induce IFNβ signalling pathways in BATF-deficient pDCs while a weaker TLR stimulus might fail to do so. This latter could be likely if BATF is a scaffold transcription factor immediately involved in initial IFNβ production by pDCs. Therefore, CpG might be an insufficient stimulus compared to a complex virus. However, it is also possible that the stimulation of BATF-deficient cells is dependent on the used doses of CpG. Therefore, it should be subject of further studies to repeat these CpG experiments and to do dose titration studies for CpG using BATF-deficient mice. In an attempt to investigate the consequences of BATF deficiency in the context of a stronger more physiological stimulus for induction of IFNβ production by pDCs, we infected BATF-deficient mice with a low dose of the LCMV Armstrong strain. From collaborative work, we know that BATF-deficient mice have significantly higher viral titres in various tissues following LCMV infection and are incapable of sustaining cytotoxic T cell responses despite normal T cell numbers (Grusdat et al., 2014). To our surprise, 8 days after LCMV infection the numbers of splenic pDC were significantly increased in BATF-deficient mice whereas this population had almost completely vanished in wildtype mice. This suggests that in the absence of BATF LCMV infection leads to enhanced recruitment of pDCs into the spleen. In line with our previous findings, splenic pDCs from BATF deficient mice exhibited a lower expression of B220 and CCR9 but, like pDCs from WT mice were highly activated upon during viral infection. Interestingly, several studies demonstrated that pDCs can undergo a phenotypic and functional switch towards cDCs under the influence of LCMV infection (Zuniga et al., 2004; Zuniga et al., 2008). Furthermore, BATF-deficient mice had increased serum levels of IFNα as

well as IFNβ, and genes involved in type I IFN signalling including IRF7 were found to be highly induced upon LCMV infection in BATF deficient compared to control mice. In conclusion, we find BATF-deficient pDCs to be strongly activated to produce type I IFN after infection with LCMV. These differences observed here could be due do pDC related defects e.g. higher numbers of immature pDCs that have the potential to differentiate to cDCs or higher viral titres in BATF-deficient mice triggering increased type I IFN production or a combination of both.

In summary, these data imply that BATF-deficient mice have overall higher numbers of pDCs, that can be activated to produce large amounts of type IFN upon proper stimulation. While, BATF-deficient pDCs develop normally in the bone marrow their continued differentiation in the periphery appears to be perturbed. In the spleen we find elevated numbers of pDCs which fail to express some classical pDC markers such CCR9 and B220 It is possible that BATF is involved in the terminal maturation steps of pDCs or maybe even in the conversion of $CCR9^-$ immature pDCs to cDCs (Segura et al., 2009) as the overall splenic pDC population in BATF-deficient mice has a lower expression of CCR9 than in the wildtype situation. Furthermore, BATF-deficient pDCs seem to have an impaired IFNβ response to weak stimuli, such as B type CpGs, while stronger stimuli, like viral infections seem to induce even higher type I IFN production than in wild type cells.

Since BATF is a transcription factor, we wondered whether it might be directly involved in the induction and expression of the IFNβ gene. We have conducted some initial experiments to address this possibility. A dual-luciferase assay involving transfection of HEK cells with *Batf* and an *Ifnb*-promoter-luciferase constructs, revealed that BATF can potentiate *Ifnb*-promoter activity and therefore may be directly involved in IFNβ production. BATF is known to form heterodimers with Jun in order to interact with transcription factors of the IRF family. This complex can bind to AIC elements on target genes and regulate their expression (Murphy et al., 2013; Li et al., 2012). So far, interactions of this nature have been shown for IRF4 and IRF8. It is possible, that BATF might also interact with IRF7, a transcription factor constitutively expressed in pDCs playing a key role in expression of IFNβ. The initial findings from our luciferase assay raise the possibility that BATF might interact with IRF7 in binding to the *Ifnb*-promoter.

However, this theory needs to be investigated with further experiments. Another strong hint to the role of BATF in regulating IFNβ production is that mice deficient for BATF are protected in a murine model of the auto-immune disease multiple sclerosis (EAE) (Schraml et al., 2009). We could show, that upon strong TLR stimulation, BATF-deficient mice produce higher amounts of IFNβ compared to control animals. Furthermore, rIFNβ is used as a therapy to limit severity of multiple sclerosis. Therefore, it is possible that elevated production of IFNβ in BATF-deficient mice, as we have observed here, could limit EAE. Another example is infection with the protozoan parasite *Toxoplasma gondii*. Here it was shown that mice deficient for BATF3, that lack $CD8\alpha^+$ cDCs and therefore show defects in IL-12 and IFNγ production are highly susceptible to this infection (Mashayekhi et al., 2011). We could show that opposed to mice lacking BATF3, BATF deficiency led to partial protection in the acute phase of infection with *T. gondii*. We suspect that early increase in IFNβ production in $BATF^{-/-}$ mice might offer a survival advantage during the early phases of infection. Also, it has been shown that treatment with rIFNβ leads to inhibition of *T. gondii* parasite growth in macrophages *in vitro* and *in vivo* (Schmitz et al., 1989; Orellana et al., 1991).

Taken together, these data imply several possible roles for BATF in IFNβ-producing pDCs. On the one hand BATF could be involved in initial induction of the IFNβ gene, for instance by targeting of *the Ifnb*-promoter in cooperation with IRF7. This first hypothesis is also supported by our findings that BATF expression in IFNβ-producing pDCs is independent of the IFNAR. On the other hand BATF could act as a negative regulator of the type I IFN response in order to limit overproduction of this cytokine. The latter case is likely since we could observe elevated level of type I IFN in the absence of BATF throughout different experimental systems. Last, but not least, BATF could have a combination of these functions, acting as a very tight regulator of induction and limiting of IFN responses. The underlying molecular mechanisms of these regulatory BATF-actions are focus of on-going studies in our lab and will help to further understand the impact of this transcription factor on type I IFN production. Ultimately this work could be of great importance for guiding therapeutic strategies using type I IFNs in the future.

4.4 PSD-93 and its role in IFNβ producing splenic pDCs

In our microarray analysis comparing gene expression profiles from splenic IFNβ-producing and non-producing pDCs we found PSD-93 highly expressed specifically in IFNβ-producing pDCs. Therefore, we hypothesized that PSD-93 might be important for differentiation of or IFNβ production in these cells.

We were able to verify the elevated expression of PSD-93 in splenic IFNβ-producing pDCs by independent qRT-PCR analysis on *ex vivo* sorted producing vs. non-producing pDCs 6 h after TLR9 stimulation with CpG. We also found that PSD-93 expression was largely independent of the type I IFN amplification loop via the IFNAR. PSD-93 is known to be expressed in neuronal membranes at postsynaptic sites (Brenman et al., 1996). Immunofluorescence stainings of bone marrow-derived Flt3-L-differentiated pDCs confirmed that PSD-93 is also expressed in the membrane of activated IFNβ-producing pDCs. Specifically, PSD-93 was undetectable in naïve pDCs, but visible in punctate distribution on the surface of IFNβ-producing pDCs 24 h after TLR9 stimulation. We hypothesize that similar expression patterns for PSD-93 in the membrane of pDCs and dendrites of neurons (El-Husseini et al., 2000) may underline similar functions of this protein in these two distinct cell types. For instance, PSD-93 builds heterodimers with its family member PSD-95 acting as scaffold proteins in assembling and subsequent signalling of the NMDA receptor (Brenman et al., 1996; Carlisle et al., 2008; Kim et al., 1996) and is involved in formation of lipid rafts (Delint-Ramirez et al., 2010). We suspect that PSD-93 may play a similar role in pDCs acting as a scaffold for receptors or membrane domains proteins important for the function of IFNβ-producing pDCs.

It is also possible that PSD-93 might be involved in terminal differentiation of IFNβ-producing pDCs or signalling processes leading to production of IFNβ by this distinct pDC subset. In order to investigate this hypothesis we made use of PSD-93-deficient mice (McGee et al., 2001). PSD-93-deficient bone marrow-derived Flt3-L-differentiated pDCs and cDCs developed normally in our hands. Our results also demonstrate that loss of PSD-93 does not affect differentiation of these cells *in vitro*. However, mice deficient for PSD-93 showed overall increased cell numbers in the spleen before and after stimulation hinting to a possible higher rate of proliferation in spleen resident immune and non-immune cells or

increased recruitment of these cells into the spleen. In contrast, liver cell numbers were decreased in PSD-93-deficient mice, indicating that cellular distribution may be broadly imbalanced in these animals. Moreover, we found that elevated cell numbers in the spleen of PSD-93-deficient mice were at least partially due to significantly increased absolute numbers of pDCs and cDCs. In general, we found increased numbers of pDCs throughout all analysed tissues in both naïve PSD-93-deficient mice and following CpG stimulation. In spite of these differences no obvious effects of PSD-93 on differentiation of bone marrow-derived pDCs were observed, suggesting that lack of PSD-93 either leads to a redistribution or enhanced recruitment of pDCs into the tissues tested or to increased proliferation of pDCs in the bone marrow subsequently leading to higher pDC numbers throughout the body. It is possible, that PSD-93 might play a role during very early differentiation of DC pre-cursors. Common DC progenitor cells (CDPs) are dependent on Flt3-L for further differentiation to either pDCs or pre-DCs that in turn give rise to cDCs (Geissmann et al., 2010; Naik et al., 2006; Onai et al., 2007; Poltorak and Schraml, 2015; Schlitzer et al., 2015b). It is conceivable that at this early stage of pDC vs. cDC commitment PSD-93 or PSD-93 in interaction with other proteins might be involved in Flt3 signalling resulting controlling differentiation of pDCs or cDCs. In *in vitro* bone marrow cultures we artificially add a defined amount of Flt3-L and would miss subtle differentiation defects driven by a lack or overproduction of Flt3-L. To take this theory further we would suspect that PSD-93 mice might have higher levels of Flt3-L, leading to higher differentiation or proliferation rates of pDCs and cDCs. Future experiments are needed to test the validity of these concepts.

Next, we asked the question of whether pDCs lacking PSD-93 exhibit the same surface marker profile as wildtype pDCs. Analysing splenic pDCs from these mice revealed that PSD-93-deficient pDCs express all classical pDC surface markers such as CD11c, mPDCA-1, B220, CCR9, SiglecH and Ly6C. Therefore it seems that even in the absence of PSD-93, and despite the increased numbers of pDCs present in these animals, these cells truly resemble pDCs, unlike what we had described for the BATF-deficient situation (4.3) where pDCs appear to exist with a heightened capacity to convert to cDCs.

Increased numbers of DCs suggest increased levels of type I IFN after stimulation of these cells. To test this concept we crossed PSD-93$^{-/-}$ mice with our IFNβ-reporter mice and generated a new mouse strain: PSD-93$^{-/-}$xIFNβ$^{mob/mob}$. We could not detect differences in percentage of IFNβ-producing cells nor in levels of IFNα or IFNβ in the supernatant of CpG or Poly(I:C) stimulated bone marrow-derived Flt3-L-differentiated DCs from PSD-deficient and wildtype mice. In contrast, infection of these BMDCs with MCMV led to more IFNβ-producing pDCs from PSD-deficient than wildtype mice, despite no differences in activation status of these cells. These data prove that even in the absence of PSD-93 BMDCs are capable of mounting type I IFN responses. Even more strikingly, we could confirm this observation *in vivo*. *In vivo*, loss of PSD-93 led to significantly higher absolute numbers of splenic IFNβ-producing pDCs. Surprisingly, in spite elevated numbers of splenic IFNβ-producing pDCs, serum levels for IFNβ were not affected. This is an interesting observation and could be explained if despite the ability to produce IFNβ these pDCs might produce lower amounts of this cytokine per cell than wildtype pDCs. PSD-93 is strongly elevated in IFNβ-producing pDCs. Furthermore it is reportedly involved in signalling processes and in lipid raft formation (Brenman et al., 1996; Carlisle et al., 2008; Kim et al., 1996; Delint-Ramirez et al., 2010). Here, we have already discussed a possible role for PSD-93 in early DC differentiation through Flt3. But it is conceivable, that PSD-93 might also be involved more directly in type I IFN signalling at different step of the signalling cascade. Stimulation with CpG or viruses leads to activation of TLR9 on pDCs. It has been reported for macrophages that TLR9 localises in lipid rafts providing an optimal platform for interaction with its ligands (Szabo et al., 2007). Therefore, on one hand formation of lipid rafts facilitated by PSD-93 could affect initial signalling via TLR9. While on the other hand, within these lipid rafts PSD-93 could optimally interact with receptors such as TLR9 involved in signal induction and transmission. Whether PSD-93 and TLR9 interact needs to be investigated in future studies e.g. by co-localisation or immunoprecipitation assays. Further, PSD-93 also could be involved in signalling processes downstream of TLR9. In order to understand PSD-93 function and its role in IFNβ production by pDCs we need to carefully analyse potential interaction partners in the type I IFN signalling pathway such as IRFs, STATs or even test for possible

cooperation with the IFNAR. In addition, in an infection model with *Toxoplasma gondii* PSD-93 deficient mice rapidly succumbed the infection. Type I IFN production by DCs is crucial in the early phase of *T. gondii* infection for induction of subsequent immune responses and survival. PSD-93-deficient mice seem to fail to properly induce these factors. This again points to an important function for PSD-93 in IFNβ production and illustrates how important it is for us to understand the function and mechanisms of PSD-93 in pDCs. A key component of this analysis is to understand different splice variants of PSD-93 to identify which variants are important in IFNβ-producing pDCs. Ten different splice variants are described for the PSD-93 gene of which four are predicted to encode functional proteins. Therefore, the PSD-93 variant identified here in IFNβ-producing pDCs could differ from those described e.g. in postsynaptic sites. Identification of the specific splice variant(s) responsible for regulating IFNβ-producing pDCs could be important for further studies of the structure-function of PSD-93 in these cells and is an ongoing effort in our lab (strategy for splice variant identification is shown in the Appendix section of this thesis).

4.5 Dendritic cells and type I IFN play a crucial role in host defence against *Toxoplasma gondii*

The intracellular parasite *Toxoplasma gondii* is one of the most prevalent human parasites worldwide. Humans are rather dead end hosts of *T. gondii* and the outcome of individual infections is uncertain and ranges from harmless to life-threatening depending on the hosts precondition. We were interested in contributing to a greater understanding of host response and resistance mechanisms towards *T. gondii* infection. The importance of cytokines like IL-12 and IFNγ and subsequent induction of mechanisms leading to parasite clearance are well described (Bierly et al., 2008; Deckert-Schluter et al., 1996; Denkers and Gazzinelli, 1998; Hunter and Sibley, 2012; Mashayekhi et al., 2011; Pepper et al., 2008). The importance of type I IFN during *T. gondii* infection has been less well analysed, despite promising early findings where administration of rIFNβ led to inhibition of parasite growth within human (*in vitro*) or murine (*in vivo*) macrophages (Orellana et al., 1991; Schmitz et al., 1989). The studies by

Schmitz et al. and Orellana et al. led us to the hypothesis that endogenously produced type I IFN, especially IFNβ might play a role in early host immune responses to *T. gondii* infection.

In order to test this hypothesis we infected wildtype mice and mice deficient for either IFNβ or the type I IFN receptor with *T. gondii* type II strain ME49 cysts. ME49 was chosen as a model because it is able to induce robust immune responses, but is considered intermediate in terms of virulence (Kim and Weiss, 2004). We found that after infection with *T. gondii* mice deficient for either IFNβ or IFNAR where highly susceptible and most rapidly succumbed during the acute phase of infection lasting until day 10, followed by a plateau phase where surviving mice seemed to be protected until a second drop in survival during the chronic phase. In comparison, wildtype mice have a significantly higher survival rate, with most animals surviving well into the chronic phase of infection. This survival experiment clearly confirms our hypothesis that type I IFN are important during the early acute phase of infection with *T. gondii*. Therefore, we were interested in the underlying mechanisms of these effects. Since IL-12 and IFNγ are crucial initiators of host protection to *T. gondii* (Hunter and Sibley, 2012) we analysed production of these two cytokines by wildtype, IFNβ- or IFNAR-deficient mice after infection. Interestingly, we found significantly lower levels of IFNγ in the serum of IFNβ- and IFNAR-deficient mice in line with lower mRNA levels for this cytokine in the liver of these animals compared to wild type controls. Only wildtype mice were able to mount a strong IFNγ response after infection with *T. gondii*. We suspect this is a key explanation for the rapid demise of IFNβ- and IFNAR-deficient mice and that type I IFN actions are important upstream of IFNγ induction. During infection with *T. gondii* IFNγ is induced in NK and T cells by IL-12 produced by DCs and monocytes (Bierly et al., 2008; Mashayekhi et al., 2011; Pepper et al., 2008; Robben et al., 2004). We also analysed IL-12 levels of all three genotypes after infection. To our surprise we could not detect any significant defects in IL-12 production in IFNβ- and IFNAR-deficient mice relative to wildtype mice. Rather, these type I IFN-deficient mice had slightly elevated serum protein or mRNA levels for IL-12 showing that they are capable of strongly inducing production of this cytokine. This result also suggests that IL-12 alone is not sufficient to trigger IFNγ production during *T. gondii* infection.

We suspect that either IFNα and IFNβ themselves or type I IFN producing cells like DCs are important for NK or T cell stimulation for IFNγ production during *T. gondii* infection. To investigate this possibility, we first analysed IFNβ production and induction of genes involved in type I IFN signalling in wildtype, IFNβ- and IFNAR-deficient mice after infection. Wildtype mice exhibited slowly increasing serum IFNβ levels throughout the course of infection. We found genes involved in type I IFN signalling such as TLR9, IRF7 and ISG56 significantly upregulated in the spleen of wildtype but not IFNβ- and IFNAR-deficient mice post infection. Conversely, IFNAR-deficient and especially IFNβ-deficient mice showed a strong induction of these same genes in the liver. These findings hint to deregulation in induction of type I IFN related genes after infection with *T. gondii* in the absence of the IFNAR or IFNβ. mGBPs, representing important effector proteins in parasite clearance (Degrandi et al., 2013), were comparably induced at the mRNA level in wildtype, IFNβ- and IFNAR-deficient mice. Therefore decreased survival of type I IFN-deficient mice is likely not due to an impaired parasite targeting and destruction through mGBPs. However, IFNβ- and IFNAR-deficient mice showed significantly higher brain cyst loads compared to wildtype mice despite normal induction of mGBPs and induction of at least some genes involved in type I IFN signalling (albeit with a different tissue distribution). Thus, although immune responses are mounted against *T. gondii* in IFNβ- and IFNAR-deficient mice, these animals are unable to control the parasite load resulting in reduced survival after *T. gondii* infection. Of note, at this point we cannot rule out toxicity directly due to parasites themselves vs. immunopathology as a consequence of parasite load.

Moreover we observed an increase in overall cell numbers in the spleen of IFNβ-deficient mice on day 7 after infection, while in wildtype mice spleen cell numbers were not elevated until day 12. This rapid increase in splenic cell numbers was accompanied by elevated numbers of pDCs and $CD11b^{+}CD11c^{+}$ cDCs in the spleen of IFNβ-deficient mice. In contrast, at this early stage after infection wildtype mice showed higher numbers of pDCs and $CD11b^{+}CD11c^{+}$ cDCs in the mesenteric LNs. In the big picture we found that IFNβ-deficient mice had increased DC numbers throughout all tissues analysed (except for mesenteric LNs) while IFNAR-deficient mice rather displayed slightly reduced numbers of

DCs. In summary, we observed a complex deregulation in cellularity in the analysed tissues in the absence of type I IFN after *T. gondii* infection. This could either be due to a differential recruitment of e.g. DCs into the various tissues or due to an altered proliferation in type I IFN deficient animals resulting in an overall higher or lower number of myeloid cells. It is not known whether *T. gondii* can affect proliferation of DCs, but there are reports stating that *T. gondii* selectively infects pDCs using those cells as 'Trojan horses' to shuttle parasites across the host's body (Lambert et al., 2009; Bierly et al., 2008). In this context it was shown, that type II *T. gondii* strains such as ME49 induces higher migration rates by DCs and also have stronger intracellular associations with DCs *in vivo* than type I *T. gondii* strains (Lambert et al., 2009). The report by Lambert et al., suggested that DCs efficiently contribute to parasite propagation in a strain-specific manner. The *T. gondii* strain ME49 used in our study has a high capacity to infect DCs and transit in these cells. It is likely that signalling programs activated within the DC after parasite invasion differ between wildtype and type I IFN-deficient mice. We suspect that these differences could result in an altered migration pattern of infected DCs and therefore contribute to the deregulated distribution of pDCs and cDCs we observed in type I IFN-deficient mice. Furthermore, putative alterations in migration patterns of *T. gondii* infected DCs between the mouse genotypes tested could be part of the explanation for the differences in host immune responses at primary sites of infection e.g. in the mesenteric LNs after i.p. infection during the acute phase of infection in wild type and type I IFN-deficient mice. Based on our results and existing literature, we assume that DCs are of great importance for host responses and initiation of protective mechanisms during infection with *T. gondii*.

In order to investigate if either DCs or macrophages are the main producers of IFNβ during *T. gondii* infection we made use of IFNβ-reporter mice. Following infection of IFNβ$^{mob/mob}$ mice we detected a low but constant production of IFNβ in all analysed tissues that was stable until at least till day 7 after infection. Of note, IFNβ-producing cells were found mostly within non-B and non-T cells expressing high or intermediate levels of CD11c. This led us to the assumption that main producers of IFNβ after *T. gondii* infection are DCs and/or macrophages. To follow up on this we generated bone marrow-derived Flt3-L-differentiated pDCs

and cDCs as well as MCSF-differentiated BMDMs and infected these with viable or heat-killed tachyzoites of ME49. Viable but not heat-killed tachyzoites should be able to actively invade DCs or macrophages while heat-killed parasites should still be recognized by TLRs on these DCs or macrophages. Surface proteins of *T. gondii* are recognised by TLR11/12 on DCs (Raetz et al., 2013; Yarovinsky, 2014; Yarovinsky et al., 2005). We observed that predominantly pDCs and cDCs not macrophages produced IFNβ. Moreover, pDCs and cDCs from wildtype mice were equally activated, as shown by the upregulation of CD86, by viable or heat-killed tachyzoites while type I IFN-deficient DCs were barely activated after this challenge. Specifically, pDCs from IFNβ-deficient mice were activated by heat-killed- but less so by viable-tachyzoites, while IFNβ-deficient cDCs were activated by both. To our surprise neither viable nor heat-killed tachyzoites efficiently activated IFNAR-deficient pDCs and cDCs. This latter result could be of significant importance in addressing why type I IFN-deficient are more susceptible to *T. gondii* infection. Presumably less activated DCs produce less or no IFNβ and other pro-inflammatory cytokines such as IL-12. This could subsequently lead to diminished induction of IFNγ and weakened immune defence mechanisms. However, we observed normal IL-12 levels in IFNβ- and IFNAR-deficient mice *in vivo* after infection with *T. gondii.* Therefore this explanation seems less likely in our context. Another potential explanation could be that IL-12 is not the only mediator for activation of IFNγ responses in *T. gondii* infection. We presume that functionally activated DCs that upregulate co-stimulatory proteins such as CD86 and MHCII and are able to secrete pro-inflammatory cytokines provide a basis for induction of IFNγ and subsequent defence mechanisms in the wildtype situation. Our results suggest that lower levels of activated DCs in the absence of type I IFN result in lower IFNγ levels after infection. This could either be due to reduced activation of downstream signalling pathways triggered by direct binding of type I IFN to NK or T cells, or due to direct interactions of DCs with NK or T cells. For instance, DC presentation of *T. gondii* specific antigens might be perturbed in IFNβ- and IFNAR-deficient mice due to potential lower reactivity of the DCs themselves, and as a result might these DCs might trigger less efficient T cell responses including lower IFNγ secretion. Whether IFNβ- and IFNAR-deficient DCs have reduced

activation *in vivo* after *T. gondii* infection, similar to our observations *in vitro,* and if this is due to reduced parasite recognition by these cells and results in altered DC-T cell interactions are important questions that need to be investigated in future experiments. Also, we found that after *T. gondii* infection IFNγ is produced mostly by NK cells in the wildtype situation, and to a lesser extent by T cells during the acute phase of infection. An interesting tissue in this regard was the lung. We found prominent IFNγ production by a different cell population in each genotype post-infection: $CD4^+$ T cells in IFNAR-deficient mice, $CD8^+$ T cells in wildtype, and NK cells in IFNβ-deficient mice. Overall we found significant differences in cytokine producing cell populations throughout the analysed tissues between wildtype and type I IFN-deficient mice, which might be critical for dictating survival or death during *T. gondii* infection. Of note, basal IFNγ levels in T cells were relatively high. Therefore the importance of IFNγ production by T cells should be studied more carefully in this context along with DC-T cell interactions in further experiments. In this study, we hypothesize that NK cells are the most important producers of IFNγ in the acute phase of infection with *T. gondii*. Thus, we conducted some initial experiments to clarify the interactions between DCs and NK cells. In brief, we generated bone marrow-derived Flt3-L-differentiated pDCs and cDCs from wildtype and IFNAR-deficient mice and activated them with CpG. Activated or unstimulated DCs then were co-cultured overnight with purified wildtype or IFNAR-deficient NK cells. Subsequent analyses of NK cell activation status revealed that only fully activated wildtype, but not IFNAR-deficient DCs were able to activate NK cells. Furthermore, rIFNβ alone was not sufficient for NK cell activation. Therefore we hypothesize that functional, activated DCs are capable of recognising *T. gondii* tachyzoites and subsequently trigger IFNβ and IL-12 production during the acute phase of infection. These cells interact with NK cells (and T cells) in order to trigger IFNγ production and subsequently induce mechanisms leading to parasite clearance. However, in an *in vivo* NK cell depletion experiment we could not observe any differences in survival of wildtype and type I IFN-deficient mice with or without NK cell depletion after infection with *T. gondii.* It is unlikely that a lack of NK cells would not affect the outcome of this infection. Rather, we think that due to injection of 200 µl of fluid every 3 days in order to deplete the NK cells we

artificially improved survival of the mice. Therefore we could not see an effect of NK cell depletion. In order to analyse, if a lack of NK cells has an impact on the outcome of infection this experiment needs to be repeated with more mice and a lower amount of fluid injected.

The above described concepts are supported by our findings that mice deficient for type I IFN are highly susceptible to *T. gondii* infection, have higher brain cyst loads, altered distribution of myeloid cells, and defects in cytokine production (e.g. low IFNγ level) and fail to fully activate DCs after *T. gondii* infection. Whether this theory of DC-NK cell interactions holds true will need to be established in further experiments. However, in this study we were nevertheless able to show that type I IFN play a crucial role in host protection during infection with the protozoan parasite *Toxoplasma gondii*.

5. References

Adams, L.B., Hibbs, J.B., Jr., Taintor, R.R., and Krahenbuhl, J.L. (1990). Microbiostatic effect of murine-activated macrophages for Toxoplasma gondii. Role for synthesis of inorganic nitrogen oxides from L-arginine. The Journal of immunology *144*, 2725-2729.

Aliberti, J., Valenzuela, J.G., Carruthers, V.B., Hieny, S., Andersen, J., Charest, H., Reis e Sousa, C., Fairlamb, A., Ribeiro, J.M., and Sher, A. (2003). Molecular mimicry of a CCR5 binding-domain in the microbial activation of dendritic cells. Nature immunology *4*, 485-490.

Apostolou, E. and Thanos, D. (2008). Virus Infection Induces NF-kappaB-dependent interchromosomal associations mediating monoallelic IFN-beta gene expression. Cell *134*, 85-96.

Asselin-Paturel, C., G. Brizard, K. Chemin, A. Boonstra, A. O'Garra, A. Vicari, and G. Trinchieri. 2005. Type I interferon dependence of plasmacytoid dendritic cell activation and migration. The Journal of experimental medicine *201*, 1157-1167.

Barchet, W., Blasius, A., Cella, M., and Colonna, M. (2005). Plasmacytoid dendritic cells: in search of their niche in immune responses. Immunologic research *32*, 75-83.

Barchet, W., Cella, M., Odermatt, B., Asselin-Paturel, C., Colonna, M., and Kalinke, U. (2002). Virus-induced interferon alpha production by a dendritic cell subset in the absence of feedback signaling in vivo. The Journal of experimental medicine *195*, 507-16.

Bierly, A.L., Shufesky, W.J., Sukhumavasi, W., Morelli, A.E., and Denkers, E.Y. (2008). Dendritic cells expressing plasmacytoid marker PDCA-1 are Trojan

horses during Toxoplasma gondii infection. The Journal of immunology *181*, 8485-8491.

Bjorck, P., Leong, H.X., and Engleman, E.G. (2011). Plasmacytoid dendritic cell dichotomy: identification of IFN-alpha producing cells as a phenotypically and functionally distinct subset. The Journal of immunology *186*, 1477-1485.

Blasius, A.L., and Beutler, B. (2010). Intracellular toll-like receptors. Immunity *32*, 305-315.

Blasius, A.L., Cella, M., Maldonado, J., Takai, T., and Colonna, M. (2006a). Siglec-H is an IPC-specific receptor that modulates type I IFN secretion through DAP12. Blood *107*, 2474-2476.

Blasius, A.L., Giurisato, E., Cella, M., Schreiber, R.D., Shaw, A.S., and Colonna, M. (2006b). Bone marrow stromal cell antigen 2 is a specific marker of type I IFN-producing cells in the naive mouse, but a promiscuous cell surface antigen following IFN stimulation. The Journal of immunology *177*, 3260-3265.

Bogdan, C., Mattner, J., and Schleicher, U. (2004). The role of type I interferons in non-viral infections. Immunological reviews *202*, 33-48.

Brenman, J.E., Chao, D.S., Gee, S.H., McGee, A.W., Craven, S.E., Santillano, D.R., Wu, Z., Huang, F., Xia, H., Peters, M.F., Froehner, S.C., and Bredt, D.S. (1996). Interaction of nitric oxide synthase with the postsynaptic density protein PSD-95 and alpha1-syntrophin mediated by PDZ domains. Cell *84*, 757-767.

Brenman, J.E., Topinka, J.R., Cooper, E.C., McGee, A.W., Rosen, J., Milroy, T., Ralston, H.J., and Bredt, D.S. (1998). Localization of postsynaptic density-93 to dendritic microtubules and interaction with microtubule-associated protein 1A. The Journal of neuroscience *18*, 8805-8813.

Carlisle, H.J., Fink, A.E., Grant, S.G., and O'Dell, T.J. (2008). Opposing effects of PSD-93 and PSD-95 on long-term potentiation and spike timing-dependent plasticity. The Journal of physiology *586*, 5885-5900.

Carotta, S., Dakic, A., D'Amico, A., Pang, S.H., Greig, K.T., Nutt, S.L., and Wu, L. (2010). The transcription factor PU.1 controls dendritic cell development and Flt3 cytokine receptor expression in a dose-dependent manner. Immunity *32*, 628-641.

Carrero, J.A., Calderon, B., and Unanue, E.R. (2004). Type I interferon sensitizes lymphocytes to apoptosis and reduces resistance to Listeria infection. The Journal of experimental medicine *200*, 535-540.

Cisse, B., Caton, M.L., Lehner, M., Maeda, T., Scheu, S., Locksley, R., Holmberg, D., Zweier, C., den Hollander, N.S., Kant, S.G., Holter, W., Rauch, A., Zhuang, Y., and Reizis, B. (2008). Cell Transcription factor E2-2 is an essential and specific regulator of plasmacytoid dendritic cell development. Cell *135,* 37-48.

Colonna, M. (2004). Viral immunosuppression: disabling the guards. The Journal of clinical investigation *113*, 660-662.

Dakic, A., Metcalf, D., Di Rago, L., Mifsud, S., Wu, L., and Nutt, S.L. (2005). PU.1 regulates the commitment of adult hematopoietic progenitors and restricts granulopoiesis. The Journal of experimental medicine *201*, 1487-1502.

Daubener, W., Remscheid, C., Nockemann, S., Pilz, K., Seghrouchni, S., Mackenzie, C., and Hadding, U. (1996). Anti-parasitic effector mechanisms in human brain tumor cells: role of interferon-gamma and tumor necrosis factor-alpha. European journal of immunology *26*, 487-492.

de Weerd, N.A., Vivian, J.P., Nguyen, T.K., Mangan, N.E., Gould, J.A., Braniff, S.J., Zaker-Tabrizi, L., Fung, K.Y., Forster, S.C., Beddoe, T.*, et al.*

(2013). Structural basis of a unique interferon-beta signaling axis mediated via the receptor IFNAR1. Nature immunology *14*, 901-907.

Decker, T., Muller, M., and Stockinger, S. (2005). The yin and yang of type I interferon activity in bacterial infection. Nature reviews. Immunology *5*, 675-687.

Deckert-Schluter, M., Rang, A., Weiner, D., Huang, S., Wiestler, O.D., Hof, H., and Schluter, D. (1996). Interferon-gamma receptor-deficiency renders mice highly susceptible to toxoplasmosis by decreased macrophage activation. Laboratory investigation. A journal of technical methods and pathology *75*, 827-841.

Degrandi, D., Konermann, C., Beuter-Gunia, C., Kresse, A., Wurthner, J., Kurig, S., Beer, S., and Pfeffer, K. (2007). Extensive characterization of IFN-induced GTPases mGBP1 to mGBP10 involved in host defense. The Journal of immunology *179*, 7729-7740.

Degrandi, D., Kravets, E., Konermann, C., Beuter-Gunia, C., Klumpers, V., Lahme, S., Wischmann, E., Mausberg, A.K., Beer-Hammer, S., and Pfeffer, K. (2013). Murine guanylate binding protein 2 (mGBP2) controls Toxoplasma gondii replication. Proceedings of the National Academy of Sciences of the United States of America *110*, 294-299.

Delint-Ramirez, I., Fernández, E., Bayés, A., Kicsi, E., Komiyama, N.H., and Grant, S.G. (2010). In vivo composition of NMDA receptor signaling complexes differs between membrane subdom*ains and is modulated by PSD-95 and PSD-93. The Journal of neuroscience 30,* 8162-70.

Denkers, E.Y., and Gazzinelli, R.T. (1998). Regulation and function of T-cell-mediated immunity during Toxoplasma gondii infection. Clinical microbiology reviews *11*, 569-588.

Edelson, B.T., Kc, W., Juang, R., Kohyama, M., Benoit, L.A., Klekotka, P.A., Moon, C., Albring, J.C., Ise, W., Michael, D.G., Bhattacharya, D., Stappenbeck, T.S., Holtzman, M.J., Sung, S.S., Murphy, T.L., Hildner, K., and Murphy K.M. (2010). Peripheral CD103+ dendritic cells form a unified subset developmentally related to CD8alpha+ conventional dendritic cells. The Journal of experimental medicine *207*, 823-836.

El-Husseini, A.E., Topinka, J.R., Lehrer-Graiwer, J.E., Firestein, B.L., Craven, S.E., Aoki, C., and Bredt, D.S. (2000). Ion channel clustering by membrane-associated guanylate kinases. Differential regulation by N-terminal lipid and metal binding motifs. The Journal biological chemistry. *275,* 23904-10.

Fang, T.C.,Schaefer, U., Mecklenbrauker, I., Stienen, A., Dewell, S., Chen, M.S., Rioja, I., Parravicini, V., Prinjha, R.K., Chandwani, R., MacDonald, M.R., Lee, K., Rice, C.M., and Tarakhovsky, A. (2012). Histone H3 lysine 9 di-methylation as an epigenetic signature of the interferon response. The Journal of experimental medicine *209,* 661-669.

Fitzjohn, S.M., Doherty, A.J., and Collingridge, G.L. (2006). Promiscuous interactions between AMPA-Rs and MAGUKs. Neuron *52*, 222-224.

Gazzinelli, R.T., and Denkers, E.Y. (2006). Protozoan encounters with Toll-like receptor signalling pathways: implications for host parasitism. Nature reviews. Immunology *6*, 895-906.

Gazzinelli, R.T., Hieny, S., Wynn, T.A., Wolf, S., and Sher, A. (1993). Interleukin 12 is required for the T-lymphocyte-independent induction of interferon gamma by an intracellular parasite and induces resistance in T-cell-deficient hosts. Proceedings of the National Academy of Sciences of the United States of America *90*, 6115-6119.

Geissmann, F., Manz, M.G., Jung, S., Sieweke, M.H., Merad, M., and Ley, K. (2010). Development of monocytes, macrophages, and dendritic cells. Science *327*, 656-661.

Ghosh, H.S., Cisse, B., Bunin, A., Lewis, K.L., and Reizis, B. (2010). Continuous expression of the transcription factor e2-2 maintains the cell fate of mature plasmacytoid dendritic cells. Immunity *33*, 905-916.

Gilliet, M., Cao, W., and Liu, Y.J. (2008). Plasmacytoid dendritic cells: sensing nucleic acids in viral infection and autoimmune diseases. Nature reviews. Immunology *8*, 594-606.

Gottenberg, J.E., Cagnard, N., Lucchesi, F.L., Mistou S., Lazure, T., Jacques, S., Ba, N., Ittah, M., Lepajolec, C., Labetoulle, M., Ardizzone, M., Sibilia, J., Fournier, C., Chiocchia, G., and Mariette, X. (2006). Activation of IFN pathways and plasmacytoid dendritic cell recruitment in target organs of primary Sjogren's syndrome. Proceedings of the National Academy of Sciences of the United States of America *103*, 2770-2775.

Grusdat, M., McIlwain, D.R., Xu, H.C., Pozdeev, V.I., Knievel, J., Crome, S.Q., Robert-Tissot, C., Dress, R.J., Pandyra, A.A., Speiser, D.E.*, et al.* (2014). IRF4 and BATF are critical for CD8(+) T-cell function following infection with LCMV. Cell death and differentiation *21*, 1050-1060.

Gunn, M.D., Tangemann, K., Tam, C., Cyster, J.G., Rsen S.D., and Williams, L.T. (1998). A chemokine expressed in lymphoid high endothelial venules promotes the adhesion and chemotaxis of naive T lymphocytes. Proceedings of the National Academy of Sciences of the United States of America *95*, 258-263.

Guo, M.L., Xue, B., Jin, D.Z., Mao, L.M., and Wang, J.Q. (2012). Interactions and phosphorylation of postsynaptic density 93 (PSD-93) by extracellular signal-regulated kinase (ERK). Brain research *1465*, 18-25.

Hacker, C., Kirsch, R.D., Ju, X.S., Hieronymus, T., Gust, T.C., Kuhl, C., Jorgas, T., Kurz, S.M., Rose-John, S., Yokota, Y., and Zenke, M. (2003). Transcriptional profiling identifies Id2 function in dendritic cell development. Nature immunology *4*, 380-386.

Hadeiba, H., Sato, T., Habtezion, A., Oderup, C., Pan, J., and Butcher, E.C. (2008). CCR9 expression defines tolerogenic plasmacytoid dendritic cells able to suppress acute graft-versus-host disease. Nature immunology *9*, 1253-1260.

Han, S.J., Melichar, H.J., Coombes, J.L., Chan, S.W., Koshy, A.A., Boothroyd, J.C., Barton, G.M., and Robey, E.A. (2014). Internalization and TLR-dependent type I interferon production by monocytes in response to Toxoplasma gondii. Immunology and cell biology *92*, 872-881.

Hildner, K., Edelson, B.T., Purtha, W.E., Diamond, M., Matsushita, H., Kohyama, M., Calderon, B., Schraml, B.U., Unanue, E.R., Diamond, M.S., Schreiber, R.D., Murphy T.L., and Murphy, K.M. (2008). Batf3 deficiency reveals a critical role for CD8alpha+ dendritic cells in cytotoxic T cell immunity. Science *322*, 1097-1100.

Hochrein, H., Shortman, K., Vremec, D., Scott, B., Hertzog, P., and O'Keeffe, M. (2001). Differential production of IL-12, IFN-alpha, and IFN-gamma by mouse dendritic cell subsets. The Journal of immunology *166*, 5448-5455.

Honda, K., Yanai, H., Negishi, H., Asagiri, M., Sato, M., Mizutani, T., Shimada, N., Ohba, Y., Takaoka, A., Yoshida, N., and Taniguchi, T. (2005). IRF-7 is the master regulator of type-I interferon-dependent immune responses. Nature *434*, 772-777.

Howard, J.C., Hunn, J.P., and Steinfeldt, T. (2011). The IRG protein-based resistance mechanism in mice and its relation to virulence in Toxoplasma gondii. Current opinion in microbiology *14*, 414-421.

Hunter, C.A., and Sibley, L.D. (2012). Modulation of innate immunity by Toxoplasma gondii virulence effectors. Nature reviews. Microbiology *10*, 766-778.

Hunter, C.A., Subauste, C.S., Van Cleave, V.H., and Remington, J.S. (1994). Production of gamma interferon by natural killer cells from Toxoplasma gondii-infected SCID mice: regulation by interleukin-10, interleukin-12, and tumor necrosis factor alpha. Infection and immunity *62*, 2818-2824.

Ichikawa, E., Hida, S., Omatsu, Y., Shimoyama, S., Takahara, K., Miyagawa, S., Inaba, K., and Taki, S. (2004). Defective development of splenic and epidermal CD4+ dendritic cells in mice deficient for IFN regulatory factor-2. Proceedings of the National Academy of Sciences of the United States of America *101*, 3909-3914.

Inaba, K., Turley, S., Iyoda, T., Yamaide, F., Shimoyama, S., Reis e Sousa, C., Germain, R.N., Mellman, I., and Steinman, R.M. (2000). The formation of immunogenic major histocompatibility complex class II-peptide ligands in lysosomal compartments of dendritic cells is regulated by inflammatory stimuli. The Journal of experimental medicine *191*, 927-936.

Inoue, M., Williams, K.L., Oliver, T., Vandenabeele, P., Rajan, J.V., Miao, E.A., and Shinohara, M.L. (2012). Interferon-beta therapy against EAE is effective only when development of the disease depends on the NLRP3 inflammasome. Science signaling *5*, ra38.

Ise, W., Kohyama, M., Schraml, B.U., Zhang, T., Schwer, B., Basu, U., Alt, F.W., Tang, J., Oltz, E.M., Murphy, T.L., and Murphy, K.M. (2011). The transcription factor BATF controls the global regulators of class-switch recombination in both B cells and T cells. Nature immunology *12*, 536-543.

Ivashkiv, L.B., and Donlin, L.T. (2014). Regulation of type I interferon responses. Nature reviews. Immunology *14*, 36-49.

Izaguirre, A., Barnes, B.J., Amrute, S., Yeow, W.S., Megjugorac, N., Dai, J., Feng, D., Chung, E., Pitha, P.M., and Fitzgerald-Bocarsly, P. (2003). Comparative analysis of IRF and IFN-alpha expression in human plasmacytoid and monocyte-derived dendritic cells. Journal of leukocyte biology *74*, 1125-1138.

Johnson, L.L. (1992). A protective role for endogenous tumor necrosis factor in Toxoplasma gondii infection. Infection and immunity *60*, 1979-1983.

Joynson; D.H., and Wreghitt, T.J. (2001). Toxoplasmosis: A Comprehensive Clinical Guide. Cambridge university press 1-42.

Karsunky, H., Merad, M., Cozzio, A., Weissman, I.L., and Manz, M.G. (2003). Flt3 ligand regulates dendritic cell development from Flt3+ lymphoid and myeloid-committed progenitors to Flt3+ dendritic cells in vivo. The Journal of experimental medicine *198*, 305-313.

Khan, I.A., Matsuura, T., and Kasper, L.H. (1994). Interleukin-12 enhances murine survival against acute toxoplasmosis. Infection and immunity *62*, 1639-1642.

Kim, E., Cho, K.O., Rothschild, A., and Sheng, M. (1996). Heteromultimerization and NMDA receptor-clustering activity of Chapsyn-110, a member of the PSD-95 family of proteins. Neuron *17*, 103-113.

Kim, K., and Weiss, L.M. (2004). Toxoplasma gondii: the model apicomplexan. International journal for parasitology *34*, 423-432.

Krug, A., Uppaluri, R., Facchetti, F., Dorner, B.G., Sheehan, K.C., Schreiber, R.D., Cella, M., and Colonna, M. (2002). IFN-producing cells respond to CXCR3 ligands in the presence of CXCL12 and secrete inflammatory chemokines upon activation. The Journal of immunology *169*, 6079-6083.

Lambert, H., Vutova, P., Adams, W.C., Lore, K., and Barragan, A. (2009). The Toxoplasma gondii-Shuttling Function of Dendritic Cells Is Linked to the Parasite Genotype. Infection and immunology. *77* 4 1679-1688.

Lambrecht, B.N., and Hammad, H. (2009). Biology of lung dendritic cells at the origin of asthma. Immunity *31*, 412-424.

Laouar, Y., Welte, T., Fu, X.Y., and Flavell, R.A. (2003). STAT3 is required for Flt3L-dependent dendritic cell differentiation. Immunity *19*, 903-912.

Le Mercier, I., Poujol, D., Sanlaville, A., Sisirak, V., Gobert, M., Durand, I., Dubois, B., Treilleux, I., Marvel, J., Vlach, J., Blay, J.Y., Bendriss-Vermare, N., Caux, C., Puisieux, I., and Goutagny, N. (2013). Tumor promotion by intratumoral plasmacytoid dendritic cells is reversed by TLR7 ligand treatment. Cancer research *1;73*, 4629-40.

Li, P., Spolski, R., Liao, W., Wang, L., Murphy, T.L., Murphy, K.M. and Leonard, W.J. (2012). BATF–JUN is critical for IRF4-mediated transcription in T cells. Nature 490, 543–546.

Liu, C., Lou, Y., Lizee, G., Qin, H., Liu, S., Rabinovich, B., Kim, G.J., Wang, Y.H., Ye, Y., Sikora, A.G., Overwijk W.W., Liu, Y.J., Wang, G., and Hwu, P. (2008). Plasmacytoid dendritic cells induce NK cell-dependent, tumor antigen-specific T cell cross-priming and tumor regression in mice. Journal of clinical investigation *118*, 1165-1175.

Liu, K., Victora, G.D., Schwickert, T.A., Guermonprez, P., Meredith, M.M., Yao, K., Chu, F.F., Randolph, G.J., Rudensky, A.Y., and Nussenzweig, M. (2009). In vivo analysis of dendritic cell development and homeostasis. Science *324*, 392-397.

Liu, K., Waskow, C., Liu, X., Yao, K., Hoh, J., and Nussenzweig, M. (2007). Origin of dendritic cells in peripheral lymphoid organs of mice. Nature Immunology *8*, 578-583.

Luther, S.A., Tang, H.L., Hyman, P.L., Farr, A.G., and Cyster, J.G. (2000). Coexpression of the chemokines ELC and SLC by T zone stromal cells and deletion of the ELC gene in the plt/plt mouse. Proceedings of the National Academy of Sciences of the United States of America *97*,12694-12699.

Luthra, P., Suna, D., Silvermanc, R.H., and Hea, B. (2001). Activation of IFN-β expression by a viral mRNA through RNase L and MDA5. Proceedings of the National Academy of Sciences of the United States of America *108*, 2118–2123.

Manz, M.G., Traver, D., Akashi, K., Merad, M., Miyamoto, T., Engleman, E.G., and Weissman, I.L. (2001). Dendritic cell development from common myeloid progenitors. Annals of the new york academy of sciences *938*, 167-173; 173-164.

Mashayekhi, M., Sandau, M.M., Dunay, I.R., Frickel, E.M., Khan, A., Goldszmid, R.S., Sher, A., Ploegh, H.L., Murphy, T.L., Sibley, L.D., and Murphy, K.M. (2011). CD8alpha(+) dendritic cells are the critical source of interleukin-12 that controls acute infection by Toxoplasma gondii tachyzoites. Immunity *35*, 249-259.

McGee, A.W., Topinka, J.R., Hashimoto, K., Petralia, R.S., Kakizawa, S., Kauer, F.W., Aguilera-Moreno, A., Wenthold, R.J., Kano, M., and Bredt, D.S. (2001). PSD-93 knock-out mice reveal that neuronal MAGUKs are not required for development or function of parallel fiber synapses in cerebellum. The Journal of neuroscience *21,* 3085-91.

McKenna, H.J., Stocking, K.L., Miller, R.E., Brasel, K., De Smedt, T., Maraskovsky, E., Maliszewski, C.R., Lynch, D.H., Smith, J., Pulendran, B., Roux, E.R., Teepe, M., Lyman, S.D., and Peschon J.J. (2000). Mice lacking flt3

ligand have deficient hematopoiesis affecting hematopoietic progenitor cells, dendritic cells, and natural killer cells. Blood *95*, 3489-3497.

McLeod, R., Boyer, K.M., Lee, D., Mui, E., Wroblewski, K., Karrison, T., Noble, A.G., Withers, S., Swisher, C.N., Heydemann, P.T.*, et al.* (2012). Prematurity and severity are associated with Toxoplasma gondii alleles. Clinical infectious diseases *54*, 1595-1605.

Mellman, I., and Steinman, R.M. (2001). Dendritic cells: specialized and regulated antigen processing machines. Cell *106*, 255-258.

Melo, M.B., Kasperkovitz, P., Cerny, A., Konen-Waisman, S., Kurt-Jones, E.A., Lien, E., Beutler, B., Howard, J.C., Golenbock, D.T., and Gazzinelli, R.T. (2010). UNC93B1 mediates host resistance to infection with Toxoplasma gondii. PLoS pathogens *6*, 1001071.

Merad, M., Ginhoux, F., and Collin, M. (2008). Origin, homeostasis and function of Langerhans cells and other langerin-expressing dendritic cells. Nature reviews. Immunology *8*, 935-947.

Moser, M., and Murphy, K.M. (2000). Dendritic cell regulation of TH1-TH2 development. Nature immunology *1*, 199-205.

Murphy, T.L., Tussiwand, R., and Murphy, K.M. (2013). Specificity through cooperation: BATF-IRF interactions control immune-regulatory networks. Nature reviews. Immunology *13*, 499-509.

Naik, S.H., Metcalf, D., van Nieuwenhuijze, A., Wicks, I., Wu, L., O'Keeffe, M., and Shortman, K. (2006). Intrasplenic steady-state dendritic cell precursors that are distinct from monocytes. Nature immunology *7*, 663-671.

Naik, S.H., Sathe, P., Park, H.Y., Metcalf, D., Proietto, A.I., Dakic, A., Carotta, S., O'Keeffe, M., Bahlo, M., Papenfuss, A., Kwak, J.Y., Wu, L., and Shortman,

K. (2007). Development of plasmacytoid and conventional dendritic cell subtypes from single precursor cells derived in vitro and in vivo. Nature immunology *8*, 1217-1226.

Nestle, F.O., Farkas, A., and Conrad, C. (2005). Dendritic-cell-based therapeutic vaccination against cancer. Current opinion in immunology *17*, 163-169.

Niess, J.H., Brand, S., Gu, X., Landsman, L., Jung, S., McCormick, B.A., Vyas, J.M., Boes, M., Ploegh, H.L., Fox, J.G.*, et al.* (2005). CX3CR1-mediated dendritic cell access to the intestinal lumen and bacterial clearance. Science *307*, 254-258.

Nussenzweig, M.C., and Steinman, R.M. (1980). Contribution of dendritic cells to stimulation of the murine syngeneic mixed leukocyte reaction. The Journal of experimental medicine *151*, 1196-1212.

Ogawa, M., Matsuzaki, Y., Nishikawa, S., Hayashi, S., Kunisada, T., Sudo, T., Kina, T., and Nakauchi, H. (1991). Expression and function of c-kit in hemopoietic progenitor cells. The Journal of experimental medicine *174*, 63-71.

Ogawa, Y., Horresh, I., Trimmer, J.S., Bredt, D.S., Peles, E., and Rasband, M.N. (2008). Postsynaptic density-93 clusters Kv1 channels at axon initial segments independently of Caspr2. The Journal of neuroscience *28*, 5731-5739.

Onai, N., Obata-Onai, A., Schmid, M.A., Ohteki, T., Jarrossay, D., and Manz, M.G. (2007). Identification of clonogenic common Flt3+M-CSFR+ plasmacytoid and conventional dendritic cell progenitors in mouse bone marrow. Nature immunology *8*, 1207-1216.

Orellana, M.A., Suzuki, Y., Araujo, F., and Remington, J.S. (1991). Role of beta interferon in resistance to Toxoplasma gondii infection. Infection and immunity *59*, 3287-3290.

Pepper, M., Dzierszinski, F., Wilson, E., Tait, E., Fang, Q., Yarovinsky, F., Laufer, T.M., Roos, D., and Hunter, C.A. (2008). Plasmacytoid dendritic cells are activated by Toxoplasma gondii to present antigen and produce cytokines. The Journal of immunology *180*, 6229-6236.

Perie, L., and Naik, S.H. (2015). Toward defining a 'lineage' - The case for dendritic cells. Seminars in cell & developmental biology *41*, 3-8.

Pfaffl, M.W. (2001). A new mathematical model for relative quantification in real-time RT-PCR. Nucleic acids research *29*, e45.

Pierre, P., Turley, S.J., Gatti, E., Hull, M., Meltzer, J., Mirza, A., Inaba, K., Steinman, R.M., and Mellman, I. (1997). Developmental regulation of MHC class II transport in mouse dendritic cells. Nature *388*, 787-792.

Pifer, R., Benson, A., Sturge, C.R., and Yarovinsky, F. (2011). UNC93B1 is essential for TLR11 activation and IL-12-dependent host resistance to Toxoplasma gondii. The Journal of biological chemistry *286*, 3307-3314.

Platanias, L.C. (2005). Mechanisms of type-I- and type-II-interferon-mediated signalling. Nature reviews. Immunology *5*, 375-386.

Poltorak, M.P., and Schraml, B.U. (2015). Fate mapping of dendritic cells. Frontiers in immunology *6*, 199.

Raetz, M., Kibardin, A., Sturge, C.R., Pifer, R., Li, H., Burstein, E., Ozato, K., Larin, S., and Yarovinsky, F. (2013). Cooperation of TLR12 and TLR11 in the IRF8-dependent IL-12 response to Toxoplasma gondii profilin. The Journal of immunology *191*, 4818-4827.

Reizis, B., Bunin, A., Ghosh, H.S., Lewis, K.L., and Sisirak, V. (2011). Plasmacytoid dendritic cells: recent progress and open questions. Annual review of immunology *29*, 163-183.

Robben, P.M., Mordue, D.G., Truscott, S.M., Takeda, K., Akira, S., and Sibley, L.D. (2004). Production of IL-12 by macrophages infected with Toxoplasma gondii depends on the parasite genotype. The Journal of immunology *172*, 3686-3694.

Sapoznikov, A., Fischer, J.A., Zaft, T., Krauthgamer, R., Dzionek, A., and Jung, S. (2007). Organ-dependent in vivo priming of naive CD4+, but not CD8+, T cells by plasmacytoid dendritic cells. The Journal of experimental medicine *204*, 1923-1933.

Satpathy, A.T., Kc, W., Albring, J.C., Edelson, B.T., Kretzer, N.M., Bhattacharya, D., Murphy, T.L., and Murphy, K.M. (2012). Zbtb46 expression distinguishes classical dendritic cells and their committed progenitors from other immune lineages. The Journal of experimental medicine *209*, 1135-1152.

Scanga, C.A., Aliberti, J., Jankovic, D., Tilloy, F., Bennouna, S., Denkers, E.Y., Medzhitov, R., and Sher, A. (2002). Cutting edge: MyD88 is required for resistance to Toxoplasma gondii infection and regulates parasite-induced IL-12 production by dendritic cells. The Journal of immunology *168*, 5997-6001.

Scharton-Kersten, T.M., Yap, G., Magram, J., and Sher, A. (1997). Inducible nitric oxide is essential for host control of persistent but not acute infection with the intracellular pathogen Toxoplasma gondii. The Journal of experimental medicine *185*, 1261-1273.

Scheu, S., Dresing, P., and Locksley, R.M. (2008). Visualization of IFNbeta production by plasmacytoid versus conventional dendritic cells under specific stimulation conditions in vivo. Proceedings of the National Academy of Sciences of the United States of America *105*, 20416-20421.

Schlitzer, A., Heiseke, A.F., Einwachter, H., Reindl, W., Schiemann, M., Manta, C.P., See, P., Niess, J.H., Suter, T., Ginhoux, F., and Krug, A.B.

(2012). Tissue-specific differentiation of a circulating CCR9- pDC-like common dendritic cell precursor. Blood *119*, 6063-6071.

Schlitzer, A., Loschko, J., Mair, K., Vogelmann, R., Henkel, L., Einwachter, H., Schiemann, M., Niess, J.H., Reindl, W., and Krug, A. (2011). Identification of CCR9- murine plasmacytoid DC precursors with plasticity to differentiate into conventional DCs. Blood *117*, 6562-6570.

Schlitzer, A., McGovern, N., and Ginhoux, F. (2015a). Dendritic cells and monocyte-derived cells: Two complementary and integrated functional systems. Seminars in cell & developmental biology *41*, 9-22.

Schlitzer, A., Sivakamasundari, V., Chen, J., Sumatoh, H.R., Schreuder, J., Lum, J., Malleret, B., Zhang, S., Larbi, A., Zolezzi, F., Renia, L., Poidinger, M., Naik, S., Newell, E.W., Robson, P., Ginhoux, F. (2015b). Identification of cDC1- and cDC2-committed DC progenitors reveals early lineage priming at the common DC progenitor stage in the bone marrow. Nature immunology *16*, 718-728.

Schmitz, J.L., Carlin, J.M., Borden, E.C., and Byrne, G.I. (1989). Beta interferon inhibits Toxoplasma gondii growth in human monocyte-derived macrophages. Infection and immunity *57*, 3254-3256.

Schraml, B.U., Hildner, K., Ise, W., Lee, W.L., Smith, W.A., Solomon, B., Sahota, G., Sim, J., Mukasa, R., Cemerski, S., Hatton, R.D., Stormo, G.D., Weaver, C.T., Russell, J.H., Murphy, T.L., and Murphy. K.M. (2009). The AP-1 transcription factor Batf controls T(H)17 differentiation. Nature *460*, 405-409.

Segura, E., Wong, J., and Villadangos, J.A. (2009). Cutting edge: B220+CCR9- dendritic cells are not plasmacytoid dendritic cells but are precursors of conventional dendritic cells. The Journal of immunology *183*, 1514-1517.

Seth, S., Qiu, Q., Danisch, S., Maier, M.K., Braun, A., Ravens, I., Czeloth, N., Hyde, R., Dittrich-Breiholz, O., Forster, R., and Bernhardt, G. (2011). Intranodal interaction with dendritic cells dynamically regulates surface expression of the co-stimulatory receptor CD226 protein on murine T cells. The Journal of biological chemistry *286*, 39153-39163.

Shortman, K., and Liu, Y.J. (2002). Mouse and human dendritic cell subtypes. Nature reviews. Immunology *2*, 151-161.

Sibley, L.D. (2009). Development of forward genetics in Toxoplasma gondii. International journal for parasitology *39*, 915-924.

Sibley, L.D., and Boothroyd, J.C. (1992). Virulent strains of Toxoplasma gondii comprise a single clonal lineage. Nature *359*, 82-85.

Sisirak, V., Ganguly, D., Lewis, K.L., Couillault, C., Tanaka, L., Bolland, S., D'Agati, V., Elkon, K.B., and Reizis, B. (2014). Genetic evidence for the role of plasmacytoid dendritic cells in systemic lupus erythematosus. The Journal of experimental medicine *211*, 1969-1976.

Steinman, R.M., and Witmer, M.D. (1978). Lymphoid dendritic cells are potent stimulators of the primary mixed leukocyte reaction in mice. Proceedings of the National Academy of Sciences of the United States of America *75*, 5132-5136.

Stockinger, S., Materna, T., Stoiber, D., Bayr, L., Steinborn, R., Kolbe, T., Unger, H., Chakraborty, T., Levy, D.E., Muller, M., and Decker, T. (2002). Production of type I IFN sensitizes macrophages to cell death induced by Listeria monocytogenes. The Journal of immunology *169*, 6522-6529.

Suzuki, S., Honma, K., Matsuyama, T., Suzuki, K., Toriyama, K., Akitoyo, I., Yamamoto, K., Suematsu, T., Nakamura, M., Yui, K., and Kumatori, A. (2004). Critical roles of interferon regulatory factor 4 in CD11bhighCD8alpha-

dendritic cell development. Proceedings of the National Academy of Sciences of the United States of America *101*, 8981-8986.

Swiecki, M., and Colonna, M. (2011). Type I interferons: diversity of sources, production pathways and effects on immune responses. Current opinion in virology *1*, 463-475.

Szabo, G., Dolganuic, A., Dai, Q., and Pruett, S.B. (2007). TLR4, Ethanol, and Lipid Rafts: A New Mechanism of Ethanol Action with Implications for other Receptor-Mediated Effects. The Journal of immunology *178* 3 1243-1249

Takaoka, A., and Yanai, H. (2006). Interferon signalling network in innate defence. Cellular microbiology *8*, 907-922.

Tussiwand, R., Lee, W.L., Murphy, T.L., Mashayekhi, M., Kc, W., Albring, J.C., Satpathy, A.T., Rotondo, J.A., Edelson, B.T., Kretzer, N.M., Wu, X., Weiss, L.A., Glasmacher, E., Li, P., Liao, W., Behnke, M., Lam, S.S., Aurthur, C.T., Leonard, W.J., Singh, H., Stallings, C.L., Sibley, L.D., Schreiber, R.D., and Murphy, K.M. (2012). Compensatory dendritic cell development mediated by BATF-IRF interactions. Nature *490*, 502-507.

Villadangos, J.A., and Schnorrer, P. (2007). Intrinsic and cooperative antigen-presenting functions of dendritic-cell subsets in vivo. Nature reviews. Immunology *7*, 543-555.

Waibler, Z., Anzaghe, M., Konur, A., Akira, S., Muller, W., and Kalinke, U. (2008). Excessive CpG 1668 stimulation triggers IL-10 production by cDC that inhibits IFN-alpha responses by pDC. European journal of immunology *38*, 3127-3137.

Waskow, C., Liu, K., Darrasse-Jeze, G., Guermonprez, P., Ginhoux, F., Merad, M., Shengelia, T., Yao, K., and Nussenzweig, M. (2008). The receptor

tyrosine kinase Flt3 is required for dendritic cell development in peripheral lymphoid tissues. Nature immunology *9*, 676-683.

Xu, W. (2011). PSD-95-like membrane associated guanylate kinases (PSD-MAGUKs) and synaptic plasticity. Current opinion in neurobiology *21*, 306-312.

Yamamoto, M., Okuyama, M., Ma, J.S., Kimura, T., Kamiyama, N., Saiga, H., Ohshima, J., Sasai, M., Kayama, H., Okamoto, T., Huang, D.C., Soldati-Favre, D., Horie, K., Takeda, J., Takeda, K. (2012). A cluster of interferon-gamma-inducible p65 GTPases plays a critical role in host defense against Toxoplasma gondii. Immunity *37*, 302-313.

Yarovinsky, F. (2014). Innate immunity to Toxoplasma gondii infection. Nature reviews. Immunology *14*, 109-121.

Yarovinsky, F., Zhang, D., Andersen, J.F., Bannenberg, G.L., Serhan, C.N., Hayden, M.S., Hieny, S., Sutterwala, F.S., Flavell, R.A., Ghosh, S., and Sher, A. (2005). TLR11 activation of dendritic cells by a protozoan profilin-like protein. Science *308*, 1626-1629.

Zhao, M., J. Zhang, H. Phatnani, S. Scheu, and T. Maniatis. 2012. Stochastic expression of the interferon-beta gene. *PLoS Biol* 10: e1001249.

Zhang, J., Raper, A., Sugita, N, Hingorani, R., Salio, M., Palmowski, M.J., Cerundolo, V., and Crocker, P.R. (2006). Characterization of Siglec-H as a novel endocytic receptor expressed on murine plasmacytoid dendritic cell precursors. Blood 107: 3600-3608

Zheng, C.Y., Seabold, G.K., Horak, M., and Petralia, R.S. (2011). MAGUKs, synaptic development, and synaptic plasticity. The Neuroscientist : a review journal bringing neurobiology, neurology and psychiatry *17*, 493-512.

Zuniga, E.I., Liou, L.Y., Mack, L., Mendoza, M., and Oldstone, M.B. (2008). Persistent virus infection inhibits type I interferon production by plasmacytoid dendritic cells to facilitate opportunistic infections. Cell Host Microbe *4*, 374-386.

Zuniga, E.I., McGavern, D.B., Pruneda-Paz, J.L., Teng, C., and Oldstone, M.B. (2004). Bone marrow plasmacytoid dendritic cells can differentiate into myeloid dendritic cells upon virus infection. Nature Immunology *5*, 1227-1234.

6. Appendix

6.1 Publications

The results of the work presented here were in part published in scientific journals or presented at international conferences.

The manuscript “IFNβ expression in the spleen is restricted to a subpopulation of pDCs exhibiting a specific immune modulatory transcriptome by Bauer, Dress et al., 2015, submitted for revision at the Journal of Immunology, is attached at the end of this thesis.

6.2 PSD-93 splice variants

Primer Set A was designed to distinguish between splice variants *Dlg2* 001, 002, 003 and 004 (ENSMUSG00000052572). PCR of splice variants *Dlg2* 001 and 003 will lead to amplification of products with the same length (150 bp). For variants 002 and 004 amplified products are distinct and lead to clear identification of the variant.

Primer Set B was designed to subsequently distinguish between splice variant *Dlg2* 001 and 003. Primers designed here bind only to variant 003, not 001. Therefore, if a product is amplified using primer Set B, this should be *Dlg2* 003.

Using Set A and Set B on *ex vivo* sorted splenic IFNβ-producing vs. non-producing pDCs after TLR9 stimulation should help clarifying which transcript variant is expressed in IFNβ-producing pDCs.

Forward primers are marked in yellow, reverse primers are marked in green, white/grey mark regions similar and different in the splice variants. For each Set multiple primer pairs were designed to increase the probability of a successful transcript variant determination.

Primer Set 1A

Splice variant	Primer binding regions	Amplified sequence in bp
001	GGTGGAAAGAAAGGAGCGTGCCCGATTGAAGACAGTGAAGTTCAATGCAAAACC TGGTGTGATTGATTCCAAAGGGGACATCCCCGGATTAGGTGACGACGGTTATGGA ACAAAGACTCTGAGAGGACAAGAAGATCTCATTCTTTCCTATGAACCTGTCACGA GGCAGGAAA	151
002	GGTGGAAAGAAAGGAGCGTGCCCGATTGAAGACAGTGAAGTTCAATGCAAAACC TGGTGTGATTGATTCCAAAGGGTCATTCAATGACAAGCGTAAAAAGAGCTTCATCT TTTCACGAAAATTCCCATTCTACAAGAACAAGGAGCAGAGTGAGCAGGAAACCAG TGATCCTGAACGAGGACAAGAAGATCTCATTCTTTCCTATGAACCTGTCACGAGG CAGGAAA	205
003	GGTGGAAAGAAAGGAGCGTGCCCGATTGAAGACAGTGAAGTTCAATGCAAAACC TGGTGTGATTGATTCCAAAGGGGACATCCCCGGATTAGGTGACGACGGTTATGGA ACAAAGACTCTGAGAGGACAAGAAGATCTCATTCTTTCCTATGAACCTGTCACGA GGCAGGAAA	151
004	GGTGGAAAGAAAGGAGCGTGCCCGATTGAAGACAGTGAAGTTCAATGCAAAACC TGGTGTGATTGATTCCAAAGGGTCATTCAATGACAAGCGTAAAAAGAGCTTCATCT TTTCACGAAAATTCCCATTCTACAAGAACAAGGAGCAGAGTGAGCAGGAAACCAG TGATCCTGAACAACACGTCTCTTCTAATGCCAGCGATAGCGAAAGTAGCTGCCGA GGACAAGAAGATCTCATTCTTTCCTATGAACCTGTCACGAGGCAGGAAA	247

Primer Set 2A

Splice variant	Primer binding regions	Amplified sequence in bp
001	GGTGGAAAGAAAGGAGCGTGCCCGATTGAAGACAGTGAAGTTCAATGCAAAACC TGGTGTGATTGATTCCAAAGGGGACATCCCCGGATTAGGTGACGACGGTTATGGA ACAAAGACTCTGAGAGGACAAGAAGATCTCATTCTTTCCTATGAACCTGTCACGA GGCAGGAAA	150
002	GGTGGAAAGAAAGGAGCGTGCCCGATTGAAGACAGTGAAGTTCAATGCAAAACC TGGTGTGATTGATTCCAAAGGGTCATTCAATGACAAGCGTAAAAAGAGCTTCATCT TTTCACGAAAATTCCCATTCTACAAGAACAAGGAGCAGAGTGAGCAGGAAACCAG TGATCCTGAACGAGGACAAGAAGATCTCATTCTTTCCTATGAACCTGTCACGAGG CAGGAAA	204
003	GGTGGAAAGAAAGGAGCGTGCCCGATTGAAGACAGTGAAGTTCAATGCAAAACC TGGTGTGATTGATTCCAAAGGGGACATCCCCGGATTAGGTGACGACGGTTATGGA ACAAAGACTCTGAGAGGACAAGAAGATCTCATTCTTTCCTATGAACCTGTCACGA GGCAGGAAA	150
004	GGTGGAAAGAAAGGAGCGTGCCCGATTGAAGACAGTGAAGTTCAATGCAAAACC TGGTGTGATTGATTCCAAAGGGTCATTCAATGACAAGCGTAAAAAGAGCTTCATCT TTTCACGAAAATTCCCATTCTACAAGAACAAGGAGCAGAGTGAGCAGGAAACCAG TGATCCTGAACAACACGTCTCTTCTAATGCCAGCGATAGCGAAAGTAGCTGCCGA GGACAAGAAGATCTCATTCTTTCCTATGAACCTGTCACGAGGCAGGAAA	246

Primer Set 3A

Splice variant	Primer binding regions	Amplified sequence in bp
001	GGTGGAAAGAAAGGAGCGTGCCCGATTGAAGACAGTGAAGTTCAATGCAAAACC TGGTGTGATTGATTCCAAAGGGGACATCCCCGGATTAGGTGACGACGGTTATGGA ACAAAGACTCTGAGAGGACAAGAAGATCTCATTCTTTCCTATGAACCTGTCACGA GGCAGGAAA	150
002	GGTGGAAAGAAAGGAGCGTGCCCGATTGAAGACAGTGAAGTTCAATGCAAAACC TGGTGTGATTGATTCCAAAGGGTCATTCAATGACAAGCGTAAAAAGAGCTTCATCT TTTCACGAAAATTCCCATTCTACAAGAACAAGGAGCAGAGTGAGCAGGAAACCAG TGATCCTGAACGAGGACAAGAAGATCTCATTCTTTCCTATGAACCTGTCACGAGG CAGGAAA	204
003	GGTGGAAAGAAAGGAGCGTGCCCGATTGAAGACAGTGAAGTTCAATGCAAAACC TGGTGTGATTGATTCCAAAGGGGACATCCCCGGATTAGGTGACGACGGTTATGGA ACAAAGACTCTGAGAGGACAAGAAGATCTCATTCTTTCCTATGAACCTGTCACGA GGCAGGAAA	150
004	GGTGGAAAGAAAGGAGCGTGCCCGATTGAAGACAGTGAAGTTCAATGCAAAACC TGGTGTGATTGATTCCAAAGGGTCATTCAATGACAAGCGTAAAAAGAGCTTCATCT TTTCACGAAAATTCCCATTCTACAAGAACAAGGAGCAGAGTGAGCAGGAAACCAG TGATCCTGAACAACACGTCTCTTCTAATGCCAGCGATAGCGAAAGTAGCTGCCGA GGACAAGAAGATCTCATTCTTTCCTATGAACCTGTCACGAGGCAGGAAA	246

Primer Set 1B

Splice variant	Primer binding regions	Amplified sequence in bp
003	ATATGAAGACAGGGGAACACTGATGCGATTGCTTCTTGTTTTTTACGAGTGTGGG AATCAAAATACTTCCCAATGAAAACATCTGCCTTTGTGCAAGTCACGCCCAGTTAT CCCCCCAAAGAAATGCTCTGATTAACTTTTTTTAAAGTCTTAAGATAGCAGTTTGTG TAGCCGATCTAATTAAGAAGTTTATGTAACAGATCTGCAGGTTTTTTTTTTTTTCCT TCTTCAACTGGGTTCTTTGAGCTCAGTTTGAATGTTACCGACTTTCGATATGCAAC GGCCAAGTGCTTCCCGAGCTGAGAATTATCAGCTTCTGTGGGATACAATTGCTTC TTTAAAACAATGTGAAGAAGCTATGCAACACGCGTTCATTCC[]GTCAATGGAACAG AAATTGAATATGAATTTGAAGAAATTACATTGGAGAGGGGAAATTCAGGTCTGGGA TTCAGTATTGCTGGAGGGACAGATAATCCCCACATTGGAGATGACCCTGGCATAT TTATTACGAAGATTATTCCAGGAGGTGCTGCGGCAGAGGATGGCAGACTCAGGG TCAACGACTGTATCTTGCGGGTGAATGAAGTTGATGTGTCAGAGGTTTCCCACAG TAAAGCAGTGGAAGCCCTCAAGGAAGCCGGCTCTATTGTGCGGCTGTACGTGCG CAGAAGGCGACCCATATTGGAGACTGTTGTGGAAATCAAACTTTTTAAAGGTCCA AAAGGTTTAGGCTTCAGTATTGCTGGAGGGGTGGGGAACCAGCACATTCCTGGA GACAACAGCATCTATGTAACAAAAATTATAGATGGTGGAGCTGCACAGAAAGATG GAAGGTTGCAAGTAGGAGACAGACTGCTAATGGTAAATAACTATAGTTTAGAAGA AGTTACACACGAAGAGGCTGTAGCGATATTGAAGAACACATCTGATGTTGTTTATC TAAAAGTTGGCAAACCCACCACTATTTATATGACTGATCCTTATGGGCCACCGGAT ATTACTCACT	153

Primer Set 2B

Splice variant	Primer binding regions	Amplified sequence in bp
003	ATATGAAGACAGGGGAACACTGATGCGATTGCTTCTTGTTTTTTACGAGTGTGGG AATCAAAATACTTCCCAATGAAAACATCTGCCTTTGTGCAAGTCACGCCCAGTTAT CCCCCCAAAGAAATGCTCTGATTAACTTTTTTTAAAGTCTTAAGATAGCAGTTTGTG TAGCCGATCTAATTAAGAAGTTTATGTAACAGATCTGCAGGTTTTTTTTTTTTTCCT TCTTCAACTGGGTTCTTTGAGCTCAGTTTGAATGTTACCGACTTTCGATATGCAAC GGCCAAGTGCTTCCCGAGCTGAGAATTATCAGCTTCTGTGGGATACAATTGCTTC TTTAAAACAATGTGAAGAAGCTATGCAACACGCGTTCATTCC[]GTCAATGGAACAG AAATTGAATATGAATTTGAAGAAATTACATTGGAGAGGGGAAATTCAGGTCTGGGA TTCAGTATTGCTGGAGGGACAGATAATCCCCACATTGGAGATGACCCTGGCATAT TTATTACGAAGATTATTCCAGGAGGTGCTGCGGCAGAGGATGGCAGACTCAGGG TCAACGACTGTATCTTGCGGGTGAATGAAGTTGATGTGTCAGAGGTTTCCCACAG TAAAGCAGTGGAAGCCCTCAAGGAAGCCGGCTCTATTGTGCGGCTGTACGTGCG CAGAAGGCGACCCATATTGGAGACTGTTGTGGAAATCAAACTTTTTAAAGGTCCA AAAGGTTTAGGCTTCAGTATTGCTGGAGGGGTGGGGAACCAGCACATTCCTGGA GACAACAGCATCTATGTAACAAAAATTATAGATGGTGGAGCTGCACAGAAAGATG GAAGGTTGCAAGTAGGAGACAGACTGCTAATGGTAAATAACTATAGTTTAGAAGA AGTTACACACGAAGAGGCTGTAGCGATATTGAAGAACACATCTGATGTTGTTTATC TAAAAGTTGGCAAACCCACCACTATTTATATGACTGATCCTTATGGGCCACCGGAT ATTACTCACT	213

Primer Set 3B

Splice variant	Primer binding regions	Amplified sequence in bp
003	ATATGAAGACAGGGGAACACTGATGCGATTGCTTCTTGTTTTTTACGAGTGTGGG AATCAAAATACTTCCCAATGAAAACATCTGCCTTTGTGCAAGTCACGCCCAGTTAT CCCCCCAAAGAAATGCTCTGATTAACTTTTTTTAAAGTCTTAAGATAGCAGTTTGTG TAGCCGATCTAATTAAGAAGTTTATGTAACAGATCTGCAGGTTTTTTTTTTTTTCCT TCTTCAACTGGGTTCTTTGAGCTCAGTTTGAATGTTACCGACTTTCGATATGCAAC GGCCAAGTGCTTCCCGAGCTGAGAATTATCAGCTTCTGTGGGATACAATTGCTTC TTTAAAACAATGTGAAGAAGCTATGCAACACGCGTTCATTCC[]GTCAATGGAACAG AAATTGAATATGAATTTGAAGAAATTACATTGGAGAGGGGAAATTCAGGTCTGGGA TTCAGTATTGCTGGAGGGACAGATAATCCCCACATTGGAGATGACCCTGGCATAT TTATTACGAAGATTATTCCAGGAGGTGCTGCGGCAGAGGATGGCAGACTCAGGG TCAACGACTGTATCTTGCGGGTGAATGAAGTTGATGTGTCAGAGGTTTCCCACAG TAAAGCAGTGGAAGCCCTCAAGGAAGCCGGCTCTATTGTGCGGCTGTACGTGCG CAGAAGGCGACCCATATTGGAGACTGTTGTGGAAATCAAACTTTTTAAAGGTCCA AAAGGTTTAGGCTTCAGTATTGCTGGAGGGGTGGGGAACCAGCACATTCCTGGA GACAACAGCATCTATGTAACAAAAATTATAGATGGTGGAGCTGCACAGAAAGATG GAAGGTTGCAAGTAGGAGACAGACTGCTAATGGTAAATAACTATAGTTTAGAAGA AGTTACACACGAAGAGGCTGTAGCGATATTGAAGAACACATCTGATGTTGTTTATC TAAAAGTTGGCAAACCCACCACTATTTATATGACTGATCCTTATGGGCCACCGGAT ATTACTCACT	171

6.3. Acknowledgements

First of all I would like to thank Prof. Dr. rer. nat. Stefanie Scheu for supervision, guidance and help during my PhD thesis. For giving me the opportunity to work in her lab, for supporting the study scientifically and financially and for giving me the possibility to attend national and international meetings to present my work – which I have enjoyed a lot!

Furthermore, I would like to thank Prof. Dr. rer. nat. Thomas Klein for being my second supervisor and careful reading of this thesis.

Also, Prof. Ingo Drexler and Prof. Philipp Lang – thank you for mentoring, discussing projects and ideas over these last 3 years.

And of course I want to thank my lab members for their support – scientifically or less scientifically, but just as important, with cakes and breakfasts, small talk,…thanks to Jens, Anja, “APu” and Sonja, and to all the other ones that passed through our lab over the last years.
Jens – I’ll never forget all these endless nights at the sorter. Thanks for suffering together with me and your friendship!
Also, I like to thank Anja, Milena, Krissi and Lisanna for their friendship, support, for one or the other glass of wine, hours of complaining, enjoying, hating and loving this world. Thanks!
Not to forget, I’ll miss our rooftop BBQs and want to thank everyone from our institute or the virology who made these evenings great – there are simply too many names to list all of them here.

I want to thank my parents, for their support throughout the past years and for letting me go wherever and do whatever I want to achieve my aims and dreams.

Last, I want to thank Dave. This thesis would not have been possible without you. Thanks you so much for feeding me on crazy experimental days, spending weekends in the lab with me, nights at the FACS, drying tears, giving scientific support and advise, help, strength, trust, for editing this thesis and still loving me - and last but not least for spreading the unicorn fairy-tale. Thanks for that! ;)
I love you!

6.4. Eidesstattliche Erklärung

Hiermit erkläre ich an Eides statt, dass ich die vorgelegte Dissertation selbstständig verfasst und keine anderen als die angegebenen Quellen und Hilfsmittel verwendet habe. Die Arbeit wurde unte Beachtung der “Grundsätze zur Sicherung guter wissenschaftlicher Praxis” an der Heinrich-Heine-Universität erstellt und weder in der vorgelegten noch in einer ähnlichen Form bei einer anderen Institution eingereicht.

Düsseldorf, den 06. Juli 2015

(Regine J.G. Dress)